

Bryn Mawr College

Scholarship, Research, and Creative Work at Bryn Mawr College

Bryn Mawr College Dissertations and Theses

2022

Khovanov Homology & Uniqueness of Surfaces in the 4-ball

Isaac Sundberg

Follow this and additional works at: <https://repository.brynmawr.edu/dissertations>



Part of the [Mathematics Commons](#)

Custom Citation

Sundberg, I. 2022. "Khovanov Homology & Uniqueness of Surfaces in the 4-ball." PhD Diss., Bryn Mawr College.

This paper is posted at Scholarship, Research, and Creative Work at Bryn Mawr College.
<https://repository.brynmawr.edu/dissertations/225>

For more information, please contact repository@brynmawr.edu.

Khovanov Homology & Uniqueness of Surfaces in the 4-ball

Isaac Sundberg

2022

Submitted to the Faculty of Bryn Mawr College
in partial fulfillment of the requirements for
the degree of Doctor of Philosophy in
the Department of Mathematics

Doctoral committee:

Paul Melvin (advisor)

Erica Graham

Leslie Cheng

Lisa Traynor

© Isaac Sundberg 2022

Abstract

We use the functoriality of Khovanov homology to examine the smooth, boundary-preserving isotopy of surfaces embedded in the 4-ball. We exemplify an infinite family of prime knots that bound an arbitrarily-large number of smoothly-distinct slice disks by distinguishing the maps they induce on Khovanov homology. Similar techniques produce an infinite family of knots that each bound a pair of exotic surfaces of arbitrary genus.

Dedication

Dedicated to Jayne

Acknowledgments

I would like to thank so many people for their support in preparing this dissertation and throughout my academic career. First and foremost, my partner, your hero, Brynn. My mother and brother, Jayne and Alec, for their constant love, support, and encouragement. My undergraduate advisor, Robert Allen, for being an amazing mentor, professor, collaborator, and friend - if you hadn't drawn the Intermediate Value Theorem for me, I don't know where I would be! All my other advisors, who have been a constant source of inspiration and support: Tushar Das, Whitney George, Erica Graham, Eddie Kim, Daisy Sudparid, Ted Wendt. To Kyle Hayden, for helping me so much the past year with my applications, while also being a sick-ass collaborator. To my office buddies: first office buddy, Dan White, fer flippin' shoot I miss you... I think I speak for us both when I say needly-nee, smash-smash-smash; second office buddy, Aisha Mechery, thank you for your friendship, conversation, and for feeding me all the interesting things you find; third office buddy, Savannah Williams, I just can't say enough how much I have appreciated your affirmations, energy, support, and interior decorating; and all my other graduate office buddies: Ziva Myer, Danielle Smiley, Samantha Pezzimenti, Hannah Schwartz, Lindsay Dever, AJ Vargas, Elsa Magness, Dalena Vien, Dee Ann Reisinger, you are all such great friends. To the undergraduates at Bryn Mawr, who have been immensely supportive and have taught me so much more than I have taught them. A few more folks who have helped me with advice, applications, and encouragement: Mikhail Khovanov, Siddhi Krishna, Adam S. Levine, and Katherine Raoux.

Table of Contents

Abstract	ii
Acknowledgments	iv
Contents	v
List of Figures	vii
List of Tables	ix
1 Introduction	1
1.1 Motivation	1
1.2 Methods	3
1.3 Results	3
1.4 Future work	6
1.5 Outline	7
1.6 Conventions	7
2 Background	9
2.1 Link cobordisms	9
2.1.1 Definition and examples	9
2.1.2 Isotopy	10
2.1.3 Surface diagrams and movies	11
2.1.4 Movie moves	13
2.1.5 Approaching link cobordisms practically	13
2.2 Khovanov homology of links	14
2.2.1 Cube of resolutions	14
2.2.2 Choosing a topological quantum field theory	15
2.2.3 Applying a topological quantum field theory	17
2.2.4 Khovanov chain complex	17
2.2.5 Labeled smoothings	19
2.2.6 Khovanov homology	21
2.3 Khovanov homology of link cobordisms	21
2.3.1 Cobordism induced maps on Khovanov homology	22
2.3.2 Explicit induced maps	24
2.3.3 Local knotting	26
3 Maps induced by surfaces in the 4-ball	33
3.1 Extending to $S^3 \times [0, 1]$	33
3.2 Induced link cobordisms and induced maps	34
3.3 Diagram dependence	36
4 Closed surfaces in the 4-ball	38
4.1 φ -numbers	38
4.2 Calculating φ -numbers	39

5	Relative surfaces in the 4-ball	41
5.1	φ -classes	41
5.2	Calculating φ -classes for familiar families of surfaces	43
5.2.1	Seifert surfaces	43
5.2.2	Surfaces bounding the unlink	44
5.3	φ -distinguished families of slice disks	44
5.3.1	A pair of slices for 9_{46}	45
5.3.2	A pair of slices for 6_1	49
5.3.3	A family of slices for $\#_k(9_{46})$	49
5.3.4	An extended family of prime knots	51
5.4	Obstructing sliceness with φ -classes	53
5.5	Reflections on φ -classes	55
6	Triviality of Khovanov homology classes	56
6.1	Boundaries in Khovanov homology	56
6.2	A SageMath program	57
6.2.1	Encoding an oriented knot diagram	57
6.2.2	Encoding labeled smoothings and chains	59
6.3	Applications	63
7	Duals and relative surfaces in the 4-ball	66
7.1	Dual link cobordisms	66
7.2	φ^* -classes	67
7.3	φ^* -distinguished pairs of surfaces	69
7.3.1	Two pairs of slice disks	70
7.3.2	A pair of exotic slice disks	71
7.3.3	Exotic slice disks bounding asymmetric knots	73
7.3.4	Higher genus exotic slices	75
7.3.5	Extensions to absolute isotopy	76
	Appendix	77
	Appendix A: Categories	77
	Appendix B: Topological quantum field theories	80
	Appendix C: Supplementary Code	83

List of Figures

1.1	A series of visuals describing a slice disk for 9_{46}	2
2.1	A schematic for visualizing a link cobordism	10
2.2	A pair of Roseman moves	12
2.3	Movie moves corresponding to the Roseman moves in Figure 2.2	13
2.4	A saddle cobordism relating a 0-smoothing and 1-smoothing	15
2.5	The cube of resolutions for the positive trefoil	16
2.6	An illustration of labeled smoothings and pqr -chains	19
3.1	The sweep-around-move	34
4.1	The map on Khovanov homology induced by a sphere	39
4.2	The map on Khovanov homology induced by a torus	40
4.3	The map on Khovanov homology induced by a second torus	40
5.1	A pair of slice disks bounding 9_{46}	45
5.2	The ϕ -cycles calculated in Figures 5.3 and 5.4	46
5.3	The calculation of the ϕ -cycle for one slice disk bounding 9_{46}	47
5.4	The calculation of the ϕ -cycle for the other slice disk bounding 9_{46}	48
5.5	A pair of slice disks bounding 6_1	49
5.6	The ϕ -cycles for the two slice disks from Figure 5.5	50
5.7	The 2^5 slice disks bounding $\#_5(9_{46})$ and a special smoothing	50
5.8	A ribbon concordance from a composite knot to a prime knot	52
5.9	A prime knot bounding 2^m slice disks	53
5.10	The prime knot from Figure 5.9 with $m = 2$	54
5.11	One of the four unique slice disks described in Figure 5.9	54
6.1	Example enumerations for encoding an oriented link diagram	58
6.2	Example enumerations for encoding labeled smoothings	59
6.3	A set of link diagrams that our SageMath program does not handle	63
6.4	Encoding a diagram of 9_{46}	64
7.1	The calculation of the ϕ^* -cycle for one slice disk bounding 9_{46}	70
7.2	Slice disks bounding $15n_{103488}$ that are ϕ^* -distinguished by a given cycle	71
7.3	Slice disks bounding $J = 17nh_{34}$ that are ϕ^* -distinguished by a given cycle	72
7.4	Handle diagrams for the exterior of a slice disk bounding J	72
7.5	The calculation that one slice disk bounding J has nontrivial ϕ^* -class	74
7.6	Slice disks bounding an asymmetric version of J that are ϕ^* -distinguished by a given cycle	75
7.7	Slice disks bounding a higher-genus version of J that are ϕ^* -distinguished by a given cycle	76
7.8	A combination of the knots and surfaces in Figures 7.6 and 7.7	76
A.1	The fundamental cobordisms in Cob^3	78

B.1	The fundamental relations for Cob^3	82
C.1	Encoding a diagram of 6_1	84
C.2	Encoding a diagram of the Conway knot	86
C.3	A movie describing a genus-1 surface bounding the Conway knot	86
C.4	Encoding another diagram of the Conway knot	87
C.5	A movie describing a genus-1 surface bounding the Conway knot	87

List of Tables

2.1	The chain maps induced by Morse moves	25
2.2	The chain maps induced by Reidemeister I moves	28
2.3	The chain maps induced by Reidemeister II moves	28
2.4	The chain map induced by one Reidemeister III move	29
2.5	The chain map induced by a Reidemeister III equivalent to the move in Table 2.4	30
2.6	The chain map induced by a second Reidemeister III move	31
2.7	The chain map induced by a Reidemeister III equivalent to the move in Table 2.6	32

Chapter 1: Introduction

This dissertation examines the maps on Khovanov homology associated to smooth, oriented, compact, properly embedded surfaces in the 4-ball. In particular, we use these maps to answer questions of existence and uniqueness for slice disks.

1.1. Motivation

A knot K in the 3-sphere S^3 is **slice** if there exists a smoothly-embedded disk D in the 4-ball B^4 for which $\partial D = K$. Such a disk is called a **slice disk** for K . It is not always easy to tell which knots are slice by looking at them; after all, they are 4-dimensional! A common technique for visualizing slice disks is to *bring them down a dimension* by looking at the 3-dimensional pieces from which they are made: their level sets with respect to the 4-ball radius. By viewing the 4-ball as a quotient space $B^4 = S^3 \times [0, 1]/S^3 \times \{0\}$, the slice disk D is described by the sets $L_i = D \cap (S^3 \times \{i\})$ with respect to the 4-ball radius $i \in [0, 1]$. These level sets will be links, except at finitely many double points and isolated singularities. For example, we have illustrated a slice disk D_ℓ for the knot 9_{46} in Figure 1.1, where we see that a single handle attachment splits the knot into a two component unlink, which are then capped off to form a disk.

Understanding which knots are slice has played an important role in low-dimensional topology, being crucial to the formation of the knot concordance group as well as to the success and failure of the Whitney trick. As a result, the sliceness of knots has been well studied and is currently known for knots with up to 13 crossings, with the final 11 crossing knot only recently being determined [Pic20]. Focusing on the slice disk, as opposed to the knot itself, this indicates that the *existence* of a slice disk for a given knot is well understood, and indeed, there is a bounty of examples of slice disks to consider. Surprisingly, there are many examples of knots having *multiple* slice disks! For example, the knot in Figure 1.1 has a second slice disk D_r , obtained by rotating the level sets, or equivalently, by attaching a 1-handle on the right side of the diagram. Because such examples exist, it is a natural to study the *uniqueness* of slice disks. Are the slice disks D_ℓ and D_r equivalent? As has already been hinted, they are related by an

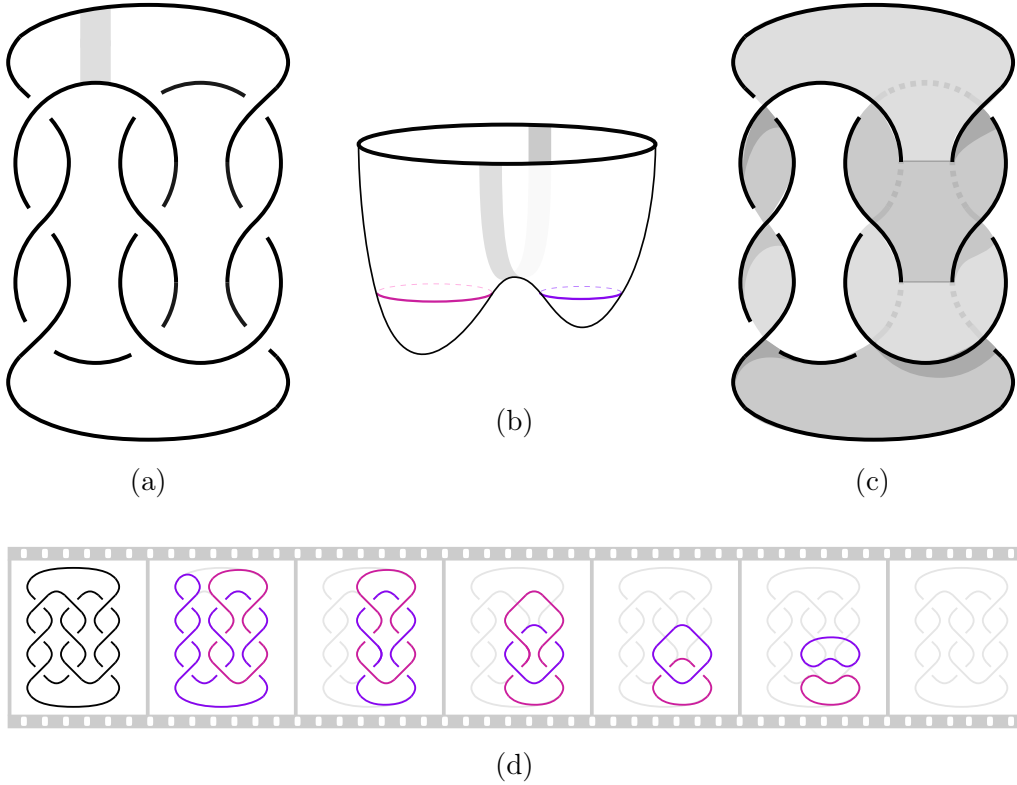


Figure 1.1: (a) a diagram for the knot 9_{46} decorated with a band describing a 1-handle attachment; (b) a schematic for the genus of the surface produced by the 1-handle; (c) the resulting slice disks D_ℓ pushed into the 3-sphere; (d) a movie describing the level sets of D_ℓ in the 4-ball.

isotopy that rotates the disk by 180° . Surprisingly, if we restrict to boundary-preserving isotopy, where the boundary knot is required to stay fixed as a set, the answer is no! The slice disks D_ℓ and D_r are not isotopic rel boundary.

Low-dimensional topologists have developed techniques for obstructing the boundary-preserving isotopy of slice disks (and more generally, surfaces in 4-manifolds) by applying tools from the fundamental group of the complement of the disks [CP21, MP19], gauge theory [Akb91, Hay21], and Heegaard Floer homology [JM16, JZ20]. In this dissertation, we discuss the application of Khovanov homology toward these questions. This innovative approach appears promising, being the only (known) technique that can smoothly distinguish topologically-equivalent surfaces without using gauge theory. Our results add to the growing list of applications of Khovanov homology toward understanding 4-dimensional information. For example, the Lee deformation of Khovanov homology [Lee02] was used to define the s -invariant [Ras05], which has been used in the groundbreaking proof that the Conway knot is not slice [Pic20], as well as in reproofs of Milnor's conjecture [Ras05] and the existence of exotic smooth structures on \mathbb{R}^4 [Ras10], both of which previously required gauge theory. Moreover, generalizing, deforming, and extending

Khovanov homology is an active field of research (c.f., [Kho06b, LS21, MN20, MWW21]). These generalizations may enhance our technique for distinguishing slice disks and may provide invariants for a broader range of surfaces within 4-manifolds.

1.2. Methods

The Khovanov homology functor \mathcal{H} developed in [Kho00] acts on the category of link cobordisms in $\mathbb{R}^3 \times [0, 1]$. It associates to an oriented link L a diagrammatically-defined homology group $\mathcal{H}(L)$, and it associates to a link cobordism $\Sigma : L_0 \rightarrow L_1$ a diagrammatically-defined homomorphism $\mathcal{H}(\Sigma) : \mathcal{H}(L_0) \rightarrow \mathcal{H}(L_1)$. The induced map is invariant, up to sign, under smooth boundary-preserving isotopy of the link cobordism [Jac04, BN05, Kho06a]. Therefore, link cobordisms can be distinguished by showing they induce distinct maps, up to sign. We adapt this invariant to surfaces in $S^3 \times [0, 1]$ and B^4 , and in particular, to slice disks.

A smooth, oriented, properly embedded surface Σ in the 4-ball can be regarded as a link cobordism from the empty link \emptyset to the link $L = \partial\Sigma$ in the boundary 3-sphere. The case where $L = \emptyset$ was first considered in [Kho00], where it was conjectured that the associated map on Khovanov homology could distinguish knotted tori. At the time (2000), the invariance under boundary-preserving isotopy had not been proven; once it was established (2004), the conjecture gained some interest. Initial calculations of the map on Khovanov homology induced by certain families of knotted tori were produced [CSS06]. Inevitably, this led to the conclusion that these maps are trivially determined by genus [Ras05, Tan06]. The relative case $L \neq \emptyset$ was later studied by Swann in [Swa10]. Although errors were found in Swann's work [Bat12], many of the results were confirmed, re-proven, and extended in [SS21]. In particular, it was shown that the relative case is nontrivial, in the sense that the associated induced maps can be used to distinguish surfaces with boundary. Additionally, the maps induced by link cobordisms $L \rightarrow \emptyset$ were studied in [HS21] with similar results proven for exotic slice disks.

1.3. Results

In this dissertation, we prove the results from [SS21] and [HS21] and highlight numerous additional applications and calculations the author has discovered in producing these works. The main results are highlighted here. There are three main results regarding the maps on Khovanov homology: they can distinguish slice disks; they can smoothly distinguish topologically isotopic

surfaces; they are invariant under local knotting.

Unique slice disks The aforementioned works [SS21, Swa10] examined the maps on Khovanov homology induced by link cobordisms $\Sigma: \emptyset \rightarrow L$. In this dissertation, we continue this analysis and prove the following two theorems.

Theorem 1.3.1. *The knots 6_1 and 9_{46} each bound a pair of slice disks that induce distinct maps on Khovanov homology, and hence, are distinct up to smooth, boundary-preserving isotopy.*

Theorem 1.3.2. *For each integer $m \geq 0$, there is a prime knot K_m bounding 2^m slice disks that induce distinct maps on Khovanov homology, and hence, are pairwise distinct up to smooth, boundary-preserving isotopy.*

The essence of these theorems is noting that the induced map $\mathcal{H}(\Sigma): \mathbb{Z} \rightarrow \mathcal{H}(L)$ is determined by where it maps the unique generator of $\mathcal{H}(\emptyset) = \mathbb{Z}$; we denote this element

$$\varphi(\Sigma) := \mathcal{H}(\Sigma)(1) \in \mathcal{H}(L)$$

This element has previously been called the *relative Khovanov-Jacobsson class* of Σ [Swa10, SS21], however, in this dissertation we will err on the side of brevity and call it the φ -class of Σ . Given the aforementioned invariance of $\mathcal{H}(\Sigma)$, the φ -class is an up-to-sign invariant of the smooth, boundary-preserving isotopy class of Σ . We prove Theorem 1.3.1 by distinguishing the φ -classes for the relevant slice disks.

The φ -classes have the benefit that they work well with the theory of Khovanov homology, and Theorem 1.3.2 is proven by exploiting the general behavior of these invariants under ribbon-concordances (i.e., genus-0 cobordisms with no local maxima). The idea is to extend a given pair of slice disks by attaching a ribbon-concordance to their boundary. Ribbon-concordances induce injections on Khovanov homology [LZ19], so if the slice disks have distinct φ -classes, then the extension of the slice disks will also have distinct φ -classes. We combine this with the fact that every knot is ribbon-concordant to a prime knot [KL79] to extend the 2^m distinct slices of $\#_m(9_{46})$ to a family of distinct slice disks for a prime knot K_m .

There are two major obstacles that φ -classes face: they are cumbersome to calculate and, even when computed, they are difficult to distinguish. In certain cases, these obstacles can be overcome. In particular, we give a SageMath program in Chapter 6 that distinguishes Khovanov homology classes associated to knot diagrams with up to 12 crossings.

Exotic slice disks The lowest dimension where the smooth and topological properties of manifolds diverge is in dimension four, and the distinction between these categories is a fundamental topic in low-dimensional topology. We say a pair of surfaces in a 4-manifold are *exotic* if they are topologically isotopic relative their boundary but not smoothly. Recall that the maps on Khovanov homology are invariant under *smooth*, boundary-preserving isotopy, and therefore, they are a natural candidate for detecting exotic surfaces. The surfaces in Theorems 1.3.1 and 1.3.2 are not even homotopic rel boundary, so a new family of slice disks must be considered. Later work used the maps on Khovanov homology to detect an infinite family of knots that each bound a pair of exotic surfaces with any chosen genus [HS21]. This dissertation reproves the following case from that work.

Theorem 1.3.3. *For each pair of non-negative integers m and n , there is a knot $J_{m,n}$ bounding a pair of exotic genus n surfaces that induce distinct maps on Khovanov homology, and hence, are distinct up to boundary-preserving isotopy.*

To prove this, we improve upon the techniques used in Theorems 1.3.1 and 1.3.2. We implement the same base strategy: a smooth, oriented, properly embedded surface in the 4-ball with boundary link $L = \partial\Sigma$ can *also* be regarded as a link cobordism $\Sigma^* : L \rightarrow \emptyset$ by reflecting the link cobordism from above through the interval factor of $\mathbb{R}^3 \times [0, 1]$. This cobordism is called the *dual cobordism*, and it induces a *dual map* $\mathcal{H}(L) \rightarrow \mathbb{Z}$ which is invariant, up to sign, under smooth, boundary-preserving isotopy of Σ . Thus, for each class $\varphi \in \mathcal{H}(L)$,

$$\varphi^*(\Sigma) := \mathcal{H}(\Sigma^*)(\varphi) \in \mathcal{H}(\emptyset) = \mathbb{Z}$$

is an up-to-sign invariant of the boundary-preserving isotopy class of Σ , called the φ^* -class of Σ . Unlike the previous approach, we may control the complexity of calculating $\varphi^*(\Sigma)$ by choosing φ wisely; moreover, we can easily distinguish φ^* -classes (up to sign), because they are integers. In Theorem 1.3.3, we show that a pair of topologically equivalent genus n surfaces $\Sigma_{0,1}$ bounding a given knot $J_{m,n}$ are smoothly distinct by giving a class $\varphi \in \mathcal{H}(J_{m,n})$ such that $\varphi^*(\Sigma_0) = 0$ and $\varphi^*(\Sigma_1) = 1$. Note that for $n = 0$, this theorem gives an infinite family of pairs of exotic slice disks for the knot $J_{m,0}$.

Local knotting A notable strength of the cobordism induced maps is their invariance under local knotting: for a surface Σ in the 4-ball and a knotted 2-sphere S , we say $\Sigma \# S$ is *locally knotted*. Locally knotting a surface generally changes its smooth, boundary-preserving isotopy class, and because there are *many* knotted 2-spheres, it is more rewarding to omit this operation

when studying boundary-preserving isotopy classes of surfaces. Fortunately, we prove that our favorite invariant is not sensitive to this operation.

Theorem 1.3.4. *The induced maps on Khovanov homology are invariant under local knotting: any link cobordism $\Sigma: L_0 \rightarrow L_1$ and knotted 2-sphere S have*

$$\mathcal{H}(\Sigma) = \pm \mathcal{H}(\Sigma \# S)$$

In particular, this implies that Theorems 1.3.2 and 1.3.3 distinguish locally *unknotted* families of surfaces in the 4-ball.

1.4. Future work

The successful application of the cobordism induced maps on Khovanov homology indicate that continued study will be promising. The work of this dissertation can be extended and applied to other related questions in low-dimensional topology. We list some of these ideas here.

Uniqueness of spanning surfaces. A spanning surface of a knot K is an oriented surface in the 3-sphere bounding K . Pairs of unique spanning surfaces for a fixed K have been found [Alf70, Lyo74, Tro75], and it is natural to ask if they remain unique when pushed into 4-ball. In [Liv82], Livingston showed that the surfaces in [Tro75] become isotopic when pushed into B^4 and posed the unlikely conjectured that all non-isotopic spanning surfaces become isotopic in the 4-ball. This conjecture remains open. Potential counterexamples exist, and the maps they induce on Khovanov homology may be able to distinguish them.

Detecting sliceness. If Σ is a genus 1 surface in the 4-ball bounding a slice knot, then the φ -class $\varphi(\Sigma)$ is nontrivial (c.f., Theorem 5.1 [SS21], or Theorem 5.4.1). In other words, the sliceness of a knot K can be obstructed by finding a genus 1 link cobordism $\Sigma: \emptyset \rightarrow K$ having trivial $\varphi(\Sigma)$. With this approach, the sliceness of a family of odd 3-stranded pretzel knots was determined [SS21, Swa10]. Initial observations indicate that this technique can be extended to a broader family of odd 3-stranded pretzel knots. Extending this to all odd 3-stranded pretzel knots would reestablish the slice-ribbon conjecture for these knots [GJ11], previously requiring gauge theory. We provide more insight for this application in Section 5.4.

Relation to knot Floer homology. A similar invariant of cobordism induced maps has been defined using knot Floer homology in [JM16] and was used to distinguish a family of slice disks

in [JZ20]. Given the general symmetry of results between Khovanov homology and knot Floer homology, it is likely that these slice disks can also be distinguished by their maps on Khovanov homology. Conversely, the maps on knot Floer homology induced by the exotic surfaces in Theorem 1.3.3 can be examined. It is also unknown if these invariants are related, perhaps by a spectral sequence.

Other versions of Khovanov homology. The definition of Khovanov homology we use is from [Kho00], however, many generalizations and deformations exist [BN05, Lee02, Kho06b]. The above techniques can be explored in these generalized settings with the hope of finding richer invariants and deeper results (c.f., [LS21]). These versions of Khovanov homology are inherent to links in S^3 and surfaces in $S^3 \times [0, 1]$, and generalizations to other 3- and 4-manifolds also exist (c.f., [MN20, MWW21]). Again, these invariants can likely be broadening to invariants for surfaces in other 4-manifolds.

1.5. Outline

This dissertation is organized into chapters, containing sections. The next chapter (Chapter 2) covers the necessary background on surfaces in $S^3 \times [0, 1]$ and their associated maps on Khovanov homology. Chapter 3 extends these maps to surfaces in the 4-ball. Chapter 4 characterizes the induced maps associated to closed surfaces. The main results of this dissertation are found in Chapters 5-7, where we examine the induced maps associated to surfaces with boundary. Chapter 5 considers link cobordisms $\emptyset \rightarrow L$, with which we define φ -classes. Chapter 6 gives a SageMath program that determines nontriviality of Khovanov homology classes, which we use in certain applications of φ -classes. We conclude with Chapter 7, which considers link cobordisms $L \rightarrow \emptyset$ and their induced maps, with which we define φ^* -classes. The dissertation contains three appendices, covering background on categories (A), topological quantum field theories (B), as well as some supplementary code (C) for Chapter 6.

1.6. Conventions

Throughout the dissertation, we will make use of certain shorthands and assumptions; these are listed here. Unless stated otherwise, we assume: all surfaces are oriented, compact, generic, and smooth; every isotopy is a smooth and boundary-preserving. The notation for pairs of objects will be confined to a common index (a pair of links $L_{0,1}$) and in certain cases, to a superscript (a

pair of links L, L'). Compositions of cobordisms $\Sigma_1 \circ \Sigma_0$ are read right to left, to be consistent with the functions that they induce. Illustrations of cobordisms should be seen as *ascending*, that is, as a cobordism *from* the link illustrated on the bottom *to* the link illustrated on the top. Occasionally, we use diagrams D interchangeably with the links L they represent, as in $\mathcal{C}(L)$ and $\mathcal{H}(L)$, which are *diagrammatically*-defined (a diagram is always clear from context).

Chapter 2: Background

This chapter discusses the necessary background for computing and utilizing the maps on Khovanov homology induced by link cobordisms. We begin by reviewing link cobordisms in Section 2.1. We summarize the link homology theory defined in [Kho00], known as Khovanov homology. This is done in two phases: the Khovanov homology groups associated to oriented link diagrams are defined in Section 2.2 and the maps on Khovanov homology induced by link cobordisms are defined in Section 2.3.

2.1. Link cobordisms

In this section we will discuss link cobordisms, which are (roughly) nice surfaces bounding pairs of links. Link cobordisms represent a large variety of surfaces of interest to low-dimensional topologists. Their breadth gives them importance, and as such, we should be careful to specify the lens through which we study them. In particular, we will discuss: their definition (2.1.1); our notion of equivalence of link cobordisms, through *boundary-preserving isotopy* (2.1.2); the methods with which we study link cobordisms, as *surface diagrams* and their associated *movies* (2.1.3); and how the methods change under this type of equivalence, through *movie moves* (2.1.4). The majority of this section reflects the theoretical usage of link cobordisms, which may lead many to be overly wary of their use in practice. In reality, we rarely think about these notions that float in the background. Link cobordisms are flexible and highly useful, which we discuss at the end of the chapter (2.1.5).

2.1.1 Definition and examples

Here we give the definition of a link cobordism which, as their name suggests, are cobordisms between links. Some examples are listed to provide context and to help visualize the objects we will work with. A useful image to reference is given in Figure 2.1.

Definition 2.1.1. Let F_g be a compact, oriented, genus- g surface with boundary. A **link cobordism** is the image Σ of a smooth, proper embedding $h: F_g \hookrightarrow \mathbb{R}^3 \times [0, 1]$. The boundary of Σ is

a pair of oriented links $L_{0,1} \subset \mathbb{R}^3 \times \{0, 1\}$. We often use the shorthand $\Sigma: L_0 \rightarrow L_1$ to describe the relevant information of a link cobordism.

Many familiar surfaces can be tailored to the above definition: Seifert surfaces, slice disks, and link concordances are all examples of link cobordisms. These surfaces do not, a priori, live in $\mathbb{R}^3 \times [0, 1]$, so some work is done to adapt them to this setting. For surfaces in S^3 and B^4 , we generally remove points and arcs from the ambient space, with the goal of producing a surface properly embedded in $\mathbb{R}^3 \times [0, 1]$. As these surfaces are generally studied up to some form of isotopy, we must be careful that the process of deleting points and arcs will guarantee consistency between the equivalence of link cobordisms and the equivalence of these other topological objects. See Chapter 3 for certain surfaces in B^4 .

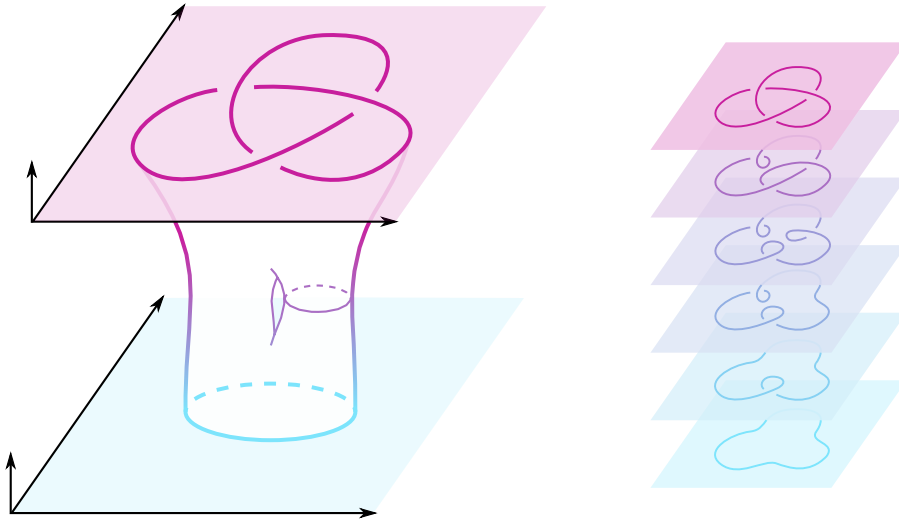


Figure 2.1: (left) a schematic for a link cobordism from the unknot to the trefoil, where the surface records the genus of the cobordism; (right) a sequence of the level sets from the link cobordism; each plane represents a copy of S^3 containing the portion of the link cobordism at that 4-ball radius.

2.1.2 Isotopy

Link cobordisms are studied up to multiple types of equivalence (e.g., boundary-preserving isotopy, ambient isotopy, or morphisms of $\mathbb{R}^3 \times [0, 1]$ carrying one surface to the other) and within two main categories (topological or smooth). In this dissertation, we consider link cobordisms up to smooth, boundary-preserving isotopy, which we define below.

We begin with a general definition for embeddings of manifolds. Let M and N be manifolds. A pair of embeddings $h_{0,1}: M \hookrightarrow N$ are *isotopic* if they are related by an *isotopy*: a smooth map $H: M \times [0, 1] \rightarrow N$ such that each $h_t = H|_{M \times \{t\}}$ is an embedding. In certain cases, such

an isotopy can be extended to a map on the entire space N . We say the embeddings $h_{0,1}$ are *ambiently isotopic* if there is an *ambient isotopy* between them: a smooth map $H: N \times [0, 1] \rightarrow N$, for which each $H_t = H|_{N \times \{t\}}$ is a diffeomorphism, $H_0 \equiv \text{id}$ and $H_1 \circ h_0 \equiv h_1$. An isotopy of embeddings of a compact manifold M can always be extended to an ambient isotopy [EK71, Corollary 1.4]. In the case at hand, we are using $M = F_g$, so for simplicity, we adopt the definition of an ambient isotopy as our base notion of isotopy, as in the following definition. For notational convenience, let $X = \mathbb{R}^3 \times [0, 1]$.

Definition 2.1.2. A pair of link cobordisms $\Sigma_{0,1}$ are **isotopic**, denoted $\Sigma_0 \sim \Sigma_1$, if their embeddings $h_{0,1}$ are ambiently isotopic: there is a smooth map $H: X \times [0, 1] \rightarrow X$ whose restrictions $H_t = H|_{X \times \{t\}}$ are diffeomorphisms satisfying $H_0 \equiv \text{id}_X$ and $H_1 \circ h_0 \equiv h_1$.

Definition 2.1.3. A pair of isotopic link cobordisms $\Sigma_{0,1}$ are **isotopic rel boundary**, denoted $\Sigma_0 \sim \Sigma_1 \text{ rel } \partial$, if the isotopy H between them fixes $\partial X \times [0, 1]$ setwise. In this case, we call H a **boundary-preserving isotopy**.

As the main focus of this dissertation is boundary-preserving isotopy, we often will err on the side of brevity and omit the phrase *boundary-preserving*. We will explicitly state when we are considering an isotopy that does not preserve the boundary.

2.1.3 Surface diagrams and movies

Just as we study links in \mathbb{R}^3 by the *diagrams* they project onto a plane, we will study link cobordisms by the *surface diagrams* they project onto a hyperplane of $\mathbb{R}^3 \times [0, 1]$. We follow the treatment of surface diagrams and movies from [Jac04].

A link cobordism $\Sigma: L_0 \rightarrow L_1$ is *generic* if, with respect to the interval factor of $\mathbb{R}^3 \times [0, 1]$, it restricts to a Morse function with distinct critical values. When generic, the level sets $L_t = \Sigma \cap (\mathbb{R}^3 \times \{t\})$ are all links, except at finitely many critical levels, where the level set contains either a transverse double point or an isolated point. A transverse double point corresponds to a Morse saddle, or equivalently, a 1-handle attachment; an isolated point corresponds to a Morse birth or death, or equivalently, a 0- or 2-handle attachment. We assume all link cobordisms are generic.

Definition 2.1.4. A *surface diagram* of a generic link cobordism $\Sigma: L_0 \rightarrow L_1$, denoted $S: D_0 \rightarrow D_1$, is the image $S \subset \mathbb{R}^2 \times [0, 1]$ of Σ under a generic projection $(p \times \text{id}): \mathbb{R}^3 \times [0, 1] \rightarrow \mathbb{R}^2 \times [0, 1]$.

By a *generic projection*, we mean that, “the only singular points in the interior of the surface diagram are double points, Whitney umbrella points and triple points. At a double point, the

diagram looks like the transversal intersection of two planes. Whitney umbrellas and triple points occur as the (isolated) boundary points of the double point set in the interior of $\mathbb{R}^2 \times [0, 1]$," [Jac04]. When Σ is generic, each level set $D_t = S \cap (\mathbb{R}^2 \times \{t\})$ is a link diagram for the link L_t except at finitely many critical points (corresponding to Morse moves) as well as finitely many singular points arising from the projection, i.e., the double and triple points (corresponding to Reidemeister moves).

Surface diagrams are used to study link cobordisms in a very similar way that diagrams are used to study links. Just as there is a set of Reidemeister moves that relate diagrams for isotopic links, there is a set of *Roseman moves* that relate surface diagrams for any pair of isotopic link cobordisms [Ros98]. We illustrate a few Roseman moves here.

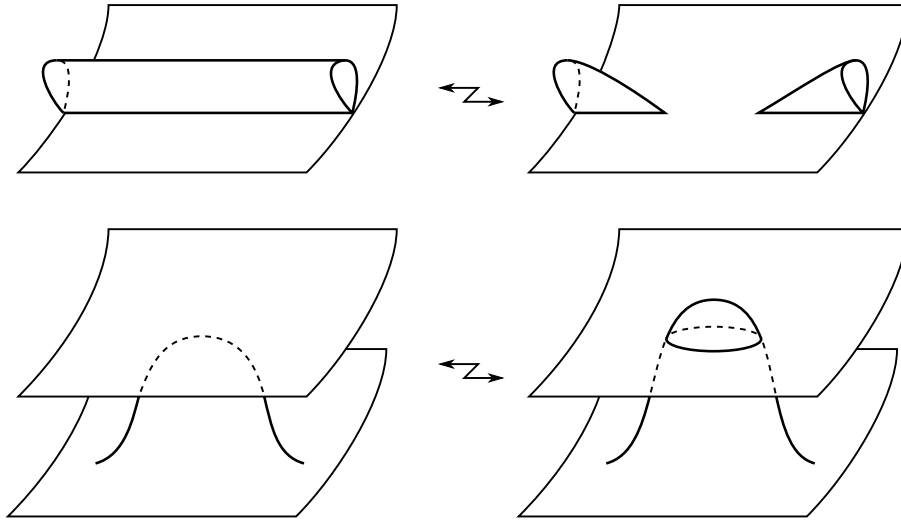


Figure 2.2: A pair of Roseman moves

Surface diagrams are not easy to visualize, having many singularities, so we often pass to a secondary tool for visualizing and studying link cobordisms, called *movies*.

Definition 2.1.5. A **movie** of a surface diagram $S : D_0 \rightarrow D_1$, representing a generic link cobordism $\Sigma : L_0 \rightarrow L_1$, is a finite sequence of diagrams, with successive pairs of diagrams related by a planar isotopy, Morse move, or Reidemeister move. Individual diagrams in the sequence are often called **frames**.

To obtain the frames of a movie, we use the following process. Let t_1, \dots, t_{m-1} be the critical points and singular points of S , as described above, ordered with respect to the interval factor of $\mathbb{R}^3 \times [0, 1]$. Then for each $i \in \{1, \dots, m-1\}$, the point t_i has a sufficiently small neighborhood $[t_i - \varepsilon(i), t_i + \varepsilon(i)]$ in which the diagrams $D_{t_i - \varepsilon(i)}$ and $D_{t_i + \varepsilon(i)}$ are related by a Morse move

or Reidemeister move. Additionally, each interval $[t_i + \varepsilon(i), t_{i+1} - \varepsilon(i+1)]$ describes an isotopy between $D_{t_i + \varepsilon(i)}$ and $D_{t_{i+1} - \varepsilon(i+1)}$. Let $t_0 = 0$ and $t_m = 1$. Then the desired movie is the sequence of diagrams corresponding to the points $\{t_0, t_i \pm \varepsilon(i), t_m\}$, which may be reindexed as $\{D_{t_i}\}_{i=0}^n$.

2.1.4 Movie moves

Movies associated to isotopic link cobordisms are related by a sequence of **movie moves**, which locally adjust the frames of a movie. A list of all necessary movie moves was given in [CS93, CRS97]. This list includes moves corresponding to the Roseman moves, mentioned above, as well as new moves which arise from the addition of a time function on the surface diagram. We list a few movie moves here.

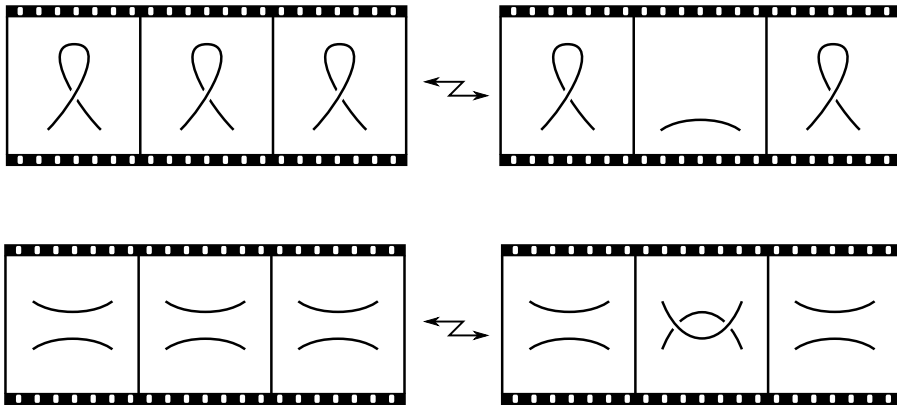


Figure 2.3: Movie moves corresponding to the Roseman moves in Figure 2.2.

2.1.5 Approaching link cobordisms practically

Link cobordisms and their surface diagrams are particularly useful from a theoretical perspective. We will later see that the important properties regarding maps on Khovanov homology are proven by understanding the subtle interplay between link cobordisms, surface diagrams, and movies. On the other hand, when we work with a link cobordism directly, this theory is not as relevant. In fact, we often define a link cobordism by working backwards through the process we have described; that is, we simply define a movie by constructing a sequence of diagrams with the desired properties of a movie. This induces a link cobordism: adjacent diagrams in the movie can be connected in $\mathbb{R}^2 \times [t_i, t_{i+1}]$ by the trace of the move through which they are related; stacking these (immersed) surfaces gives a surface in $\mathbb{R}^2 \times [0, 1]$; the result can be lifted into $\mathbb{R}^3 \times [0, 1]$ to remove any singularities, yielding a link cobordism.

2.2. Khovanov homology of links

Now that we have a strong foundational understanding of link cobordisms, we are ready to define Khovanov homology. We give the classical definition of Khovanov homology, first defined in [Kho00]. In particular, we will define the cube of resolutions for an oriented knot diagram, define and apply a topological quantum field theory \mathcal{G} , and finally, obtain a chain complex whose homology is the *Khovanov homology*. The reader may benefit from reading Appendices A and B, which review some relevant categories and discuss topological quantum field theories (tqft's).

2.2.1 Cube of resolutions

The cube of resolutions is an organized collection of objects and morphisms in the cobordism category Cob^3 (defined in Appendix A). The organization into a cube is not necessary, but it does anticipate the chain complex structure we will obtain. This is achieved in the following sections, where we show that a suitable tqft takes the cube of resolutions to a collection of modules and linear morphisms (objects and morphisms in Mod_R) that form a chain complex.

To begin, let L be an oriented link in \mathbb{R}^3 , represented by a diagram D with n crossings, of which n_+ are positive and n_- are negative ($n = n_+ + n_-$). Enumerate these crossings; we then refer to specific crossings by this enumeration as *the i th crossing* for some $1 \leq i \leq n$. We build the cube of resolutions for D through the process below; it is useful to refer to Figure 2.5 regularly, where we illustrate the cube of resolutions associated to a diagram of the positive trefoil.

Definition 2.2.1. A crossing \times in the diagram D can be **smoothed** by replacing it with a **0-smoothing** \succ or a **1-smoothing** \smile . The result of smoothing every crossing in D is a planar 1-manifold, which we call a **smoothing** of D .

A smoothing of D is an object in Cob^3 . Relative to the enumeration of the crossings in D , we may write a smoothing of D as a binary sequence

$$\sigma = (\sigma_1, \dots, \sigma_n) \tag{2.1}$$

where $\sigma_i \in \{0, 1\}$ indicates that the i th crossing is σ_i -smoothed. We refer to the smoothing and binary sequence interchangeably. One may check that our given diagram has 2^n possible smoothings. It is often convenient to record the value

$$|\sigma| = \sum_{i=1}^n \sigma_i \tag{2.2}$$

which records the number of 1-smoothings in σ .

Given a smoothing $\sigma = (\sigma_1, \dots, \sigma_n)$, we define a smoothing

$$\sigma^i = (\sigma_1, \dots, \sigma_{i-1}, 1, \sigma_{i+1}, \dots, \sigma_n) \quad (2.3)$$

which changes the i th smoothed crossing to a 1-smoothing. When $\sigma_i = 1$, we have $\sigma = \sigma^i$. Note that any pair of smoothings that differ in a single coordinate can be written as a pair σ, σ^i for some $1 \leq i \leq n$.

Definition 2.2.2. The pair of smoothings σ, σ^i are related by a **smoothing cobordism** $S_\sigma^i : \sigma \rightarrow \sigma^i$ which is a product cobordism away from the i th smoothed crossing, where it contains a saddle (illustrated in Figure 2.4).

A smoothing cobordism is a morphism in Cob^3 . We may record a smoothing cobordism as a sequence $S_\sigma^i = (\sigma_1, \dots, \sigma_{i-1}, \star, \sigma_{i+1}, \dots, \sigma_n)$ where the \star is used to indicate the index in which the 0-smoothing is changed to a 1-smoothing: for $\star = 0$, the binary sequence describes σ , and for $\star = 1$, it describes σ^i .

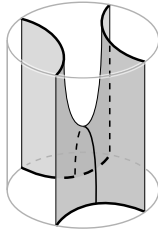


Figure 2.4: A local cobordism relating a 0-smoothing and 1-smoothing by a saddle.

The cube of resolutions is formed by noting that the smoothings of D resemble the corners of the n -cube $[0, 1]^n$ and the smoothing cobordisms resemble the cube's edges. Thus, one may visualize the cube of resolutions as a flattened cube in the plane. We have done this for the positive trefoil in Figure 2.5.

Definition 2.2.3. The **cube of resolutions** for a link diagram D is the collection of all possible smoothings of D and all possible smoothed cobordisms between them.

2.2.2 Choosing a topological quantum field theory

We now define a $(2+1)$ -dimensional tqft \mathcal{G} on Cob^3 using the procedure described in Appendix B. In particular, we construct a module A and linear maps on A , and we assign these to the necessary collection of objects and morphisms in Cob^3 in a way that guarantees the resulting tqft is well-defined.

Let R be a commutative ring with unity 1, and let A be a free, graded R -module of rank 2

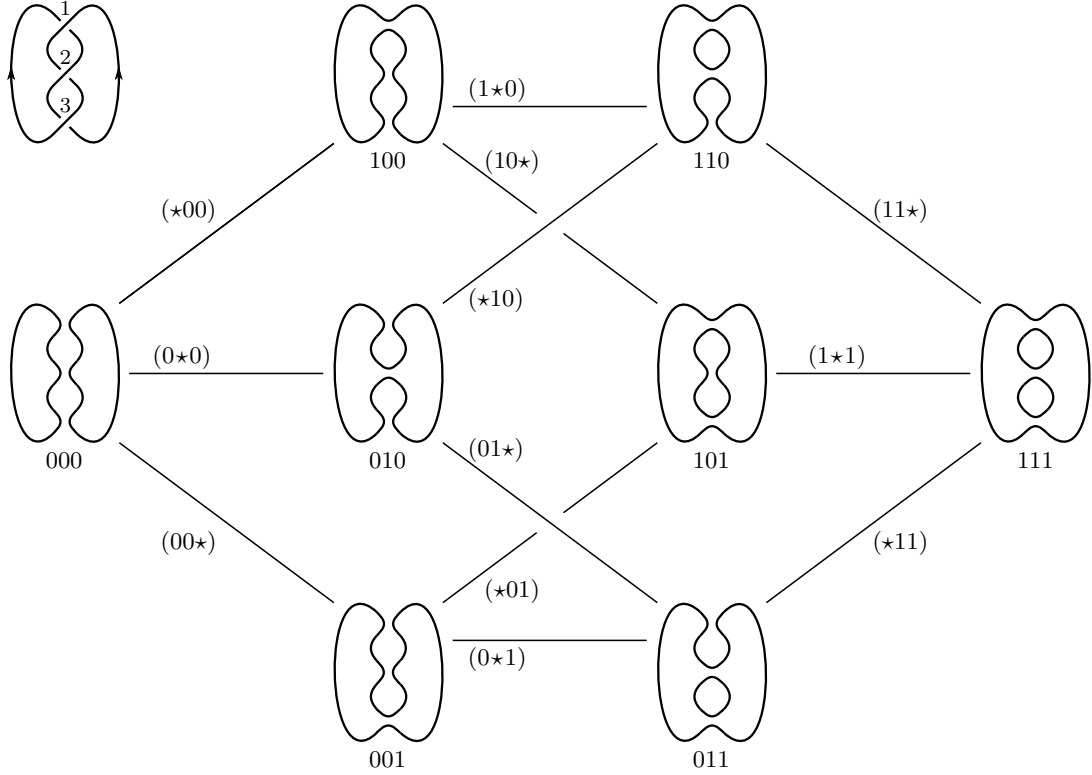


Figure 2.5: The cube of resolutions for the positive trefoil.

generated by $\mathbf{1}$ and \mathbf{x} , where $\deg(\mathbf{1}) = 1$ and $\deg(\mathbf{x}) = -1$. Extend this grading linearly across finite R -tensor products of A ; that is,

$$\deg(a_1 \otimes \cdots \otimes a_\ell) = \sum_{i=1}^{\ell} \deg(a_i) \quad a_i \in A \quad (2.4)$$

We equip A with an associative, commutative algebra structure with unit $\mathbf{1}$ and multiplication $m: A \times A \rightarrow A$ defined by

$$m(\mathbf{1}, \mathbf{1}) = \mathbf{1} \quad m(\mathbf{1}, \mathbf{x}) = m(\mathbf{x}, \mathbf{1}) = \mathbf{x} \quad m(\mathbf{x}, \mathbf{x}) = 0 \quad (2.5)$$

For notational convenience, we will occasionally write the multiplication as $m(a, b) = ab$. Note that by the universal property of tensor products, m extends uniquely to a map $m: A \otimes A \rightarrow A$. A unit map $\iota: R \rightarrow A$ is defined by

$$\iota(\mathbf{1}) = \mathbf{1} \quad (2.6)$$

We also equip A with a coalgebra structure with counit $\epsilon: A \rightarrow R$ defined by

$$\epsilon(\mathbf{1}) = 0 \quad \epsilon(\mathbf{x}) = 1 \quad (2.7)$$

and coassociative, cocommutative comultiplication $\Delta: A \rightarrow A \otimes A$ defined by

$$\Delta(\mathbf{1}) = (\mathbf{1} \otimes \mathbf{x}) + (\mathbf{x} \otimes \mathbf{1}) \quad \Delta(\mathbf{x}) = \mathbf{x} \otimes \mathbf{x} \quad (2.8)$$

The degrees of these maps are $\deg(m) = -1$, $\deg(\iota) = 1$, $\deg(\epsilon) = 1$, and $\deg(\Delta) = -1$.

To define \mathcal{G} on $\mathbf{ob}(\mathbf{Cob}^3)$, we set $\mathcal{G}(\bigcirc^\ell) = A^{\otimes \ell}$. To define \mathcal{G} on $\mathbf{mor}(\mathbf{Cob}^3)$, recall that it suffices to define $\mathcal{G}(S)$ for each of the fundamental cobordisms S in Appendix A. Using the shorthand given there, we define

$$\begin{aligned} \mathcal{G}(\bowtie) &= \epsilon & \mathcal{G}(\bigcirc\text{-}\bigcirc) &= m & \mathcal{G}(\text{id}) &= \text{id} \\ \mathcal{G}(\oplus) &= \Delta & \mathcal{G}(\text{perm}) &= \rho & \mathcal{G}(\otimes) &= \iota \end{aligned} \tag{2.9}$$

This definition of \mathcal{G} extends to a definition on an arbitrary morphism $S \in \mathbf{mor}(\mathbf{Cob}^3)$ by decomposing S as a composition $S = S_n \circ \cdots \circ S_1$ of local fundamental cobordisms and setting $\mathcal{G}(S) = \mathcal{G}(S_n) \circ \cdots \circ \mathcal{G}(S_1)$. By local we mean that each S_i can be expressed as a disjoint union of cylinders and one non-trivial fundamental cobordism \bowtie , $\bigcirc\text{-}\bigcirc$, \oplus , perm, or \otimes . In this form, we see that the map $\mathcal{G}(S_i)$ factors as a tensor product of morphisms acting on the factors of $A^{\otimes \ell}$. To ensure that this definition is well-defined, we must ensure that it does not depend on the decomposition of S . This is done by ensuring Equation 7.3 holds. We leave this as an exercise for the reader.

2.2.3 Applying a topological quantum field theory

We are now ready to apply our tqft \mathcal{G} to the cube of resolutions. Recall that the cube is a collection of objects and morphisms in \mathbf{Cob}^3 . Applying \mathcal{G} produces a collection of R -modules and R -linear maps in Mod_R , which we then turn into a chain complex in the next section.

To a smoothing $\sigma = (\sigma_1, \dots, \sigma_n)$, we associate an R -module

$$\mathcal{G}(\sigma) = A^{\otimes \ell} \tag{2.10}$$

where ℓ is the number of components in the smoothing. A generator of $\mathcal{G}(\sigma)$ is an element of the form $a_1 \otimes \cdots \otimes a_\ell$ where $a_i \in \{\mathbf{1}, \mathbf{x}\}$. We commonly denote these elements as α_σ .

To a smoothing cobordism $S_\sigma^i: \sigma \rightarrow \sigma^i$, we associate an R -linear map

$$\mathcal{G}(S_\sigma^i): A^{\otimes \ell} \rightarrow A^{\otimes \ell \pm 1} \tag{2.11}$$

that decomposes as a tensor product of identity maps id and exactly one m or Δ , depending on the type of saddle (note that this determines the number of factors in the codomain $A^{\otimes \ell \pm 1}$).

2.2.4 Khovanov chain complex

We are now ready to define the Khovanov chain complex. Applying the tqft \mathcal{G} to the cube of resolutions yielded a collection of R -modules $\mathcal{G}(\sigma)$ and R -linear maps $\mathcal{G}(S_\sigma^i)$. These objects and morphisms in Mod_R form their own cube, however, we must reorganize them to form a

chain complex.

To define the chain groups, we begin by assigning a bigrading to the generators α_σ of $\mathcal{G}(\sigma)$. These gradings are called the *homological grading* and *quantum grading*, respectively, and they draw on the values from Equations 2.2 and 2.4.

$$\mathbf{h}(\alpha_\sigma) = |\sigma| - n_- \quad (2.12)$$

$$\mathbf{q}(\alpha_\sigma) = \deg(\alpha_\sigma) + h(\alpha_\sigma) + n_+ - n_- \quad (2.13)$$

The shift by n_\pm ensures the gradings are invariant under Reidemeister moves, which we will care about later. With respect to the homological grading, we will form a (co)chain complex, as in the following definition.

Definition 2.2.4. Let D be a diagram for an oriented link, and let \mathcal{D} be the set of all smoothings of this diagram. The R -module

$$\mathcal{C}(D) := \bigoplus_{\sigma \in \mathcal{D}} \mathcal{G}(\sigma)$$

is called the **Khovanov chain group** associated to D .

The Khovanov chain group is notoriously bigraded, and with respect to the homological grading, it will form a cochain complex. We highlight the homological grading with

$$\mathcal{C}^h(D) = \bigoplus_{\{\sigma \in \mathcal{D} \mid \mathbf{h}(\sigma) = h\}} \mathcal{G}(\sigma) \quad (2.14)$$

This allows us to express the Khovanov chain group with an equivalent definition, as a graded R -module:

$$\mathcal{C}(D) = \bigoplus_{h=1}^n \mathcal{C}^h(D) \quad (2.15)$$

Incorporating the quantum grading, we have a bigraded R -module

$$\mathcal{C}^{h,q}(D) = \{\alpha_\sigma \in \mathcal{C}^h(D) \mid \mathbf{q}(\alpha_\sigma) = q\}$$

To define a (co)differential on $\mathcal{C}^h(D)$, we will combine all maps $\mathcal{G}(S_\sigma^i)$ associated to a smoothing σ with $\mathbf{h}(\sigma) = h$. As this ranges over multiple smoothings σ , and each smoothing has multiple associated smoothing cobordisms S_σ^i ranging over admissible i , we will first collect all of the maps leaving a fixed smoothing $\mathcal{G}(\sigma)$. Namely, we set

$$d_\sigma := \bigoplus_{\{i \mid \sigma_i \neq 1\}} (-1)^{\xi_\sigma^i} \mathcal{G}(S_\sigma^i) \quad (2.16)$$

where $\xi_\sigma^i = \sum_{j < i} \sigma_j$. This sign adjustment ensures we obtain a chain complex (the reader is encouraged to verify $d \circ d = 0$). The differential is then defined by the following.

Definition 2.2.5. For a diagram D of an oriented link, the **Khovanov differential**

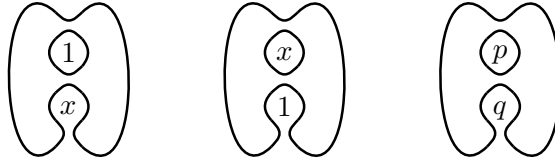


Figure 2.6: Left, center: labeled smoothings for the (110) smoothing of the positive trefoil from Figure 2.5. Right: a pqr -chain representing the sum of the two labeled smoothings to the left.

$d^h: \mathcal{C}^h(D) \rightarrow \mathcal{C}^{h+1}(D)$ is the R -linear map

$$d^h := \bigoplus_{\{\sigma \mid \mathbf{h}(\sigma)=h\}} d_\sigma$$

The pair $(\mathcal{C}(D), d)$ is called the **Khovanov chain complex** of D .

2.2.5 Labeled smoothings

The above definition of the Khovanov chain complex is certainly adequate, however, the author never found it very intuitive. We present a more visual approach here. Recall that a generator in $\mathcal{G}(\sigma)$ is an element of the form $\alpha_\sigma = a_1 \otimes \cdots \otimes a_\ell$ for $a_i \in \{\mathbf{1}, \mathbf{x}\}$. We can visualize α_σ as a labeling of each of the ℓ connected components of σ with their corresponding generator a_i of A . This motivates the following definition.

Definition 2.2.6. For a generator $\alpha_\sigma = a_1 \otimes \cdots \otimes a_\ell$ of $\mathcal{C}(\sigma)$, a **labeled smoothing** of σ is a decoration of the components of σ with their corresponding generators $a_i \in \{\mathbf{1}, \mathbf{x}\}$ from A , which we call **labels**.

We will use the generator α_σ and its corresponding labeled smoothing interchangeably. This allows us to use α_σ algebraically as an element of $A^{\otimes \ell}$ while also being able to visualize and depict it as a decorated smoothing, as in the following figure.

Labeled smoothings and the differential The definition of $\mathcal{G}(S_\sigma^i)$ is easier to internalize by thinking in terms of labeled smoothings: applying the map $\mathcal{G}(S_\sigma^i)$ to a labeled smoothing α_σ will:

- locally alter the smoothing σ by changing the i th smoothed crossing from a 0-smoothing to a 1-smoothing, yielding σ^i ;
- adjust the labels on α_σ corresponding to the component(s) within the smoothing-change by applying the map m or Δ (depending on the number of components) and relabeling the new component(s) in σ^i with the resulting label(s);
- preserve all other connected components of σ and their labels.

On a general element in $\mathcal{G}(\sigma)$, this map factors linearly onto each labeled smoothing.

Similarly, the definition of d^h is easier to internalize with labeled smoothings: applying the map d^h to a labeled smoothing α_σ repeats the process (above) of applying $\mathcal{G}(S_\sigma^i)$ to α_σ for all i where $\sigma_i \neq 1$. The resulting collection of labeled smoothings is then combined as a sum. This allows us to easily determine when a labeled smoothing is a cycle, as in the following proposition.

Proposition 2.2.7. *A labeled smoothing α_σ is a cycle if and only if every 0-smoothing merges a pair of distinct, x -labeled components on σ .*

Labeled smoothings and pqr -chains The visual appeal of labeled smoothings begins to break down when we consider a general element in the Khovanov chain complex $\mathcal{C}(D)$, which may contain many generators. For this purpose, it is helpful to build a shorthand for a certain class of elements in $\mathcal{C}(D)$, called pqr -chains.

We give a very algebraic definition of these chains below, but to better visualize them, one may think of them as follows. A pqr -chain is a decorated smoothing whose labels consist of $\mathbf{1}$'s, \mathbf{x} 's, and some number of letters p_1, \dots, p_m . For each letter p_i , we create a new labeled smoothing by changing each letter to a label: $p_i = 1$ and $p_{j \neq i} = \mathbf{x}$. We then collect each of these labeled smoothings into a sum, which we also refer to as the pqr -chain. For example, we illustrate a pqr -chain in Figure 2.6 as a labeling of a smoothing (right), which is interpreted as a sum of labeled smoothings. Alternatively, we have the following algebraic definition.

Definition 2.2.8. A pqr -chain is a finite sum of labeled smoothings α_σ of the form

$$\sum_{j=1}^{\ell} a_{1,j} \otimes \cdots \otimes a_{\ell,j}$$

for which there is a subset $K \subset \{1, \dots, \ell\}$ such that for each $k \in K$,

$$\bullet a_{k,j} = \begin{cases} \mathbf{1} & \text{if } j = k \\ \mathbf{x} & \text{if } j \in K \text{ and } j \neq k \\ 0 & \text{if } j \notin K \end{cases}$$

$$\bullet a_{i,j} = a_{i,j'} \text{ for all } i \notin K \text{ and } 1 \leq j, j' \leq \ell.$$

For example, a pqr -chain on a smoothing σ with ℓ components might take the form

$$(\mathbf{1} \otimes \mathbf{x} \otimes \mathbf{1} \otimes \mathbf{x} \otimes \mathbf{x}) + (\mathbf{x} \otimes \mathbf{x} \otimes \mathbf{1} \otimes \mathbf{1} \otimes \mathbf{x}) + (\mathbf{x} \otimes \mathbf{x} \otimes \mathbf{1} \otimes \mathbf{x} \otimes \mathbf{1})$$

Here we have $K = \{1, 4, 5\}$. The convenience of pqr -chains comes from the fact that they are labelings on a common smoothing, and as a result, can be visualized as a single labeling of this smoothing: for each $1 \leq j \leq \ell$, if $j \in K$, label the j th loop with a letter of the alphabet; if $j \notin K$, label the j th loop with its unique label $a_{j,\star}$. We can extend this notation further: if the letter we use on a loop is capitalized, we make the corresponding summand negative. We will

use this notation throughout the dissertation; for reference, the first occurrence is in Figure 4.2.

2.2.6 Khovanov homology

The Khovanov chain complex produces homology groups in the usual way, by setting

$$\mathcal{H}^h(D) = \ker(d^h)/\text{im}(d^{h-1})$$

So far, we do not have an excellent way of thinking of elements in $\ker(d^h)$ or $\text{im}(d^{h-1})$, although Proposition 2.2.7 is somewhat useful. This makes visualizing elements in $\mathcal{H}^h(D)$ difficult, but one can go a long way by simply working with elements in the chain complex $\mathcal{C}^h(D)$. In any case, we have the following definition.

Definition 2.2.9. For a diagram D of an oriented link, the homology groups $\mathcal{H}(D)$ of the Khovanov chain complex $(\mathcal{C}(D), d)$ are called the **Khovanov homology** of D .

These groups are finitely-generated and bigraded via the bigrading on the chain groups. One important aspect of Khovanov homology groups is that they form a link invariant, in the sense of the following two results (these results are proven by examining the maps on Khovanov homology induced by Reidemeister moves, which we discuss in the next section).

Theorem 2.2.10 ([Kho00]). *Any pair of diagrams $D_{0,1}$ representing isotopic links $L_{0,1}$ have quasi-isomorphic Khovanov chain complexes $\mathcal{C}(D_0) \simeq \mathcal{C}(D_1)$, and therefore, isomorphic Khovanov homology groups $\mathcal{H}(D_0) \cong \mathcal{H}(D_1)$.*

As a result, one can talk about the Khovanov homology associated to a link, in the sense that a link L has an associated quasi-isomorphism class $\mathcal{C}(L)$ of chain complexes $\mathcal{C}(D)$, taken over all diagrams D representing any link isotopic to L . Similarly, we may consider the isomorphism class $\mathcal{H}(L)$ of homology groups $\mathcal{H}(D)$. This notation is, however, not conventional and goes against the standard notation throughout the literature, where $\mathcal{C}(L)$ and $\mathcal{H}(L)$ are used *in place* of $\mathcal{C}(D)$ and $\mathcal{H}(D)$, with the choice of diagram D being understood from context. We adopt this convention, for consistency.

2.3. Khovanov homology of link cobordisms

In this section, we discuss the link cobordism induced maps on Khovanov homology. We begin by discussing their construction [Kho00] and their up-to-sign equivalence under boundary-preserving isotopy [Jac04]. Our future calculations will rely on explicit computations of these induced maps, so we record the isotopy, Morse, and Reidemeister induced maps, as calculated in

[BN05]. We conclude by discussing the invariance of these maps under local knotting (connect summing with a knotted 2-sphere).

2.3.1 Cobordism induced maps on Khovanov homology

In [Kho00], it was shown that a link cobordism $\Sigma: L_0 \rightarrow L_1$, represented by a surface diagram $S: D_0 \rightarrow D_1$, induces a bigraded chain map

$$\mathcal{C}(\Sigma): \mathcal{C}^{h,q}(D_0) \rightarrow \mathcal{C}^{h,q+\chi(\Sigma)}(D_1) \quad (2.17)$$

with induced R -linear map $\mathcal{H}(\Sigma): \mathcal{H}(D_0) \rightarrow \mathcal{H}(D_1)$ that is similarly bigraded. We recall the definition of this chain map here. First, recall that a surface diagram has an associated movie $\{D_{t_i}\}_{i=1}^n$, where adjacent frames D_{t_i} and $D_{t_{i+1}}$ are related by an isotopy, Morse move, or Reidemeister move. We define a chain map for each of these relations. A planar isotopy induces the expected chain map: on a labeled smoothing α_σ , the isotopy is performed on σ and the labels from α_σ are preserved for each component in σ throughout the isotopy. A Morse move induces the chain map that it was assigned in Equation 2.9 by the tqft defining the Khovanov chain complex. The reader is encouraged to check that any Morse move that changes the Euler characteristic $\chi(\Sigma)$ will equally change the homological grading. Finally, a Reidemeister move induces a quasi-isomorphism on the relevant chain complexes; note that we have not yet defined such quasi-isomorphisms explicitly, however, we will do this the following section (for now, it is enough that such maps exist). Thus, there is an associated chain map $\mathcal{C}(D_{t_i}) \rightarrow \mathcal{C}(D_{t_{i+1}})$ between any adjacent pair of frames in the movie. The map $\mathcal{C}(\Sigma)$ is the composition of all such maps, and it induces the map $\mathcal{H}(\Sigma)$.

Definition 2.3.1. For a movie $\{D_{t_i}\}_{i=0}^n$ representing a link cobordism $\Sigma: L_0 \rightarrow L_1$, we call the associated chain map $\mathcal{C}(\Sigma): \mathcal{C}(D_0) \rightarrow \mathcal{C}(D_1)$ the **induced chain map** for Σ .

The induced chain map depends entirely on the choice of movie (or equivalently, the choice of surface diagram), which fixes a (co)domain for the map. A different surface diagram has an entirely distinct induced chain map, and therefore, we study a link cobordism with a fixed projection $\mathbb{R}^3 \times [0, 1] \rightarrow \mathbb{R}^2 \times [0, 1]$ in mind (and when studying multiple link cobordisms, we use a consistent same projection). For this reason, it is often convenient to occasionally include the surface diagram in the notation for the induced map: a link cobordism Σ represented by surface diagram S induces the chain map $\mathcal{C}_S(\Sigma)$.

Remark 2.3.2. One might ask to what extent the induced chain maps associated to distinct

surface diagrams differ: for a link cobordism $\Sigma: L \rightarrow L'$ represented by surface diagrams $S_{0,1}: D_{0,1} \rightarrow D'_{0,1}$, do the Reidemeister induced maps $\rho_{0,1}: D_{0,1} \rightarrow D'_{0,1}$ produce an up-to-sign commutative diagram:

$$\begin{array}{ccc} \mathcal{C}(D_0) & \xrightarrow{\rho_0} & \mathcal{C}(D'_0) \\ \downarrow c_S(\Sigma) & & \downarrow c_{S'}(\Sigma) \\ \mathcal{C}(D_1) & \xrightarrow{\rho_1} & \mathcal{C}(D'_1) \end{array}$$

As far as the author is aware, this need not hold in general. Moreover, it is not overly important for it to hold, as we tend to study the induced chain maps with respect to a specific surface diagram, as we have just mentioned. We will see later that this property does hold for specific link cobordisms and specific classes of Reidemeister moves (Proposition 3.3.2).

The potential significance of the induced chain maps associated to a link cobordism were first noted within [Kho00], where they were conjectured to be invariant under isotopy of Σ . This conjecture was made while working over the coefficient group $R = \mathbb{Z}[c]$, and it was later shown that, in this case, the conjecture does not hold [Jac03]. It was later shown that the conjecture also doesn't hold under ambient isotopy [Jac04], however, the same work proved that the conjecture holds when we restrict to boundary-preserving isotopy and work over $R = \mathbb{Z}$, as in the following theorem. From here, we use $R = \mathbb{Z}$.

Theorem 2.3.3 ([Jac04]). *For a link cobordism $\Sigma: L_0 \rightarrow L_1$, with boundary links represented by diagrams D_0 and D_1 , the chain map*

$$\mathcal{C}(\Sigma): \mathcal{C}(D_0) \rightarrow \mathcal{C}(D_1)$$

is invariant, up to sign and up to chain homotopy, under smooth isotopy of Σ fixing $\partial\Sigma$ setwise; as a result, the induced map $\mathcal{H}(\Sigma): \mathcal{H}(D_0) \rightarrow \mathcal{H}(D_1)$ is invariant, up to sign, under boundary-preserving isotopy of Σ .

This theorem is proven by first recalling that movies for isotopic link cobordisms $\Sigma_0 \simeq \Sigma_1$ are related by a sequence of movie moves. It is then shown that the mini-movies describing each movie move induce equivalent chain maps, up to chain homotopy and up to sign. Thus, the sequence of movie moves between movies for Σ_0 and Σ_1 induces a sequence of chain homotopies between the maps induced by those movies, as desired.

2.3.2 Explicit induced maps

We now define the chain maps induced by planar isotopy, Morse moves, and Reidemeister moves, which we used in the previous section to define the induced maps on Khovanov homology. In particular, we focus on an explicit definition of the Reidemeister induced maps, as planar isotopy and Morse induced maps have been defined.

Isotopy induced chain maps The chain map induced by a planar isotopy of diagrams is defined on a labeled smoothing α_σ by applying the isotopy to the underlying smoothing σ and preserving the labels from α_σ throughout this isotopy.

Ornaments We pause to develop a convenient shorthand based on [BN05]. The Morse and Reidemeister moves only change a diagram locally within some tangle. As a result, for a labeled smoothing α_σ , it suffices to define the induced chain maps on the portion of α_σ within this tangle, while leaving the rest of the labeled smoothing unchanged. In order to properly define the chain map, we must account for all possible smoothings of the tangle, as well as all possible labels for each smoothing. As a result, it is convenient to have a shorthand that simplifies the amount of information necessary to express these maps. The idea is to reduce the definition to the level of smoothings by defining a set of local *ornaments* that can be placed on a smoothing, each of which corresponds to a predetermined chain map on the portion of the smoothing it adorns. A chain map can then be defined on all possible labelings of a smoothing σ by simply decorating σ with these ornaments: to any given labeled smoothing α_σ , apply each of the predetermined chain maps corresponding to the ornaments decorating σ .

The ornaments we need correspond, perhaps not surprisingly, to the three Morse moves: births, deaths, and saddles. These decorations were described in Appendix A, and we have used them in defining the tqft \mathcal{G} , however, we recall them here for completeness. A birth will locally add a crossingless unknot to an empty tangle; we decorate a smoothing with the ornament \odot consisting of a crossingless unknot with 4 external antennae to indicate this addition. Similarly, a death removes a crossingless unknot, in which case we decorate the smoothing with the ornament \oslash consisting of 4 internal antennae adorning the component being removed. A saddle acts on a tangle with two unknotted arcs \succ by either merging or splitting the component(s) to which the arcs belong; in either case, the result is a tangle $\succ\langle$. We decorate the smoothing with the ornament $\succ\langle$ consisting of a thin line that perpendicularly intersects the two components being merged or split.

Morse Move	Ornament	Chain Map	Definition of chain map
Birth	\otimes	ι	$1 \mapsto \begin{array}{c} \textcircled{1} \\ \textcircled{} \end{array}$
Death	\oslash	ϵ	$\begin{array}{c} \textcircled{1} \\ \textcircled{} \end{array} \mapsto 0$ $\begin{array}{c} \textcircled{x} \\ \textcircled{} \end{array} \mapsto 1$
Saddle	\bowtie	m	$\begin{array}{c} \textcircled{1} \\ \textcircled{1} \end{array} \mapsto \begin{array}{c} \textcircled{1} \\ \textcircled{} \end{array}$ $\begin{array}{c} \textcircled{1} \\ \textcircled{x} \end{array} \mapsto \begin{array}{c} \textcircled{x} \\ \textcircled{} \end{array}$ $\begin{array}{c} \textcircled{x} \\ \textcircled{1} \end{array} \mapsto \begin{array}{c} \textcircled{x} \\ \textcircled{} \end{array}$ $\begin{array}{c} \textcircled{x} \\ \textcircled{x} \end{array} \mapsto 0$
		Δ	$\begin{array}{c} \textcircled{1} \\ \textcircled{} \end{array} \mapsto \begin{array}{c} \textcircled{1} \\ \textcircled{x} \end{array} + \begin{array}{c} \textcircled{x} \\ \textcircled{1} \end{array}$ $\begin{array}{c} \textcircled{x} \\ \textcircled{} \end{array} \mapsto \begin{array}{c} \textcircled{x} \\ \textcircled{} \end{array}$

Table 2.1: The chain maps induced by Morse moves.

The chain maps induced by each ornament was defined in Equations 2.5-2.8. We also state them here (Table 2.1) to see how they act locally on a labeled smoothing.

One additional decoration \blacktriangleright will be needed to define the Reidemeister induced maps, consisting of a dot on any component of the smoothing. This decoration indicates the application of two saddles (one splitting and then one re-merging) on the decorated component. Using Table 2.1, one can verify that the map induced by this local cobordism kills an x -labeled arc, but sends a 1-labeled arc to twice an x -labeled arc.

Morse induced chain maps The chain map induced by a Morse move is defined on a labeled smoothing α_σ by decorating the smoothing σ with the ornament corresponding to the given Morse move.

Reidemeister induced chain maps The chain map induced by a Reidemeister move is defined on a labeled smoothing α_σ by decorating the smoothing σ with the ornaments given in Tables 2.2-2.7. Note that the Reidemeister III induced maps, given in Tables 2.4-2.7, are defined on a given labeled smoothing α_σ by finding the correct smoothing in the leftmost column and applying the sum of maps in the corresponding row. We use I to denote an isotopy; empty cells correspond to the 0 map.

As any given decoration can consist of multiple ornaments, there is a natural question of the order in which the corresponding chain maps should be applied; this will either be irrelevant (i.e., the moves and their induced maps commute) or clear from context (e.g., a dotted arc on a birth requires the birth to occur before the map induced by the dotted arc can be applied).

Remark 2.3.4. Note the $\frac{1}{2}$ in the definition of the Reidemeister I induced chain map in Table 2.2 does not conflict with \mathbb{Z} as our coefficient group: the dotted arc will always produce an even coefficient, so overall, the map will maintain an integral coefficient.

2.3.3 Local knotting

A link cobordism is *locally knotted* if it can be written as $\Sigma \# S$ for a surface Σ and a knotted 2-sphere $S \subset \mathbb{R}^3 \times [0, 1]$. Locally knotting a surface will generally change the boundary-preserving isotopy class of the surface. As such, we tend to omit this operation from consideration, and consider the equivalence classes of surfaces in the 4-ball up to boundary-preserving isotopy and up to local knotting. In order for an invariant to distinguish these classes of surfaces, it must be invariant under both boundary-preserving isotopy and local knotting. We have already seen that the induced maps on Khovanov homology are invariant under boundary-preserving isotopy (Theorem 2.3.3), therefore, we wish to guarantee they are also invariant under local knotting.

Theorem 2.3.5. *The cobordism induced maps on Khovanov homology are invariant under local*

knotting: given a link cobordism $\Sigma : L_0 \rightarrow L_1$ and a knotted 2-sphere S , the induced maps $\mathcal{H}(\Sigma)$ and $\mathcal{H}(\Sigma \# S)$ agree up to multiplication by ± 1 .

Proof. The case $L_0 = \emptyset$ was first established in [SS21], and this argument can be adapted to the case where $L_0 \neq \emptyset$. Let B be a 4-ball intersecting $\Sigma \# S$ along the disk $S \setminus \mathring{D}^2$ bounded by an unknot U in $\partial B \cong S^3$. We may perform a boundary-preserving isotopy of $\Sigma \# S$ that drags B near L_0 . It then suffices to show that locally knotting the product cobordism $C : L_0 \rightarrow L_0$ induces the identity map. We can isolate B so that $C \# S$ decomposes into a link cobordism $C \sqcup (S \setminus \mathring{D}^2) : L_0 \rightarrow L_0 \sqcup U$ followed by a saddle merging L_0 and U . By [SS21, Theorem 4.2], which is also proven in this dissertation as Theorem 5.2.2, the map induced by $S \setminus \mathring{D}^2$ is identical to the map induced by the link cobordism induced by a standard D^2 in B . Moreover, the map on Khovanov homology induced by a split cobordism will split as the tensor product of the individual cobordism-induced maps, so $C \sqcup (S \setminus \mathring{D}^2)$ induces the same map as $C \sqcup D^2$. Stacking the saddle on the latter cobordism yields a surface isotopic to C rel boundary, so by Theorem 2.3.3 they induce the same map, as desired. \square

Reidemeister Move	Smoothing	Chain Map
		0
		$\frac{1}{2} \left(\text{circle with loop on right and dot on left} - \text{circle with loop on right and dot on right} \right)$
		0
		$\frac{1}{2} \left(\text{circle with loop on right and dot on left} - \text{circle with loop on right and dot on right} \right)$
		0

Table 2.2: The chain maps induced by Reidemeister I moves.

Reidemeister Move	Smoothing	Chain Map
		$- \text{circle with two small circles between them}$
		0
		0

Table 2.3: The chain maps induced by Reidemeister II moves.

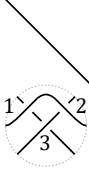
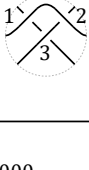

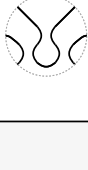



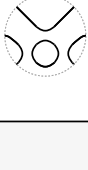


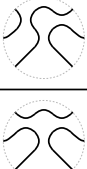
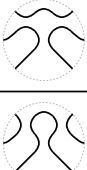





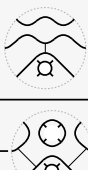
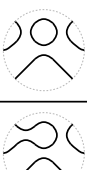


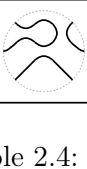
		000	100	010	001	110	101	011	111
									
000		<i>I</i>							
100			<i>I</i>		<i>-I</i>				
010				<i>I</i>					
001									
110						<i>I</i>			
101								<i>I</i>	
011									
111									

Table 2.4: The chain map induced by one of the Reidemeister III moves.

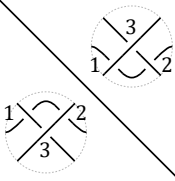
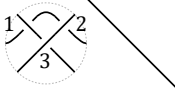



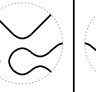
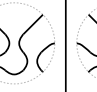
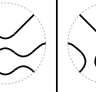
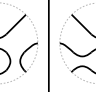






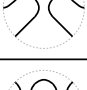



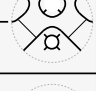
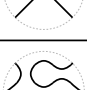
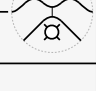

		000	100	010	001	110	101	011	111
									
000		<i>I</i>							
100									
010				<i>-I</i>	<i>I</i>				
001			<i>I</i>						
110						<i>I</i>			
101									
011							<i>I</i>		
111									

Table 2.5: The chain map induced by one of the Reidemeister III moves, equivalent up to isotopy, to the move in Table 2.4.

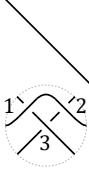
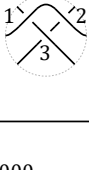
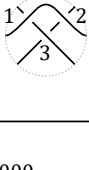

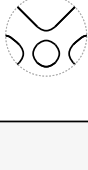



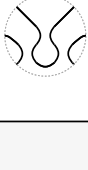



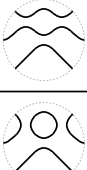
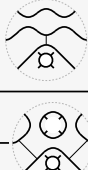





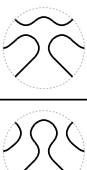
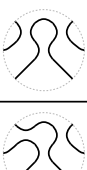
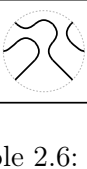
		000	100	010	001	110	101	011	111
									
000									
100			 I						
010			 I	 I					
001					I				
110								I	
101							I		
011								I	
111									$-I$

Table 2.6: The chain map induced by one of the Reidemeister III moves.

	000	100	010	001	110	101	011	111
000								
100								
010			I					
001					I			
110						I		
101						I		
011					I			
111								$-I$

Table 2.7: The chain map induced by one of the Reidemeister III moves, equivalent up to isotopy, to the move in Table 2.6.

Chapter 3: Maps induced by surfaces in the 4-ball

The main purpose of this dissertation is to distinguish pairs of surfaces in the 4-ball up to boundary-preserving isotopy through the 4-ball, and we do this by showing that these surfaces induce distinct maps on Khovanov homology. When taken literally, this approach is ill-conceived: surfaces in B^4 are not the same as link cobordisms in $\mathbb{R}^3 \times [0, 1]$, and isotopy of these surfaces in either setting is, a priori, unique to their ambient manifold. This chapter addresses the interplay between isotopy of surfaces in B^4 and the link cobordisms they induce in $S^3 \times [0, 1]$ and $\mathbb{R}^3 \times [0, 1]$.

In Section 3.1, we discuss the extension of Khovanov homology to link cobordisms in $S^3 \times [0, 1]$. In Section 3.2, we show that a surface in B^4 induces a link cobordism in $S^3 \times [0, 1]$, and this association preserves boundary-preserving isotopy classes: surfaces in B^4 are isotopic if and only if their induced link cobordisms in $S^3 \times [0, 1]$ are isotopic. Finally, Section 3.3 discusses the diagram dependence of the maps induced by surfaces in the 4-ball.

3.1. Extending to $S^3 \times [0, 1]$

The entirety of Chapter 2 can *almost* be repeated verbatim with S^3 replacing \mathbb{R}^3 . We summarize the differences here. Let $S^3 = \mathbb{R}^3 \cup \{\infty\}$. Note that a link cobordism in $S^3 \times [0, 1]$, defined by replacing \mathbb{R}^3 with S^3 in Definition 2.1.1, will generically miss the arc $\{\infty\} \times [0, 1]$, inducing a link cobordism in $\mathbb{R}^3 \times [0, 1]$. Thus, we may extend the definition of Khovanov homology to links and link cobordisms: to a link in S^3 we can associate the Khovanov homology of the link in $S^3 \setminus \{\infty\} = \mathbb{R}^3$, and to a link cobordism in $S^3 \times [0, 1]$ we can associate the map on Khovanov homology induced by the associated link cobordism in $(S^3 \times [0, 1]) \setminus (\{\infty\} \times [0, 1]) = \mathbb{R}^3 \times [0, 1]$. Note that this is only possible for a *fixed* link cobordism in $S^3 \times [0, 1]$.

The sticky point is when we consider isotopy of link cobordisms in $S^3 \times [0, 1]$, as they do not generally induce isotopies in $\mathbb{R}^3 \times [0, 1]$. In particular, a generic isotopy will not necessarily miss the arc $\{\infty\} \times [0, 1]$. Fortunately, there is the only additional isotopy we need to consider. A link cobordism in $S^3 \times [0, 1]$ can still be represented by a surface diagram in $\mathbb{R}^2 \times [0, 1]$ (through the link cobordism it induces in $\mathbb{R}^3 \times [0, 1]$), and the surface diagrams associated to a pair of

isotopic link cobordisms in $S^3 \times [0, 1]$ are related by a sequence of Carter-Rieger-Satio moves (see Section 2.1.4) and one additional *sweep-around-move*, illustrated in Figure 3.1. This additional move was first addressed in [MWW21], with the purpose of creating a functorial link homology theory for links in $S^3 \times [0, 1]$. In particular, they prove that the movies for the sweep-around move induce identity maps on Khovanov-Rozansky homology; later work reproved this theorem for the Bar-Natan and Lee deformations of Khovanov homology, as well as the undeformed Khovanov homology we use here [LS21]. We summarize this in the following theorem.

Theorem 3.1.1. *The maps on Khovanov homology are invariant under the isotopy described in the sweep-around-move, i.e. they associate the identity map to this movie.*

As a result, Theorem 2.3.3 holds for link cobordisms in $S^3 \times [0, 1]$, implying that Khovanov homology is functorial over link cobordisms in $S^3 \times [0, 1]$.

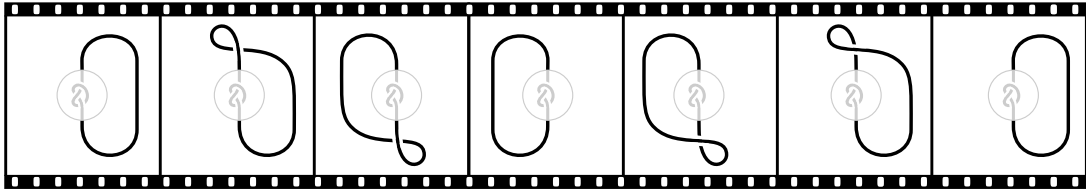


Figure 3.1: The additional *sweep-around-move* on movies of surfaces in $S^3 \times [0, 1]$.

3.2. Induced link cobordisms and induced maps

In this section, we extend Khovanov homology to surfaces in B^4 , much like the previous section did for $S^3 \times [0, 1]$. As we have done previously, we view the 4-ball as a quotient space $B^4 = (S^3 \times [0, 1]) / (S^3 \times \{0\})$ with center $\mathbf{0} = \pi(S^3 \times \{0\})$. A smooth, compact, oriented surface properly embedded in B^4 will miss the center, inducing a link cobordism in $B^4 \setminus N(\mathbf{0}) \cong S^3 \times [0, 1]$. More importantly, a generic isotopy of such surfaces will also miss the neighborhood of a point in the complement of the surface, inducing an isotopy between the associated link cobordisms in $S^3 \times [0, 1]$. We make this precise below.

Let E be a smooth, compact, oriented surface that is properly embedded in B^4 and has boundary link $L = \partial E$ in the boundary $S^3 = \partial B^4$. For any point $p \in (B^4 \setminus E)^\circ$, there is a neighborhood $N(p)$ missing E (by compactness), with which we have $B^4 \setminus \overset{\circ}{N}(p) \cong S^3 \times [0, 1]$. The image of E under this identification is a link cobordism $\Sigma: \emptyset \rightarrow L$.

Definition 3.2.1. For a smooth, compact, oriented surface E that is properly embedded in the 4-ball, the link cobordism $\Sigma: \emptyset \rightarrow L$ produced in the previous paragraph is called the **induced**

link cobordism of E .

As in the previous section, we may then associate the Khovanov homology of the induced link cobordism to the surface E , as in the following definition.

Definition 3.2.2. For a link cobordism $\Sigma: \emptyset \rightarrow L$ induced by a surface E in the 4-ball, the associated map on the Khovanov chain complex $\mathcal{C}(\Sigma): \mathbb{Z} \rightarrow \mathcal{C}(L)$ is called the **induced chain map** associated to E , and the map it induces on Khovanov homology $\mathcal{H}(\Sigma): \mathbb{Z} \rightarrow \mathcal{H}(L)$ is called the **induced map** on Khovanov homology associated to E .

Previously, we saw that in order to extend from $\mathbb{R}^3 \times [0, 1]$ to $S^3 \times [0, 1]$, we needed to consider an additional sweep-around-move. This was because an isotopy of link cobordisms in $S^3 \times [0, 1]$ did not necessarily induce an isotopy in $\mathbb{R}^3 \times [0, 1]$. Fortunately for the case at hand, an isotopy of surfaces in B^4 *does* induce an isotopy of the corresponding link cobordisms in $S^3 \times [0, 1]$.

Proposition 3.2.3. *A pair of surfaces $E_{0,1}$ in the 4-ball are isotopic rel boundary in the 4-ball if and only if their induced link cobordisms $\Sigma_{0,1}$ in $S^3 \times [0, 1]$ are isotopic rel boundary in $S^3 \times [0, 1]$.*

Corollary 3.2.4. *The induced map on Khovanov homology associated to a surface in the 4-ball is invariant, up to sign, under boundary-preserving isotopy of the surface.*

Remark 3.2.5. Put more generally, Khovanov homology is a functorial link homology theory for surfaces in the 4-ball. This is, however, somewhat misleading, since we have not defined a category of surfaces in the 4-ball. One could, perhaps, consider the category whose objects are surfaces in the 4-ball up to boundary-preserving isotopy, and whose morphisms are link cobordisms $\Sigma: L \rightarrow L'$ in $S^3 \times [0, 1]$, applied to a surface $E: \emptyset \rightarrow -L$ by composition $\Sigma \circ E: \emptyset \rightarrow L'$ (that is, by attaching a collar containing Σ to B^4 that stacks Σ onto E).

Proof of 3.2.4. Suppose that $E_{0,1}$ are surfaces in the 4-ball having distinct induced maps on Khovanov homology, up to sign. We will show $E_{0,1}$ are not isotopic surfaces relative to their boundary. As the induced maps are distinct, the induced link cobordisms $\Sigma_{0,1}$ are not isotopic rel boundary in $S^3 \times [0, 1]$ (by Theorem 2.3.3, extended to $S^3 \times [0, 1]$ in the previous section). Surfaces in the 4-ball whose induced link cobordisms are distinct in $S^3 \times [0, 1]$ are distinct themselves in B^4 (by Proposition 3.2.3), thus E and E' are not isotopic rel boundary in the 4-ball. \square

Proof of 3.2.3. Let F_g be a genus- g surface with boundary and $h_{0,1}: F_g \hookrightarrow B^4$ be embeddings of F_g into the 4-ball that define $E_{0,1} = h_{0,1}(F_g)$. By assumption, there is a boundary-preserving isotopy $H: B^4 \times [0, 1] \rightarrow B^4$ from E_0 to E_1 . Our goal is to produce an isotopy of link cobordisms

in $S^3 \times [0, 1]$ by regarding each surface $E_t = H(F_g \times \{t\})$ as a link cobordism with respect to a consistent identification of $S^3 \times [0, 1]$ with $B^4 \setminus (N(p))^\circ$, as produced in Definition 3.2.1. We do this by isolating a ball B that is never touched by the image of this isotopy $\cup_t E_t$.

The space $F_g \times [0, 1]$ is compact, so its image $\cup_t E_t$ is compact in the 4-ball. For some point $q \in \partial B^4 \setminus L$, there is a sufficiently small half-ball B in the 4-ball centered at q that is disjoint from the image of the isotopy (if not, then some E_t must contain q by compactness, contradicting that each E_t is properly embedded). If the ball has radius $\varepsilon > 0$, then choose a point $p \in B^\circ$ such that $d(p, q) = \varepsilon/2$. The open ball of radius $\varepsilon/4$ centered at p is disjoint from $\cup_t E_t$, and its complement can be identified with $S^3 \times [0, 1]$. Restricting H to this subspace defines a boundary-preserving isotopy between the induced link cobordisms $\Sigma_{0,1}$ of the surfaces $E_{0,1}$ in the 4-ball. \square

3.3. Diagram dependence

In this section we discuss the diagram dependence of the induced chain maps associated to certain link cobordisms. For an arbitrary link cobordism in $\mathbb{R}^3 \times [0, 1]$, the induced chain map depends on the chosen surface diagram, and more precisely, on the chosen diagram for the boundary links. This diagram fixes a chain group for the domain and codomain for the map, and when we change the surface diagram, these groups change by a Reidemeister induced equivalence, as mentioned in Remark 2.3.2. We will show that when we restrict to link cobordisms $\Sigma: \emptyset \rightarrow L$, different surface diagrams induce maps that commute with certain Reidemeister induced maps.

Remark 3.3.1. Because we are studying the boundary-*preserving* isotopy class of Σ , this dissertation only considers the link L , and not its isotopy class. Moreover, the permissible chain homotopies defining $\mathcal{C}(L)$ arise from a sequence of *link specific* Reidemeister moves, and not by *any* sequence of Reidemeister moves. More precisely, a diagram for a link L is the image of some projection $p: \mathbb{R}^3 \rightarrow \mathbb{R}^2$ onto a codimension-one, linear subspace. Projections $p, p': \mathbb{R}^3 \rightarrow \mathbb{R}^2$ defining diagrams D, D' are related by a one-parameter family of rotations $r_t: \mathbb{R}^3 \times I \rightarrow \mathbb{R}^3$ with $r_0 = \text{id}$ taking one projection onto the other $p' = p \circ r_1$. A small perturbation of r makes $p \circ r_t$ generic as a link projection, whereby $(p \circ r_t)(L)$ describes a sequence of *link-specific* Reidemeister moves from D to D' , meaning each Reidemeister move relates a pair of diagrams specific to L . The maps induced by these Reidemeister moves will be called *link-specific Reidemeister induced maps*.

In our setting, $\mathcal{C}(L)$ denotes the chain homotopy class of $\mathcal{C}(D)$ up to link specific Reidemeister induced chain homotopy equivalences, and $\mathcal{H}(L)$ denotes the isomorphism class of $\mathcal{H}(D)$ under

link-specific Reidemeister induced isomorphisms.

Proposition 3.3.2. *For a link cobordism $\Sigma: \emptyset \rightarrow L$ with surface diagrams $S, S': \emptyset \rightarrow D, D'$, the following diagram commutes, up to sign and up to homotopy, for link-specific Reidemeister induced maps φ .*

$$\begin{array}{ccc}
 \mathcal{C}(D') & \xrightarrow{\varphi} & \mathcal{C}(D) \\
 \swarrow \mathcal{C}_{S'}(\Sigma) & & \nearrow \mathcal{C}_S(\Sigma) \\
 & \mathbb{Z} &
 \end{array}$$

Corollary 3.3.3. *The induced map on Khovanov homology associated to a surface in the 4-ball is independent, up to isomorphism, of the chosen surface diagram.*

Proof of Proposition 3.3.2. The idea is to construct a pair of link cobordisms inducing $\varphi \circ \mathcal{C}(S')$ and $\mathcal{C}(S)$ that are isotopic relative to L , whereby Theorem 2.3.3 implies the diagram commutes in the desired manner. The tricky part is producing isotopic cobordisms whose boundaries produce identical diagrams *with respect to the same projection*.

Let $p, p': \mathbb{R}^3 \rightarrow \mathbb{R}^2$ be the projections defining the surface diagrams S and S' . Remark 3.3.1 gives a one-parameter family of rotations r_t with $r_0 = \text{id}$ and $p' = p \circ r_1$ that induces a movie $(p \circ r_t)(L)$ describing a sequence of link-specific Reidemeister moves from D to D' . Consider the one-parameter family of link cobordisms describing the trace of L under this movie:

$$A_s = r|_{L \times [0, 1-s]}: r_0(L) \rightarrow r_{1-s}(L)$$

The link cobordism $A_0^{-1}: r_1(L) \rightarrow L$ has surface diagram $p(A_0^{-1}): D' \rightarrow D$, so with respect to p , the link cobordism $A_0^{-1} \circ r_1(\Sigma)$ induces the map $\varphi \circ \mathcal{C}(S')$. Since Σ induces $\mathcal{C}(S)$ with respect to p , it suffices to show $A_0^{-1} \circ r_1(\Sigma)$ and Σ are isotopic relative to L . Indeed, $A_s^{-1} \circ r_{1-s}(\Sigma)$ describes a boundary-preserving isotopy between these link cobordisms, as desired. \square

Remark 3.3.4. As a result of this proposition, we tend to omit the surface diagram from the notation $\mathcal{C}_S(\Sigma)$, opting for the shorthand $\mathcal{C}(\Sigma)$, as in Definition 3.2.2. In general, the surface diagram is either clear from context or unnecessary for the argument. When necessary, we will specify a surface diagram.

Chapter 4: Closed surfaces in the 4-ball

The first consideration of induced maps on Khovanov homology toward obstructing isotopy of surfaces appeared in [Kho00], where it was conjectured that the maps induced by a closed surface $\Sigma: \emptyset \rightarrow \emptyset$ could be used to distinguish knotted surfaces in \mathbb{R}^4 . This was later proven impossible in [Ras05, Tan06]. This chapter summarizes these results. We may choose to work in B^4 , in $S^3 \times [0, 1]$, or as it was done originally, in $\mathbb{R}^3 \times [0, 1]$. To remain consistent with the text, the results are phrased in the setting of the 4-ball.

4.1. φ -numbers

A smooth, closed, oriented surface Σ embedded in the 4-ball can be regarded as a link cobordism $\Sigma: \emptyset \rightarrow \emptyset$. This link cobordism induces a map $\mathcal{H}(\Sigma): \mathbb{Z} \rightarrow \mathbb{Z}$. Note that there is only one diagram for the empty-link, so Theorem 2.3.3 guarantees that $\mathcal{H}(\Sigma)$ is invariant, up to sign, under *ambient* isotopy of Σ . More concisely, this map is determined by where it maps the generator of \mathbb{Z} , leading to the following definition.

Definition 4.1.1. The φ -number of a smooth, closed, oriented surface $\Sigma \subset B^4$ is the integer

$$\varphi(\Sigma) := \mathcal{H}(\Sigma)(1) \in \mathbb{Z}$$

determining the induced map $\mathcal{H}(\Sigma): \mathbb{Z} \rightarrow \mathbb{Z}$.

The φ -number is a concise way of encoding the induced map on Khovanov homology, and it shares the same up-to-sign invariance under ambient isotopy of Σ as the induced map. For completeness, we summarize this through the following result.

Proposition 4.1.2. *The φ -number of a smooth, closed, oriented surface Σ embedded in the 4-ball is an up-to-sign invariant of the ambient isotopy class of Σ .*

The φ -numbers were originally conjectured to distinguish knotted tori. The restriction to knotted tori is justified in the following proposition.

Proposition 4.1.3. *The φ -number of a surface $\Sigma \subset B^4$ is trivial unless it has genus 1.*

Proof. The induced map is $(0, \chi(\Sigma))$ -graded, so the φ -number can be written explicitly

$$\varphi(\Sigma) = \mathcal{H}(\Sigma)(1) \in \mathcal{H}^{0, \chi(\Sigma)}(\emptyset).$$

Because $\mathcal{H}(\emptyset)$ is supported in the $(0, 0)$ -grading, the φ -number is necessarily trivial for $\chi(\Sigma) \neq 0$, or equivalently for $g(\Sigma) = 1$. \square

In later work [CSS06], the φ -numbers were calculated for certain families of knotted tori; in that work, they used the name *Khovanov-Jacobsson* numbers for what we call φ -numbers. Eventually, φ -numbers were fully classified in an unexpected way.

Theorem 4.1.4 ([Ras05, Tan06]). *The φ -number of a connected surface Σ in the 4-ball is completely determined by genus $g(\Sigma)$. In particular, $\varphi(\Sigma) = \pm 2$ when $g(\Sigma) = 1$.*

For disconnected surfaces, this result acts multiplicatively on the components of the surface, i.e., $\varphi(\Sigma) = 2^m$ when Σ has m components.

4.2. Calculating φ -numbers

It is useful to calculate the φ -number of certain closed surfaces in the 4-ball, as it provides insight into the constructions from Chapter 2. Below, we calculate the φ -number of an unknotted 2-sphere, as well as the φ -class associated to movies of the unknotted torus.

Example 4.2.1. In Figure 4.1, we calculate the φ -number $\varphi(S)$ associated to an unknotted 2-sphere S . The 2-sphere may be decomposed as $S = \mathcal{O} \circ \mathcal{O}$, whereby $\mathcal{H}(S): \mathbb{Z} \rightarrow \mathbb{Z}$ decomposes into $\mathcal{H}(S) = \epsilon \circ \iota$, which we calculate diagrammatically below. As expected, the resulting map is trivial.

Example 4.2.2. In Figure 4.2, we calculate the φ -number associated to a knotted torus, resulting in a map $1 \mapsto 2$, as expected. This is done similarly in 4.3, where the result is a map $1 \mapsto -2$. Note that these movies both represent unknotted tori. More complicated movies representing knotted tori can be obtained, and in light of Theorem 4.1.4, they will nevertheless produce maps $1 \mapsto \pm 2$.

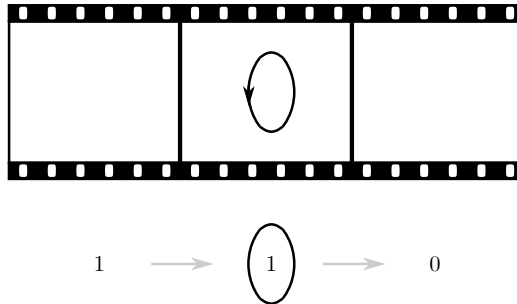


Figure 4.1: The map on Khovanov homology induced by a sphere.

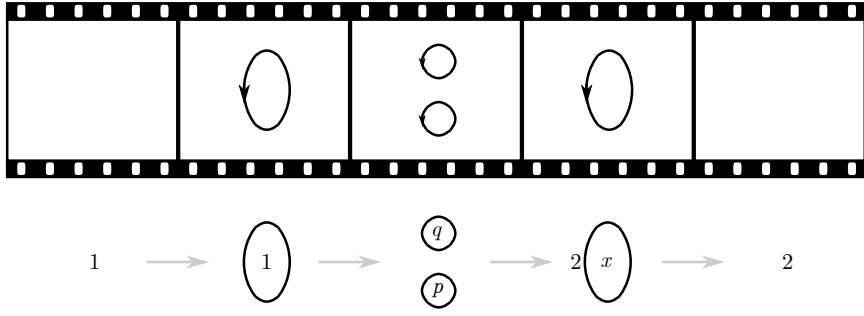


Figure 4.2: The map on Khovanov homology induced by a torus.

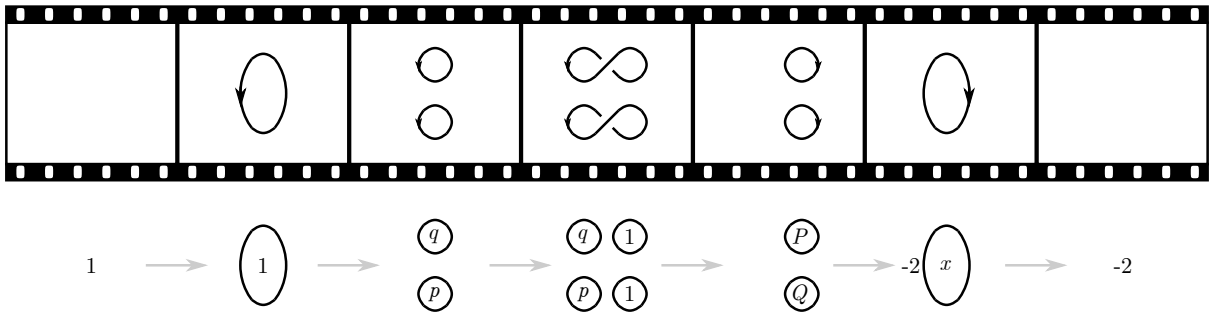


Figure 4.3: The map on Khovanov homology induced by a second torus.

Chapter 5: Relative surfaces in the 4-ball

In this chapter, we consider the natural extension of Chapter 4 to surfaces with boundary. Analogous to the definition of φ -numbers, in Section 5.1, we use the maps on Khovanov homology induced by surfaces with boundary to extract an invariant of the boundary-preserving isotopy class of Σ , called the φ -class of the surface. In Section 5.2, we characterize this invariant for Seifert surfaces and surfaces bounding the unlink. In Section 5.3, we use φ -classes to produce families of unique slice disks bounding a common link. Finally, in Section 5.4, we show that this invariant can be used to obstruct sliceness of certain knots

5.1. φ -classes

A smooth, compact, oriented surface $\Sigma \subset B^4$ bounding a link $L \subset S^3$ can be regarded as a link cobordism $\Sigma: \emptyset \rightarrow L$, as described in Section 3.2. The associated induced map on Khovanov homology is invariant, up to sign, under boundary-preserving isotopy of Σ . More concisely, this map is determined by where it maps the generator of $\mathcal{H}(\emptyset) = \mathbb{Z}$.

Definition 5.1.1. The φ -class of a smooth, compact, oriented surface $\Sigma \subset B^4$ with boundary link $L \subset S^3$, represented by a diagram D , is the Khovanov homology class

$$\varphi(\Sigma) := \mathcal{H}(\Sigma)(1) \in \mathcal{H}(D)$$

represented by the cycle

$$\phi(\Sigma) := \mathcal{C}(\Sigma)(1) \in \mathcal{C}(D)$$

which we call the ϕ -cycle of Σ .

The φ -class is a concise way of encoding the induced map on Khovanov homology, and it shares the same up-to-sign invariance under boundary-preserving isotopy of Σ as the induced map. For completeness, we summarize this through the following result.

Corollary 5.1.2. *The φ -class of a smooth, compact, oriented surface Σ properly embedded in the 4-ball is an up-to-sign invariant of the boundary-preserving isotopy of Σ .*

When calculating the induced maps on Khovanov homology, we generally work on the chain

level, so it is important to note the relevance of the ϕ -cycle: these are the cycles that we calculate and that, in order to use as an invariant, we hope to distinguish. As a sanity check, we note that the ϕ -cycle represents a homology class, i.e., it is a cycle in $\mathcal{H}(D)$. This fact follows by construction: $1 \in \mathcal{C}(\emptyset)$ is a cycle (because $\mathcal{C}(\emptyset)$ is supported in the $(0, 0)$ -grading so $d(1)$ must be 0) and $\mathcal{C}(\Sigma)$ is a chain map (which sends cycles to cycles), so $\phi(\Sigma) = \mathcal{C}(\Sigma)(1)$ must be a cycle. More directly, we have

$$d(\phi(\Sigma)) = d(\mathcal{C}(\Sigma)(1)) = \mathcal{C}(\Sigma)(d(1)) = \mathcal{C}(\Sigma)(0) = 0$$

so $\phi(\Sigma)$ is a cycle in $\mathcal{C}(D)$ representing the homology class $\varphi(\Sigma)$ in $\mathcal{H}(D)$.

Corollary 5.1.3. *The ϕ -cycle is a cycle representing the φ -class.*

Diagram independence of the ϕ -cycle and φ -class follows from the discussion in Section 3.3, however, we discuss diagram dependence of the φ -class, with the aim of proving Corollary 5.1.4 below. For the surface diagram $S: \emptyset \rightarrow D$ of the given link cobordism, defined with the same projection as D , recall the notation from 2.3.1 and write

$$\varphi_D(\Sigma) := \mathcal{H}_S(\Sigma)(1) \in \mathcal{H}(D)$$

Suppose we have two diagrams $D_{0,1}$ for the boundary link L of the given link cobordism. By Proposition 3.3.2, any sequence of link-specific Reidemeister moves relating D_0 and D_1 induces an equivalence $\Psi: \mathcal{H}(D_0) \rightarrow \mathcal{H}(D_1)$ satisfying $\Psi \circ \mathcal{H}_{S_0}(\Sigma) = \pm \mathcal{H}_{S_1}(\Sigma)$. In particular, we have the following up-to-sign equivalence

$$\Psi(\varphi_{D_0}(\Sigma)) = \Psi(\mathcal{H}_{S_0}(\Sigma)(1)) = (\Psi \circ \mathcal{H}_{S_0}(\Sigma))(1) = \mathcal{H}_{S_1}(\Sigma)(1) = \varphi_{D_1}(\Sigma)$$

We conclude that the φ -classes φ_{D_0} and φ_{D_1} vary, up to sign, by a Reidemeister induced isomorphism.

Corollary 5.1.4. *The φ -class is independent, up to isomorphism, of the chosen diagram.*

Remark 5.1.5. The author has been asked many times if *any* sequence of Reidemeister moves will preserve the φ -class of a link cobordism $\Sigma: \emptyset \rightarrow L$. This question can be interpreted in two ways, and both are not relevant to our work. First, one might ask that instead of the link-specific Reidemeister moves used in Proposition 3.3.2, we use any sequence of Reidemeister moves. This is not necessary to consider in the category with which we work: we are considering the link L itself, not its isotopy class. Moreover, in this setting, the Proposition would relate the two maps induced by two surface diagrams for Σ with a completely unrelated map induced by an arbitrary sequence of Reidemeister moves. This map has nothing to do with the surface Σ or its boundary-preserving isotopy class. A second interpretation of this question might be that,

given a sequence of Reidemeister moves between diagrams D_0 and D_1 representing links L_0 and L_1 , the cylinder $A: L_0 \rightarrow L_1$ produced by tracing the isotopies induced by each move should preserve the ϕ -cycle and φ -class. This is, of course, true! The following diagram is commutative by construction:

$$\begin{array}{ccc} \mathcal{H}(D_0) & \xrightarrow{\mathcal{H}(A)} & \mathcal{H}(D_1) \\ & \swarrow \mathcal{H}(\Sigma) & \nearrow \mathcal{H}(A \circ \Sigma) \\ & \mathbb{Z} & \end{array}$$

whereby the φ -class for Σ and for $A \circ \Sigma$ will be preserved by $\mathcal{H}(A)$.

Throughout the remainder of this chapter, we will discuss certain methods for calculating and applying the ϕ -cycle associated to surfaces in the 4-ball. Next up, we calculate the φ -class for two families of surfaces in the 4-ball.

5.2. Calculating φ -classes for familiar families of surfaces

Here, we discuss the classification of φ -classes for certain familiar families of surfaces, namely, Seifert surfaces and surfaces bounding the unlink, proven in [Swa10, SS21].

5.2.1 Seifert surfaces

For a diagram D of a link $L \subset S^3$, recall that Seifert's algorithm produces a surface $\Sigma_D \subset S^3$, called the Seifert surface of D . Pushing this surface into the 4-ball produces a link cobordism $\Sigma: \emptyset \rightarrow L$, and the associated map

$$\mathcal{H}(\Sigma): \mathbb{Z} \rightarrow \mathcal{H}(D)$$

has been completely classified, which we briefly mention here. In [Swa10, SS21], it was shown that the associated ϕ -cycle is a collection of labeled smoothings on the orientation induced smoothing σ_D of the diagram D . Moreover, they produce a graph Γ from σ_D , with vertices the connected components and edges the 0- and 1-smoothings, that completely determines the ϕ -cycle: the homotopy type of the subgraph Γ_0 (containing only 0-smoothings as edges) determines $\phi_D(\Sigma_D)$.

Theorem 5.2.1 ([Swa10, SS21]). *The φ -class $\varphi_D(\Sigma_D)$ associated to a Seifert surface Σ_D is determined by graphical conditions on the positive and negative crossings in the diagram D .*

This result is a computational advance, being a quick way to find the φ -class for some surfaces. It has been applied for good use though: using the Seifert class $\varphi(\Sigma_D)$ associated to certain pretzel knots, their sliceness was verified, as in Corollary 26-27 of [Swa10] or Theorem

2.5 of [SS21].

5.2.2 Surfaces bounding the unlink

Here, we classify φ -classes for surfaces bounding the unlink, as in the following theorem.

Theorem 5.2.2. *Let U be the n -component unlink and D its crossingless diagram. The ϕ -cycle for a connected link cobordism $\Sigma : \emptyset \rightarrow U$ is determined by its genus:*

- (a) *if $g(\Sigma) = 0$, then $\phi_D(\Sigma)$ is, up to sign, a pqr -chain on the components of D ;*
- (b) *if $g(\Sigma) = 1$, then $\phi_D(\Sigma)$ is, up to sign, twice the all x -label on D ;*
- (c) *if $g(\Sigma) \geq 2$, then $\phi_D(\Sigma) = 0$.*

This theorem is proven by utilizing Theorem 4.1.4 and the bigrading. This result is also a computational advance, however, it was put to good use in Theorem 2.3.5.

Remark 5.2.3. Theorem 5.2.2 assumes that Σ is a connected surface. In the case that there are multiple components, [GL20] shows that for split links, the induced map $\mathcal{C}(\Sigma)$ is determined by the maps induced between components of Σ , independent of their potential linking. Thus, this theorem can be applied to each component of Σ individually.

5.3. φ -distinguished families of slice disks

The motivation for defining and studying φ -classes is to distinguish smooth, compact, oriented surfaces that are properly embedded in the 4-ball up to boundary-preserving isotopy. In the absolute case, the φ -numbers were unable to distinguish any closed surfaces in the 4-ball. We will see that this is not the case for φ -classes, which are able to distinguish families of slice disks for a given knot.

Definition 5.3.1. A family of smooth, oriented, compact surfaces $\Sigma_1, \dots, \Sigma_n$ that are properly embedded in the 4-ball and share a common boundary link $L \subset S^3$ are **φ -distinguished** by their maps on Khovanov homology if they have pairwise distinct φ -classes up to sign, that is, $\varphi(\Sigma_i) \neq \pm\varphi(\Sigma_j)$ for all $i \neq j$.

Remark 5.3.2. Because the induced maps on Khovanov homology do not detect local knotting (connect summing with a knotted 2-sphere, see Section 2.3.3), then a pair of surfaces $\Sigma_{0,1}$ that are φ -distinguished cannot be related by a local knotting, namely, $\Sigma_0 \not\cong \Sigma_1 \# S$ for any knotted 2-sphere S .

5.3.1 A pair of slices for 9_{46}

Here, we distinguish a pair of slice disks for the knot 9_{46} . A diagram for this knot is recorded in the center of Figure 5.1, and a pair of slice disks D_ℓ and D_r for 9_{46} are given by the two bands ℓ and r (left and right). To the left and right hand side, we see the corresponding disks D_ℓ and D_r after being pushed into the boundary 3-sphere.

These slice disks have been known to be distinct, up to boundary-preserving isotopy, and therefore, they are perfect candidates for testing the abilities of the φ -classes. Indeed, we have the following theorem, proving half of Theorem 1.3.1.

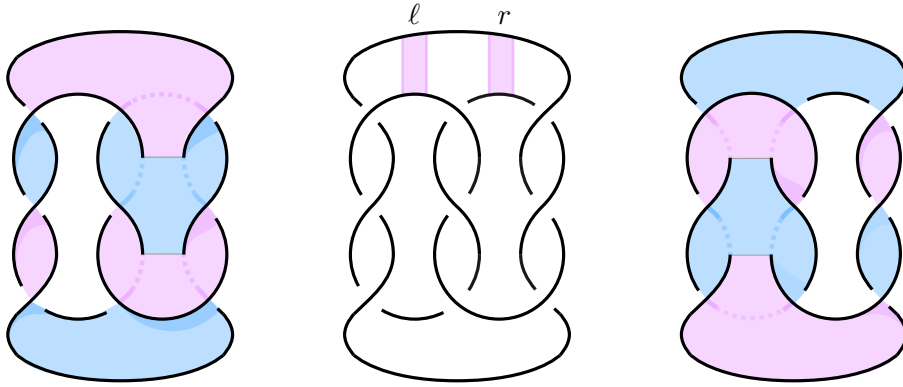


Figure 5.1: A diagram for the knot 9_{46} together with a pair of slice disks (drawn in S^3), described by the indicated band moves ℓ and r .

Theorem 5.3.3. *The slice disks D_ℓ and D_r for 9_{46} are φ -distinguished.*

Proof. In Figures 5.3 and 5.4 we calculate the φ -cycles for D_ℓ and D_r , which for reference, are listed in Figure 5.2. Note that our movies are obtained by reversing the movies that the band moves ℓ and ℓ' describe. To see that D_ℓ and D_r are φ -distinguished we show that the given ϕ -cycles represent distinct homology classes, up to sign; or equivalently,

$$\Phi_\pm = \phi(D_\ell) \pm \phi(D_r)$$

are both nontrivial cycles in $\mathcal{C}(9_{46})$. Nontriviality of this cycle can be determined quickly with the code from Section 6.2, which shows that the cycles Φ_\pm are not boundaries in $\mathcal{C}(9_{46})$ (see Appendix C). We apply a second method for determining nontriviality, with the intention of extending this result to a broader family of φ -distinguished slice disks. This method uses (so-called) trim maps $T: L \rightarrow L'$, which resolve a crossing by attaching a 1-handle, thus *trimming* the link L to produce a link L' represented by a diagram with one fewer crossing. The idea is that, if the resulting cycle $T(\Phi_\pm)$ represents a nontrivial class, then it must have been that Φ_\pm also represented something

nontrivial. These maps are explicitly calculated in [SS21, Section 5]. Applying three trim maps to the crossings in the left column of the diagram, any labeled smoothing with a 1-smoothing in the left column is killed. There is only one such labeled smoothing whose left column contains only 0-smoothings. As a result, the three resolution maps produce a single labeled smoothing: the all 1-label of the 1-smoothing for the trimmed diagram. An analysis on the differential entering this extreme homological grading shows that this cycle is never a boundary (see [Ell09, Example 2.2] and [Swa10, Proposition 10]). \square

$$\begin{aligned} \phi(D_\ell) = & \text{Diagram 1} + \text{Diagram 2} + \text{Diagram 3} + \text{Diagram 4} + \text{Diagram 5} + \text{Diagram 6} + \text{Diagram 7} + \text{Diagram 8} \\ \phi(D_r) = & \text{Diagram 1} + \text{Diagram 2} + \text{Diagram 3} + \text{Diagram 4} + \text{Diagram 5} + \text{Diagram 6} + \text{Diagram 7} + \text{Diagram 8} \end{aligned}$$

Figure 5.2: The ϕ -cycles for D_ℓ (top) and D_r (bottom).

Remark 5.3.4. Although the movie descriptions for these surfaces produce cycles belonging to Khovanov chain complexes associated to the same diagram of $\mathfrak{9}_{46}$, these chain complexes differ in their enumeration of the diagram's crossings. This is fine, as these complexes are related by a chain homotopy that only affects the signs of certain labeled smoothing in $\phi(\Sigma_\ell)$ and $\phi(\Sigma_r)$. These sign changes will not cause any unwanted cancellation, or the effect of the resolution maps. The net result is that the sign of the resulting labeled smoothing may change, and this will have no effect on the nontriviality of c_\pm .

Remark 5.3.5. The above trim maps produce non-orientable surfaces, but they still induce chain maps on Khovanov homology. In fact, [LS21] proved that Khovanov homology is functorial over non-orientable surfaces. Additionally, they noted the above proof of Theorem 5.3.3 says more than what we have presented: attaching the non-orientable cobordism produced by the trim maps produces examples of φ -distinguished, non-orientable surfaces. One trim gives a pair of Möbius bands for 8_{20} , two produces a pair of Klein bottles for 6_1 , and three produces non-orientable surfaces bounding $3_1 \# 3_1$.

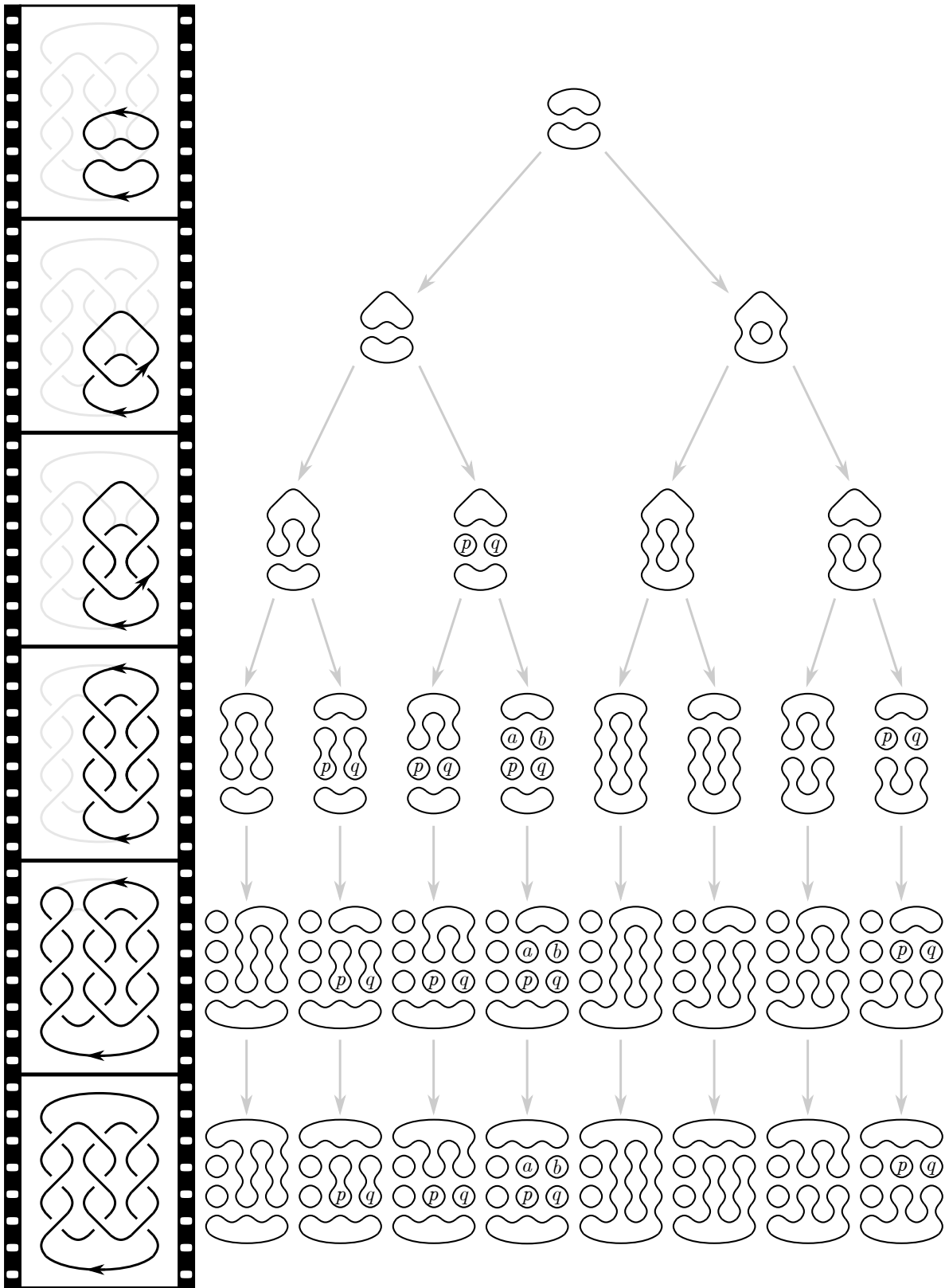


Figure 5.3: A movie description of the surface Σ_ℓ and the calculation of its ϕ -cycle.

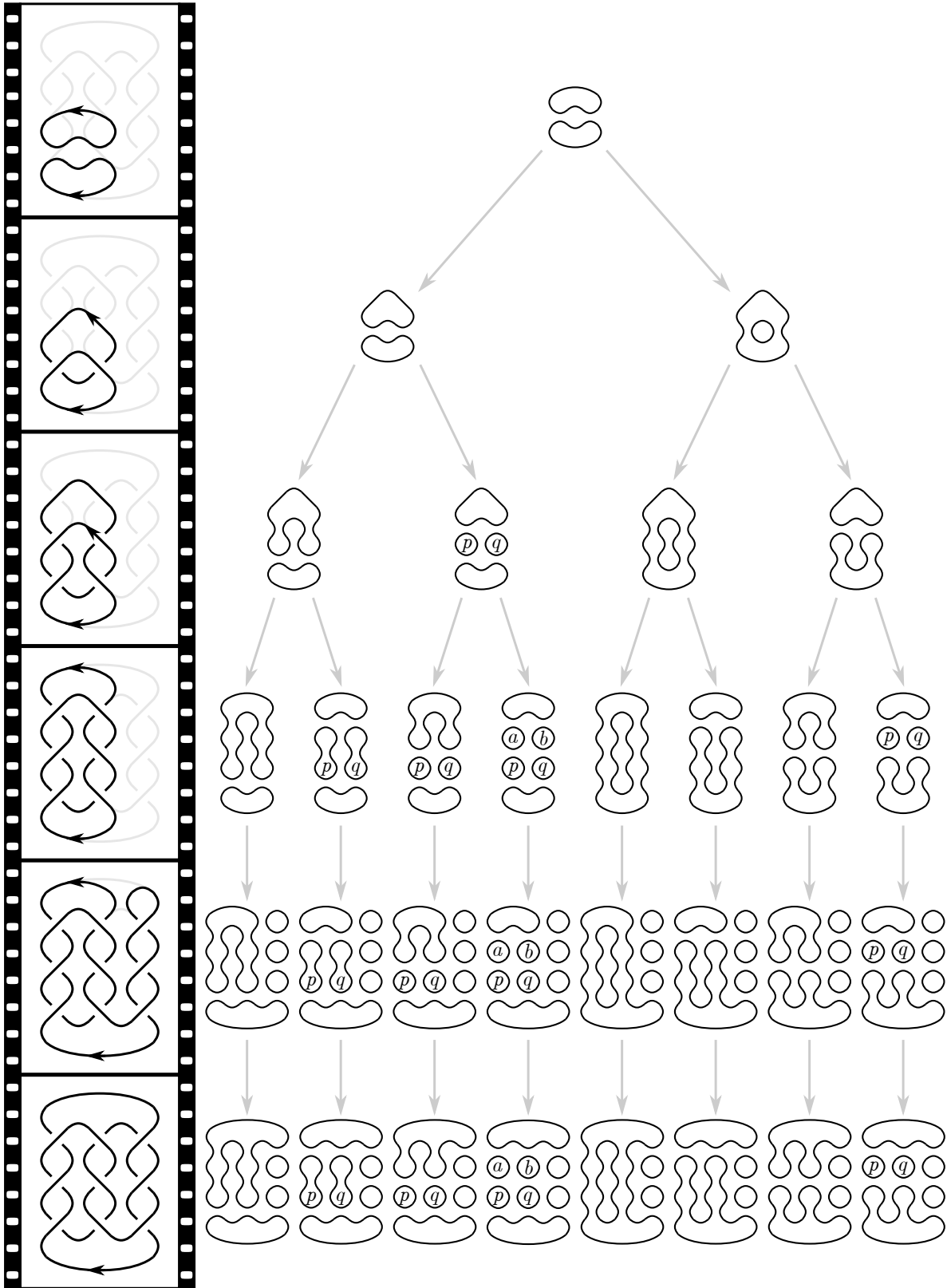


Figure 5.4: A movie description of the surface Σ_r , and the calculation of its ϕ -cycle.

5.3.2 A pair of slices for 6_1

In Figure 5.5, we see a pair of slice disks E_ℓ and E_r for the knot 6_1 , again expressed by a pair of band moves recorded on the given diagram D for 6_1 . Unlike the slices for 9_{46} , it is not easily to see E_ℓ and E_r after pushing them into S^3 , as they have far too many layers and intersections to be seen plainly on a page.

It is known that E_ℓ and E_r are distinct up to boundary-preserving isotopy, but it is interesting that they can be distinguished by their φ -classes, as in the following theorem. This proves the remaining half of Theorem 1.3.1.

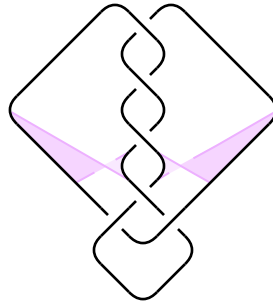


Figure 5.5: A pair of slice disks bounding 6_1 .

Theorem 5.3.6. *The slice disks E_ℓ and E_r for 6_1 are φ -distinguished.*

Proof. We give the ϕ -cycles in Figure 5.6. The calculations are done similar to those for the slices of 9_{46} , with the additional use of a Reidemeister III move. As before, the enumerations induced by the two movies differ, however, in this case, there is a common smoothing between the cycles. Following the enumerations for these crossings, we see that both enumerations express this smoothing with the binary sequence 101000, and therefore, they chain homotopy relating the two chain complexes will be the identity on this element. We distinguish these cycles in Appendix C using the SageMath program from Section 6.2. \square

5.3.3 A family of slices for $\#_k(9_{46})$

The above distinction of slice disks for 9_{46} generalizes to an infinite family of knots that exhibit an arbitrarily large number of slice disks.

Corollary 5.3.7. *The knot $\#_m(9_{46})$ bounds at least 2^m -many φ -distinguished slice disks.*

Proof. First, observe that there are 2^m -many slice disks for $\#_m(9_{46})$ obtained by boundary-summing m -many disks chosen from the two slice disks D_ℓ and D_r from Theorem 5.3.3. We

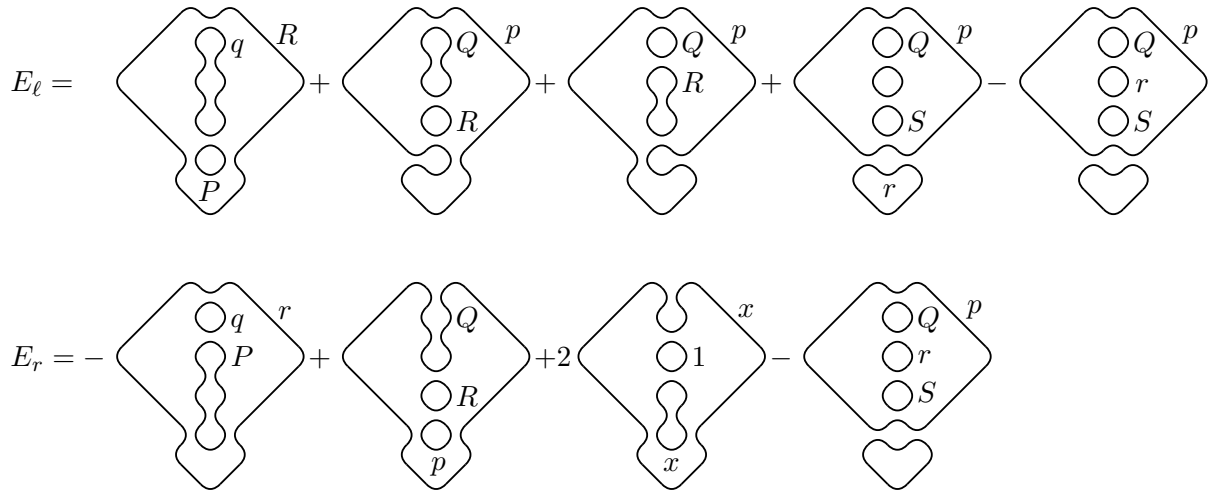


Figure 5.6: The ϕ -cycles for the two slice disks from Figure 5.5.

illustrate these disks in Figure 5.7 with a *windmill* diagram, with m -many inward-facing copies of 9_{46} as the *sails* of the windmill and m -many *windshafts* which connect the sails in the center of the diagram. Movies for the 2^m -many slices are obtained by choosing either of the movies from Theorem 5.3.3 for each sail and using m -many Morse saddles to merge their final frames along the windshafts.

Now, choose a pair of slices $\Sigma_{0,1}$ from the 2^m -many slices described above, and produce

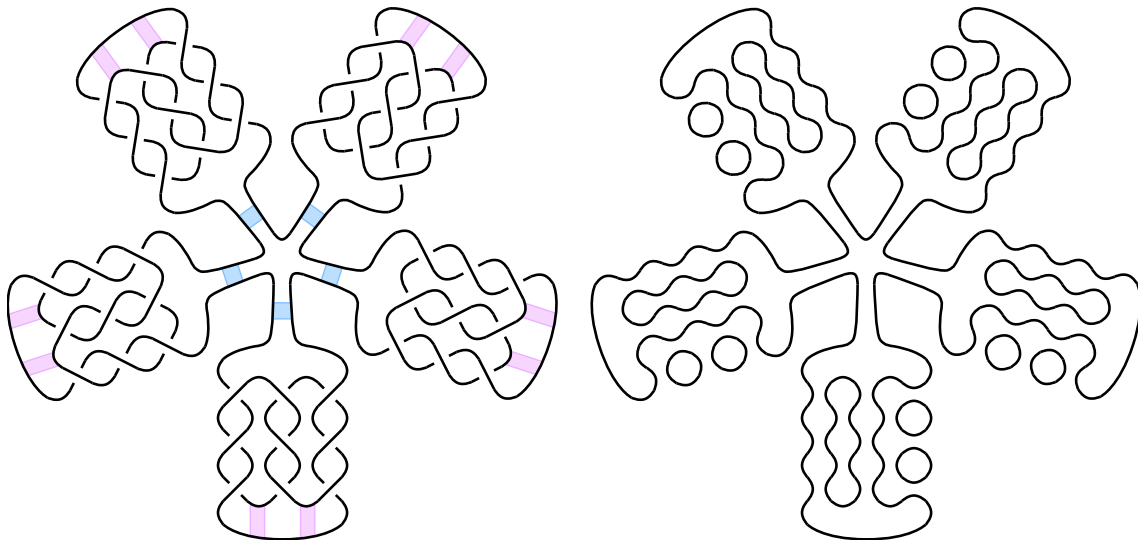


Figure 5.7: The windmill diagram (left) for $\#_5(9_{46})$ and a smoothing (right) from the ϕ -cycle associated to one of its slice disks.

their ϕ -cycles per the given movie descriptions. As in the proof of Theorem 5.3.3, we will trim the diagrams to simplify the cycles, although in this case, we must trim each sail. Trim the left column of a sail when the movie of Σ_0 shows Σ_r and trim the right column when it shows Σ_ℓ . Because Σ_0 and Σ_1 differ in their choice of movies for the sails, one of the trims will kill $\phi(\Sigma_1)$.

The only remaining element of $\phi(\Sigma_0)$ will be the all 1-label of the 1-smoothing of the trimmed diagram of $\#_m(9_{46})$. As before, such an element represents a nontrivial homology class in the Khovanov homology of this trimmed diagram. The result follows just as it did in the previous two results. \square

Slight generalizations to the above techniques allow us to produce even more families of knots with large numbers of slice disks. We simply increase the crossing count in each column of the odd, three-stranded pretzel knots.

Corollary 5.3.8. *For n odd and $|n| > 1$, the pretzel knot $P(n, -n, n)$ bounds at least two distinct slice disks.*

Corollary 5.3.9. *For n odd and $|n| > 1$, the knot $\#_m(P(n, -n, n))$ bounds at least 2^m -many distinct slice disks.*

5.3.4 An extended family of prime knots

The above calculations can be extended to produce examples of prime knots with an arbitrarily large number of φ -distinguished slices. Our methods work broadly for any family of φ -distinguished surfaces, so we describe them in generality before giving a specific example. The trick is to extend a family of φ -distinguished link cobordisms by a ribbon concordance, i.e., a genus-0 surface with no local maxima. Ribbon concordances are well suited to φ -classes because they induce injections on Khovanov homology [LZ19], and thus, preserve the uniqueness of φ -classes. Let $\Sigma, \Sigma' : \emptyset \rightarrow K$ be a pair of φ -distinguished link cobordisms, $\varphi(\Sigma) \neq \varphi(\Sigma')$. Any ribbon concordance $C : K \rightarrow K'$ induces an injection $\mathcal{H}(C) : \mathcal{H}(K) \rightarrow \mathcal{H}(K')$ on Khovanov homology, whereby the link cobordisms $C \circ \Sigma$ and $C \circ \Sigma'$ are also φ -distinguished, having

$$\varphi(C \circ \Sigma) = \mathcal{H}(C)(\varphi(\Sigma)) \neq \mathcal{H}(C)(\varphi(\Sigma')) = \varphi(C \circ \Sigma')$$

This allows us to produce (potentially) new families of φ -distinguished link cobordisms by simply extending any known family of φ -distinguished link cobordisms. In Theorem 5.3.10 below, this is done for a specific family of slice disks extended by the ribbon concordance from [KL79], illustrated in Figure 5.8, proving Theorem 1.3.2.

Theorem 5.3.10. *The prime knot K_m in Figure 5.9 bounds at least 2^m -many φ -distinguished slice disks.*

Proof. We begin by describing a general ribbon concordance from any given knot K to a prime

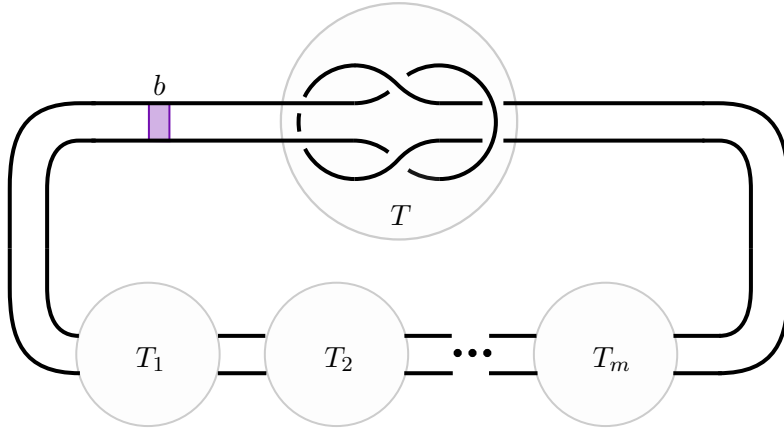


Figure 5.8: The band move b on the given diagram describes the ribbon concordance defined in [KL79] between a composite knot, expressed as a sum of prime tangles, and a prime knot.

knot K' , which was defined in [KL79]. We can express K as a sum of prime knots, and in particular, we may find a knot diagram that is a tangle-sum of finitely many prime tangles T_1, T_2, \dots, T_m . With these tangles, produce the knot K' in Figure 5.8, consisting of a tangle T and the tangles from K . The aforementioned paper proved that this knot is prime, and moreover, they noted that the band move b describes a link cobordism from K' to a two-component unlink consisting of K together with an unknot, which we will cap off. Reversing this cobordism produces a ribbon concordance $C: K \rightarrow K'$ from the (arbitrary) knot K to a prime knot K' .

Applying this construction to $K = \#_m(9_{46})$ produces the prime knot K_m in Figure 5.9. The bands on the diagram describe the 2^m slice disks for K_m . As Corollary 5.3.7 φ -distinguished the 2^m slice disks for $\#_m(9_{46})$, these slice disks for K_m are also φ -distinguished, as desired. \square

For reference, we have drawn K_2 in Figure 5.10 and one of the four φ -distinguished slice disks (pushed into S^3) in Figure 5.11.

It is interesting to note that it is much harder to produce an extended family of slice disks for the knot $\#_m(6_1)$ and its corresponding prime knot. In particular, it was crucial that we show that the slice disks for $\#_m(9_{46})$ were φ -distinguished. In that case, the ϕ -cycle was fairly tame and acted nicely during the boundary-summing of the disks. In the $\#_m(6_1)$ case, the ϕ -cycles are unpleasant, to say the least. Nevertheless, we expect that with sufficient tenacity, the same conclusion can be reached.

5.4. Obstructing sliceness with φ -classes

We now change direction and discuss another application of φ -classes: obstructing sliceness of knots. In particular, by implementing the characterization of φ -classes for closed surfaces (Theorem 4.1.4), we obtain the following result.

Theorem 5.4.1 ([Swa10]). *For a slice knot K , the φ -class of a link cobordism $\Sigma : \emptyset \rightarrow K$ is nontrivial if $g(\Sigma) \leq 1$. In particular, slice disks have nontrivial φ -classes.*

Proof. For $g(\Sigma) = 0$, produce a closed surface $\Sigma' = -(\Sigma \# T^2) \circ \Sigma$ with genus 1. By Theorem 4.1.4, we must have $\mathcal{H}(\Sigma')(1) = 2$, and therefore

$$2 = \mathcal{H}(\Sigma')(1) = (\mathcal{H}(-(\Sigma \# T^2)) \circ \mathcal{H}(\Sigma))(1) = \mathcal{H}(-\Sigma \# T^2)(\varphi(\Sigma)).$$

A trivial $\varphi(\Sigma)$ kills the right-most term, producing a contradiction. The proof with $g(\Sigma) = 1$ is done similarly: compose Σ with a slice disk to yield an identical calculation. \square

Remark 5.4.2. In [SS21, Swa10], the above result was used to obstruct the sliceness of certain odd, three-stranded pretzel knots. In particular, it was shown that the φ -class associated to the Seifert surface bounding these knots is trivial. More generally, one can attempt to characterize the sliceness of all odd, three-stranded pretzel knots; this was done in [GJ11] using numerous tools, including gauge theory. It is not known if this result can be recovered using only φ -classes. Initial attempts seem promising: the Seifert surface for $P(3, 5, 7)$ has a trivial φ -class, and so by Theorem 5.4.1 is not slice, and moreover, this knot is not obstructed from being slice in [SS21, Swa10].

Remark 5.4.3. More generally, any knot with unknotting number 1 will bound a genus-1 surface: describe the crossing change that produces an unknot-diagram as a sequence of 1-

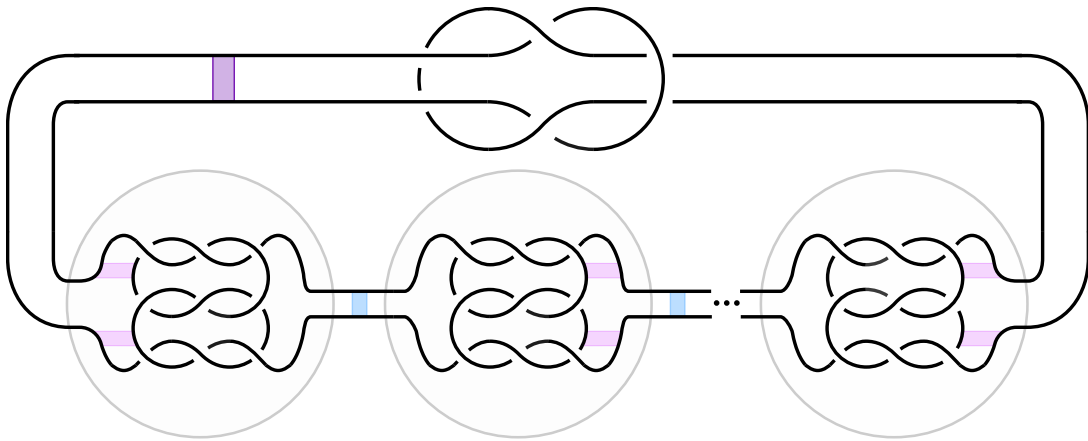


Figure 5.9: The prime knot K_m with band moves describing the 2^m slice disks.

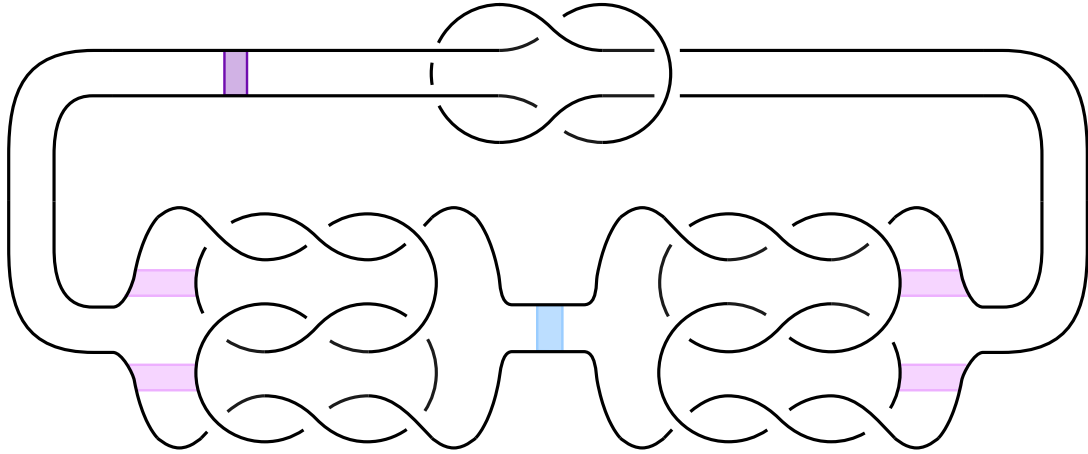


Figure 5.10: The knot K_2 with band moves describing the four slice disks it bounds.

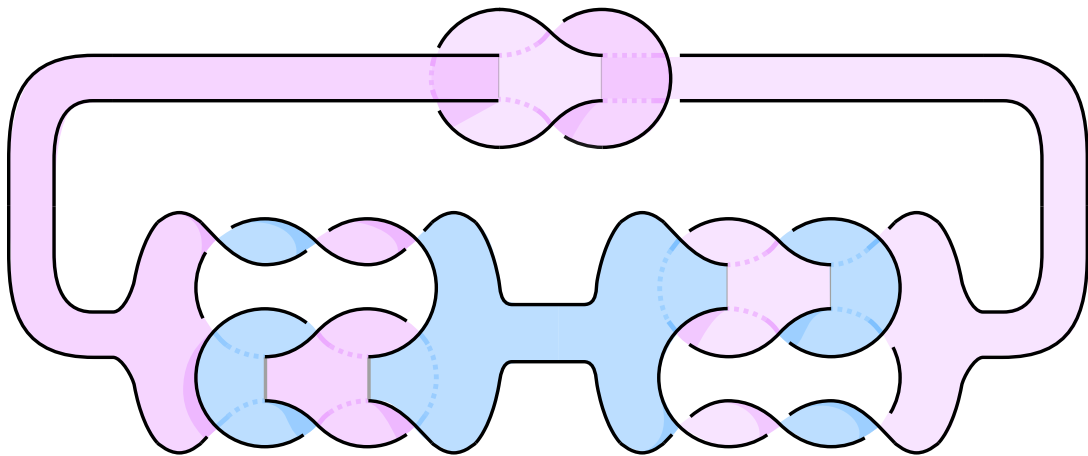


Figure 5.11: One of the four unique slice disks bounding K_2 , viewed in the 3-sphere.

handle attachments and Reidemeister I moves; untangle the unknot-diagram with Reidemeister moves; attach a 2-handle. As there are many unknotting number 1 knots (e.g., any Whitehead double), this might lead to a broader examination of sliceness obstructions through φ -classes. One such example, or perhaps non-example, is the Conway knot, which has unknotting number 1. For two genus-1 surfaces bounding the Conway knot, we calculate the φ -class, only to find that they are nontrivial Khovanov homology classes (see Appendix C).

Remark 5.4.4. The s -invariant is known to provide information on the 4-ball genus of knots. It is perhaps not surprising that the φ -class can also be used to produce information regarding the 4-ball genus of knots. It is unknown if there is a relationship between the s -invariant and φ -classes. In light of the result above, it would be of interest to find examples of a knot K bounding a genus-1 surface Σ for which $s(K) = 0$ and $\varphi(\Sigma) = 0$, or alternatively, $s(K) > 0$ and $\varphi(\Sigma) \neq 0$. This would imply that, in terms of detecting sliceness, one invariant is stronger than the other. It seems less likely that they are equivalent as sliceness obstructions.

5.5. Reflections on φ -classes

Using φ -classes can be very difficult. They work well with the theory of Khovanov homology, as we saw in the prime examples, but they are exceedingly difficult to calculate and to distinguish. In the best situations, they require significant levels of endurance to compute and a completely separate technique to distinguish. Unfortunately, in most cases, the level of endurance is inhuman and the (known) technique to distinguish cannot be done by a computer. Nevertheless, in the next chapter, we describe this technique for distinguishing Khovanov homology classes.

Chapter 6: Triviality of Khovanov homology classes

In the previous chapter, we saw that many arguments hinged on the ability to distinguish Khovanov homology classes, or equivalently, to show that their difference is nontrivial. What does it mean to be trivial in Khovanov homology? We answer this question in Section 6.1. The following Section 6.2 gives a computer program that determines triviality of Khovanov homology classes. The final Section 6.3 shows how to use this program for a specific application.

6.1. Boundaries in Khovanov homology

Suppose D is a diagram for some oriented link, and consider the Khovanov homology $\mathcal{H}(D)$. Fix a homological grading $h \in \mathbb{Z}$, and choose an arbitrary generator $\varphi \in \mathcal{H}^h(D)$. This class is represented by a cycle $\phi \in \ker(d^h) \subset \mathcal{C}^h(D)$. By definition,

$$\mathcal{H}^h(D) = \ker(d^h)/\text{im}(d^{h-1})$$

Thus, φ is trivial if $\phi \in \text{im}(d^{h-1})$, i.e., if it is a boundary. To determine when an arbitrary class is trivial, it suffices to understand when it is a boundary in the Khovanov chain complex. Previous work has attempted to describe when certain cycles are boundaries [Ell09, Ell10]. Namely, these works considered cycles that consist of a single labeled smoothing $\beta \in \mathcal{C}^h(D)$. Unfortunately, this is not reflective of a general cycle in the Khovanov chain complex, which is generally a combination of labeled smoothings

$$\phi = \sum_{i=1}^n b_i \beta_i \quad b_i \in \mathbb{Z}, \beta_i \in \mathcal{C}^h(D)$$

Many of these labeled smoothings do not appear in the aforementioned work because they themselves are not cycles. Moreover, for ϕ to be a boundary, it is not necessary that each labeled smoothing α_i is itself a boundary.

We will use a more direct approach to showing a cycle is a boundary. First, chose a basis for

each chain complex with a relevant homological grading

$$\mathcal{C}^{h-1}(D) = \langle \alpha_1, \dots, \alpha_m \rangle$$

$$\mathcal{C}^h(D) = \langle \beta_1, \dots, \beta_n \rangle$$

With respect to these bases, we may express ϕ and d^{h-1} as matrices \mathbf{b} and \mathbf{M} , respectively. In particular, the basis for $\mathcal{C}^h(D)$ allows us to write $\phi = \sum_{i=1}^n b_i \beta_i$, with which we define a column vector $\mathbf{b} = (b_i)$. Similarly, the map d^{h-1} can be written as a matrix by determining how it acts on the basis vectors for $\mathcal{C}^{h-1}(D)$, namely

$$d(\alpha_i) = \sum_{j=1}^n b_{i,j} \beta_j$$

We then set $\mathbf{M} = (b_{i,j})$. Finally, to determine whether b is a boundary, it suffices to find a solution to the equation $\mathbf{M}\mathbf{x} = \mathbf{b}$. This can be done with numerous methods in linear algebra (e.g., by row-reducing the augmented matrix $[\mathbf{M}|\mathbf{b}]$). The chosen method should be sensitive to the coefficient group in use (here we have specified \mathbb{Z} coefficients).

6.2. A SageMath program

In this section, we describe a SageMath program which determines the triviality of a Khovanov homology class. The program takes in an oriented link diagram and cycle, with which it calculates the Khovanov chain complex and applies the above argument to determine if the cycle represents a boundary.

Our program uses Python, with the exception of a single SageMath command. The description we give below will be from the perspective of a SageMath terminal running on a Windows machine. To begin, download the `triviality.py` file (available [here](#)) and save it to your desktop. Open SageMath and load the file by executing the following:

```
1 sage: load('/home/sage/Desktop/triviality.py')
```

The path to your file may change depending on your OS.

6.2.1 Encoding an oriented knot diagram

Let D be an oriented link diagram with n crossings. We encode a knot diagram by using a similar method to [BN02], which was inspired by Dowker-Thistlethwaite notation. The extra information from this method allows us to encode elements in the Khovanov chain complex. To begin, choose an enumeration x_i of the crossings, an enumeration c_i of the link components,

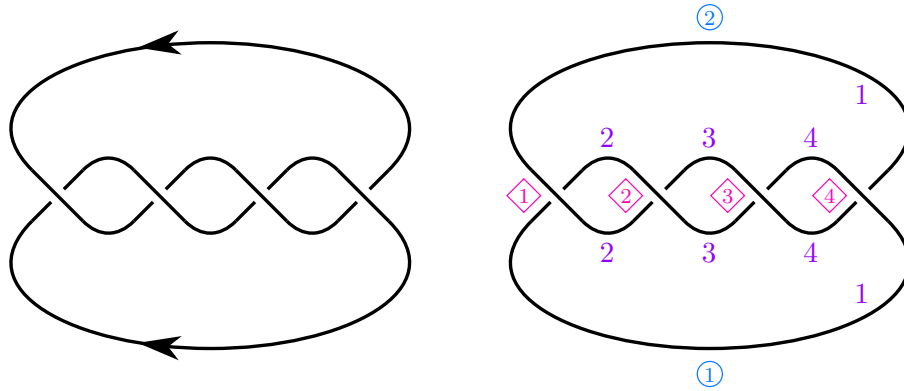


Figure 6.1: An enumeration for the **crossings**, **components**, and **strands** of a link.

and an enumeration s_i of the strands¹ of each link component so that successive strands in the enumeration agree with the orientation of the link. This is done for a link in Figure 6.1; we have used colors and shapes to help indicate which numbers correspond to which enumerations. Note that each strand corresponds uniquely to a pair of positive integers s_i and c_i for the chosen enumerations of the link. These pairs of positive integers allow us to uniquely represent each crossing x_m in D as a pair of 4-tuples $S_m = (s_i, s_j, s_k, s_l)$ and $C_m = (c_i, c_j, c_k, c_l)$, beginning with the positive integers s_i and c_i associated to the incoming under-strand, and proceeding anticlockwise around the diagram. We encode D as a **Diagram** object via the n -tuples $S = (S_1, \dots, S_n)$ and $C = (C_1, \dots, C_n)$. For example, the link diagram in Figure 6.1 is encoded in lines 2-4 of the code below. Note that when we are given a diagram for a knot, the n -tuple C consists of n -many 4-tuples $(1, 1, 1, 1)$ and is unnecessary to input into the program.

```

2 sage: S = [[1, 2, 2, 1], [2, 3, 3, 2], [3, 4, 4, 3], [4, 1, 1, 4]]
3 sage: C = [[1, 2, 1, 2], [2, 1, 2, 1], [1, 2, 1, 2], [2, 1, 2, 1]]
4 sage: D = Diagram(S, C)

```

From the sequence $S = (S_1, \dots, S_n)$, we can obtain the number of positive/negative crossings by examining the strand-values s_j and s_l from each S_m . The crossing is positive when $s_l < s_j$ and is negative otherwise. The **Diagram** object has these values as attributes; see lines 5-6 of the code below.

```

5 sage: # .n returns the number of crossings; .np and .nn return the
      number of positive and negative crossings, respectively
6 sage: [D.n, D.np, D.nn]
      [4, 4, 0]

```

Other values are used within the code, such as the largest strand number and the number of components, and are obtained similarly.

¹By a strand, we mean any connected component of the diagram with double points removed.

6.2.2 Encoding labeled smoothings and chains

The information provided by these n -tuples is sufficient to build the Khovanov chain complex $\mathcal{C}(D)$ associated to the given link diagram D . We will first describe how a labeled smoothing is encoded into the program and then describe how the program produces the Khovanov chain complex associated to a diagram D .

A labeled smoothing α_σ is encoded using information from the **Diagram** object, namely the tuples S and C . First, a smoothing can be represented as a binary sequence $\sigma = (\sigma_1, \dots, \sigma_n)$, as described in Section 2.2. To label the smoothing, we wish to associate a label to each loop \mathcal{L} in σ , which requires a method for uniquely referencing these loops. This is done by carrying over the enumeration of the strands s_i and components c_i in D to the strands² in σ : label each strand in σ with its strand enumeration s_j and the component enumeration c_k . To each loop \mathcal{L} , we associate the unique pair of sequences (s_j) and (c_k) beginning with the strand $s_{j'}$ and component $c_{k'}$ that represent the first lexicographic pair $(s_{j'}, c_{k'}) \in S \times C$ on the strands of \mathcal{L} , followed by successive labels as we traverse \mathcal{L} with respect to the direction of the strand $s_{j'}$ from component $c_{j'}$ in the diagram D . We may obtain these sequences using an illustration of the smoothing, as in Figure 6.2; the program does this for itself using the binary sequence for σ .

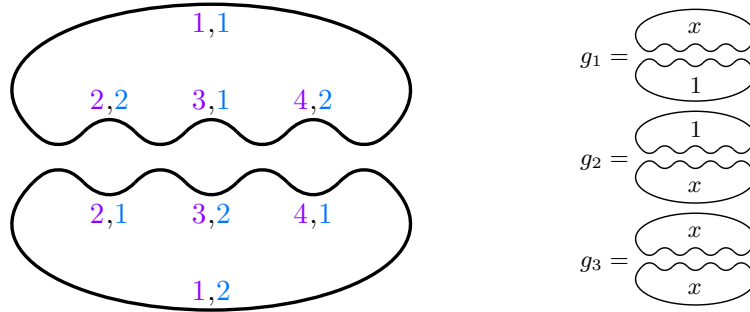


Figure 6.2: The $\sigma = (0, 0, 0, 0)$ smoothing of D decorated with the enumerations s_i and c_i from Figure 6.1 (left) and three labeled smoothings α_σ (right).

The loop \mathcal{L} in σ is then a sequence $\mathcal{L} = (s_j, c_j)$ of elements in $S \times C$. For a smoothing with ℓ loops, we may enumerate the loops $\mathcal{L}_i = (s_{i,j}, c_{i,j})$ lexicographically by their first pair $(s_{i,1}, c_{i,1}) \in S \times C$. A labeling of σ is an element $v = (v_k) \in \{\mathbf{1}, \mathbf{x}\}^\ell$, where v_i indicates the label of the loop \mathcal{L}_i . Therefore, a labeled smoothing is encoded as a **Generator** object by three attributes: the **Diagram** object D , a binary sequence σ , and a label v . As mentioned, the binary sequence uses the enumerations from D to enumerate its loops. The choice of labels is dependent

²By a strand of the smoothing, we mean a connected component of the smoothing once all smoothed crossings have been removed; these correspond directly to the strands for a diagram.

on the user-input, i.e., one's own ability to correctly enumerate the loops with respect to the input enumerations chosen for the **Diagram** object. For example, the three labeled smoothings $g_1, g_2, g_3 \in \mathcal{C}(D)$ in Figure 6.2 are encoded in lines 7-9 of the code below. Generators in $\mathcal{C}(D)$ have a print method (line 10) to reveal their binary sequence, strand sequences (s_j) , component sequences (c_j) , label, and bigrading (calculated using Equations 2.12 and 2.13).

An arbitrary chain element in $\mathcal{C}(D)$ is a linear combination of generators $\sum_{i=1}^m a_i \alpha_i$ and is encoded as a **Chain** object, whose attributes consist of an m -tuple (α_i) of Generator objects and an m -tuple (a_i) of coefficients. We have encoded the chain $c = g_1 + g_2$ in line 11. These objects have a similar print method to generators (line 12). They also have the ability to add a summand $a_{m+1} \alpha_{m+1}$ to the chain (line 13).

```

7 sage: g1 = Generator(D, "0000", "x1")
8 sage: g2 = Generator(D, "0000", "1x")
9 sage: g3 = Generator(D, "0000", "xx")
10 sage: g1.printGenerator()
-----
Generator
  binary sequence:      0000
  strand sequences:    [[1,2,3,4], [2,3,4,1]]
  component sequences: [[1,2,1,2], [1,2,1,2]]
  label:               x1
  grading:             (0,4)
-----
11 sage: c = Chain(D,[g1,g2],[1,1])
12 sage: c.printChain()
-----
Chain
  bigrading: (0,4)
-----
Generator #1
  binary sequence:      0000
  strand sequences:    [[1,2,3,4], [2,3,4,1]]
  components sequences: [[1,2,1,2], [1,2,1,2]]
  label:               x1
  grading:             (0,4)
  coefficient:         1
Generator #2

```

```

binary sequence:      0000
strand sequences:    [[1,2,3,4], [2,3,4,1]]
components sequences: [[1,2,1,2], [1,2,1,2]]
label:              1x
grading:            (0,4)
coefficient:        1
-----
13 sage: c.addSummand(g2,-1) #prints the same as line 10

```

A **ChainComplex** object takes as input the **Diagram** D and produces the generators of the Khovanov chain groups $\mathcal{C}(D)$ by creating a labeled smoothing for each admissible labeling of the 2^n binary sequences of length n . This object has a method for printing the generators of a specific bigrading (line 15). The differential of the chain complex $\mathcal{C}(D)$ is encoded as a pair of methods, acting either on a **Generator** (line 16) or a **Chain** (line 18). We may check if a given a chain c is a cycle using the method from line 19. In particular, the code checks if $d(c) = 0$ by comparing the trivial **Chain** object 0 with the output of the method from line 18 applied to the **Chain** representing c . Finally, we also allow for the differential from a specific bigrading

$$d^{h,q}: \mathcal{C}^{h,q}(D) \rightarrow \mathcal{C}^{h+1,q}(D)$$

to be printed as an array (line 21).

```

14 sage: CC = ChainComplex(D)
15 sage: CC.printChainGroup(0,4) #returns the same as line 12
16 sage: CC.d(g1).printChain()
-----
Chain
  bigrading: (1,4)
-----
Generator #1
  binary sequence:      0001
  strand sequences:    [[1,2,3,4,4,3,2,1]]
  components sequences: [[1,2,1,2,1,2,1,2]]
  label:              x
  grading:            (1,4)
  coefficient:        1
Generator #2
  binary sequence:      0010
  strand sequences:    [[1,2,3,3,2,1,4,4]]
  components sequences: [[1,2,1,2,1,2,1,2]]

```



```

label:          x
grading:        (1,4)
coefficient:    1
Generator #3
binary sequence: 0100
strand sequences: [[1,2,2,1,4,3,3,4]]
components sequences: [[1,2,1,2,1,2,1,2]]
label:          x
grading:        (1,4)
coefficient:    1
Generator #4
binary sequence: 1000
strand sequences: [[1,1,4,3,2,2,3,4]]
components sequences: [[1,2,1,2,1,2,1,2]]
label:          x
grading:        (1,4)
coefficient:    1
-----
17 sage: CC.d(g2).printChain() #returns the same as line 16
18 sage: CC.dChain(Chain(D,[g1,g2],[1,-1]).printChain()
0
19 sage: print(CC.isCycle(Chain(D,[g1,g2],[1,-1]))
True
20 sage: CC.printChainGroup(1,4) #returns the same as line 16
21 sage: CC.printChainMap(-1,4)
-----
Chain Map (-1,4) --> (0,4)
-----
[[0], [0]]
22 sage: CC.printVector(Chain(D,[g2,g1],[-1,1]))
[1, -1]
23 sage: print(CC.isBoundary(Chain(D,[g1,g2],[1,-1])))
False

```

From here it should be clear how we determine if a chain in $\mathcal{C}^{h,q}(D)$ represents a trivial homology class. We have already seen that we can: check that the chain is a cycle; calculate the chain groups $\mathcal{C}^{h,q}(D)$ and $\mathcal{C}^{h+1,q}(D)$; represent the cycle as a vector \mathbf{b} in $\mathcal{C}^{h+1,q}(D)$, with respect to the chosen basis (line 22); calculate the chain map $d^{h,q}$ as a matrix \mathbf{M} (line 21); and finally,

check if \mathbf{b} is in the image of \mathbf{M} (line 23).

Remark 6.2.1. There are two main restrictions to this code. First, the diagram for the knot cannot contain either of the images from Figure 6.3. This is because the code cannot detect the orientation of the unknot component by examining the strands. Second, the code does not run efficiently enough to work for knots with more than 13 crossings.

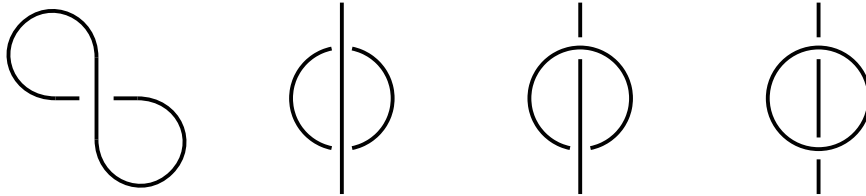


Figure 6.3: A set of link diagrams that our SageMath program does not handle.

6.3. Applications

To give an explicit application of the SageMath program from the previous section, we will reprove Theorem 5.3.3 by showing that the slice disks D_ℓ and D_r bounding 9_{46} produce distinct φ -classes. Previously, we proved this theorem by showing $\varphi(D_\ell) \pm \varphi(D_r)$ are mapped nontrivially by a (nonorientable) cobordism $C: 9_{46} \rightarrow 3_1 \# 3_1$. Here, we will directly show that $\varphi(D_\ell) \pm \varphi(D_r)$ are nontrivial in $\mathcal{H}(9_{46})$.

The ϕ -cycles associated to D_ℓ and D_r were calculated in Section 5.3, and are given in Figure 5.2. We will show these cycles represent distinct homology classes by showing their sum/difference is not a boundary in the chain complex associated to the diagram from Figure 6.4. We encode the chain complex $\mathcal{C}(9_{46})$ in lines 1-3 using enumerations from the same figure. The generators that make up the ϕ -cycles representing the relevant φ -classes are encoded in lines 4-31. The chains $\phi_l + \phi_r$ and $\phi_l - \phi_r$ are encoded in lines 32-33. We ensure these chains are cycles and conclude that they are not boundaries in $\mathcal{C}(9_{46})$ in lines 34 and 35, respectively.

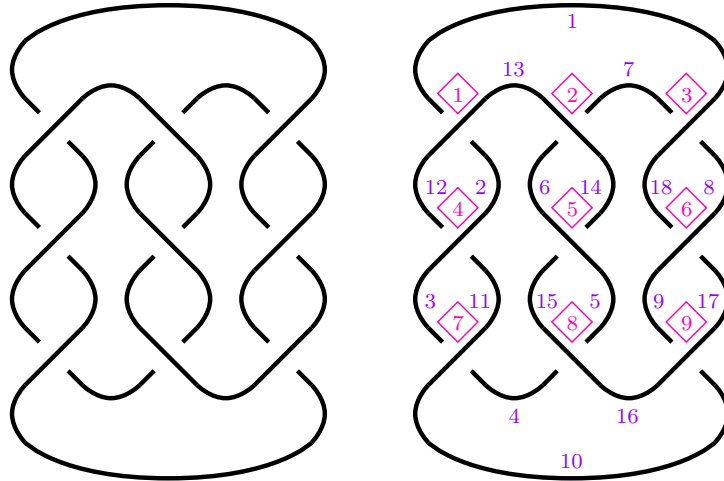


Figure 6.4: A diagram for 9_{46} with enumerations of its crossings and strands.

```

1 sage: crossings = [[1,12,2,13],[6,14,7,13],[7,18,8,1],[11,2,12,3],
2 sage:               [14,6,15,5],[17,8,18,9],[3,10,4,11],[4,16,5,15],[9,16,10,17]]
3 sage: D = Diagram(crossings)
4 sage: CC = ChainComplex(D)
5 sage: l1 = Generator(D, "011011101", "1111")
6 sage: l2 = Generator(D, "101011101", "111x11")
7 sage: l3 = Generator(D, "101011101", "1x1111")
8 sage: l4 = Generator(D, "011101101", "111x11")
9 sage: l5 = Generator(D, "011101101", "1x1111")
10 sage: l6 = Generator(D, "101101101", "11x11x11")
11 sage: l7 = Generator(D, "101101101", "11x1x111")
12 sage: l8 = Generator(D, "101101101", "1x111x11")
13 sage: l9 = Generator(D, "101101101", "1x11x111")
14 sage: l10 = Generator(D, "011011011", "1111")
15 sage: l11 = Generator(D, "101011011", "1111")
16 sage: l12 = Generator(D, "011101011", "1111")
17 sage: l13 = Generator(D, "101101011", "111x11")
18 sage: l14 = Generator(D, "101101011", "1x1111")
19 sage: r1 = Generator(D, "111111100", "1111")
20 sage: r2 = Generator(D, "101111101", "11111x")
21 sage: r3 = Generator(D, "101111101", "1111x1")
22 sage: r4 = Generator(D, "111101101", "11111x")
23 sage: r5 = Generator(D, "111101101", "1111x1")
24 sage: r6 = Generator(D, "101101101", "11111x1x")
25 sage: r7 = Generator(D, "101101101", "11111xx1")
26 sage: r8 = Generator(D, "101101101", "1111x11x")

```

```

26 sage: r9 = Generator(D, "101101101", "1111x1x1")
27 sage: r10 = Generator(D, "111111111", "1111")
28 sage: r11 = Generator(D, "101111111", "1111")
29 sage: r12 = Generator(D, "111101111", "1111")
30 sage: r13 = Generator(D, "101101111", "1111x")
31 sage: r14 = Generator(D, "101101111", "1111x1")
32 sage: c1 = Chain(D, [l1,...,l14,r1,...,r14],[1,...,1, 1,..., 1])
33 sage: c2 = Chain(D, [l1,...,l14,r1,...,r14],[1,...,1,-1,...,-1])
34 sage: [CC.isCycle(c1), CC.isBoundary(c1)] #Returns [True, False]
35 sage: [CC.isCycle(c2), CC.isBoundary(c2)] #Returns [True, False]

```

Chapter 7: Duals and relative surfaces in the 4-ball

In this chapter, we reverse the approach from Chapter 5 by considering the maps induced by link cobordisms $L \rightarrow \emptyset$. In Section 7.1, we discuss these cobordisms and their induced maps. In Section 7.2, we use these maps to extract an invariant of the boundary-preserving isotopy class of the surface, analogous to the φ -class. Finally, in Section 7.3, we apply this invariant to distinguish numerous pairs of surfaces in the 4-ball, including exotic pairs.

7.1. Dual link cobordisms

As we have seen, a smooth, compact, oriented surface Σ embedded in the 4-ball can be regarded as a link cobordism $\Sigma: \emptyset \rightarrow L$. We may obtain a second link cobordism $\Sigma^*: L \rightarrow \emptyset$ by reflecting Σ through the interval factor of $S^3 \times [0, 1]$, having the effect of reversing the cobordism¹. As a result, a movie for Σ^* is obtained by reversing the movie for Σ .

Definition 7.1.1. The link cobordism $\Sigma^*: L \rightarrow \emptyset$ induced by a smooth, compact, oriented surface Σ properly embedded in the 4-ball is called the **dual link cobordism** of Σ . Given a surface diagram $S: D \rightarrow \emptyset$ of the link cobordism, the associated map on the Khovanov chain complex $\mathcal{C}_S(\Sigma^*): \mathcal{C}(D) \rightarrow \mathbb{Z}$ is called the **dual chain map** associated to Σ , and the map it induces on Khovanov homology $\mathcal{H}_S(\Sigma^*): \mathcal{H}(D) \rightarrow \mathbb{Z}$ is called the **induced dual map** on Khovanov homology associated to Σ .

All of the hard work from Section 3 can be reproduced for dual link cobordisms and their associated maps. In particular, we highlight analogous results regarding isotopy in $S^3 \times [0, 1]$ and B^4 (Corollary 3.2.4) and diagram independence (Corollary 3.3.3). Note that because the domain and codomain have switched, Corollary 3.3.3 has been strengthened. As before, Corollary 7.1.3 means the surface diagram can be removed from our notation.

Corollary 7.1.2. *The induced dual map on Khovanov homology associated to a surface in the 4-ball is invariant, up to sign, under boundary-preserving isotopy of the surface.*

Corollary 7.1.3. *The induced dual map is independent of the chosen surface diagram.*

¹To be clear, we define $r: S^3 \times [0, 1] \rightarrow S^3 \times [0, 1]$ by $r(s, t) = (s, 1 - t)$ and set $\Sigma^* = r(\Sigma)$.

Remark 7.1.4. Dual link cobordisms get their name from the fact that the associated dual chain map is, loosely, the dual of the induced chain map, up to isomorphism. That is, we have the following diagram:

$$\begin{array}{ccccc}
\mathcal{C}(K_1) & \xrightarrow{\Psi_1} & (\mathcal{C}(K_1))^* & \xrightarrow{\psi_1} & \mathcal{C}(\bar{K}_1) \\
\uparrow c(\Sigma) & & \downarrow (c(\Sigma))^* & & \downarrow c(\Sigma^*) \\
\mathcal{C}(K_0) & \xrightarrow{\Psi_0} & (\mathcal{C}(K_0))^* & \xrightarrow{\psi_0} & \mathcal{C}(\bar{K}_0)
\end{array}$$

where $(\cdot)^*$ indicates the dual, $(\bar{\cdot})$ indicates the mirror image of a knot diagram, $\Psi_{0,1}$ are the dual maps ($v \mapsto v^*$), and $\psi_{0,1}$ are isomorphisms ($1^* \mapsto x; x^* \mapsto 1$). The requirement to mirror the knot diagrams is simply there to make things work.

Remark 7.1.5. As might be expected, we do not typically go through the long process of taking a surface in the 4-ball, considering its induced link cobordism $\Sigma: \emptyset \rightarrow L$, constructing a movie for Σ , and finally producing a movie for the desired dual cobordism $\Sigma^*: L \rightarrow \emptyset$. Instead, we simply write down a movie beginning with a diagram D for L and ending with an empty link \emptyset , and this movie induced a surface in the 4-ball.

7.2. φ^* -classes

As in the exploration of φ -classes (Section 5.1), we employ the fact that the induced dual map acts as an invariant of the boundary-preserving isotopy class of the associated surface in the 4-ball (Corollary 7.1.2). In particular, we extract specific invariants from the induced dual maps, and in comparison to φ -classes, the current invariants carry a new degree of flexibility. Previously, we saw that a link cobordism $\Sigma: \emptyset \rightarrow L$ and diagram D for L gave rise to a single class $\varphi(\Sigma) \in \mathcal{H}(D)$, which acted as a proxy for the the associated induced map $\mathcal{H}(\Sigma): \mathbb{Z} \rightarrow \mathcal{H}(D)$, in the sense that $\varphi(\Sigma)$ determined the entire map $\mathcal{H}(\Sigma)$, through which it itself acted as an invariant of the boundary-preserving isotopy of Σ . In the current setting, the dual link cobordism $\Sigma^*: L \rightarrow \emptyset$ induces a map $\mathcal{H}(\Sigma^*): \mathcal{H}(D) \rightarrow \mathbb{Z}$ that is not (necessarily) determined by a single class.

Definition 7.2.1. For a smooth, compact, oriented surface $\Sigma \subset B^4$ with boundary link represented by a diagram D , and a Khovanov homology class $\varphi \in \mathcal{H}(D)$, the integer

$$\varphi^*(\Sigma) := \mathcal{H}(\Sigma^*)(\varphi) \in \mathbb{Z}$$

is called the φ^* -class of Σ . Similarly, for the cycle $\phi \in \mathcal{C}(D)$ representing φ , the integer

$$\phi^*(\Sigma) := \mathcal{C}(\Sigma^*)(\phi) \in \mathbb{Z}$$

is called the ϕ^* -cycle of Σ .

Remark 7.2.2. It should be noted that a ϕ^* -cycle is not necessarily the dual of the ϕ -cycle. We do not mean $\phi^*(\Sigma) = (\phi(\Sigma))^*$ when defining a ϕ^* -cycle for a surface. This is only the case when we set $\phi = \phi(\Sigma)$, which (in practice) counteracts the idea of *simplifying* calculations through the choice of ϕ .

Note that each class $\varphi \in \mathcal{H}(D)$ will produce an associated φ^* -class via the induced dual map. As the map $\mathcal{H}(\Sigma^*)$ is invariant under boundary-preserving isotopy of Σ^* , each φ^* -class is also an invariant of the boundary-preserving isotopy of Σ^* . In particular, a pair of surfaces $\Sigma_{0,1}$ having a common boundary link L and inducing dual maps that disagree on a chosen φ^* -class,

$$\varphi^*(\Sigma_0) = \mathcal{H}(\Sigma_0^*)(\varphi) \neq \mathcal{H}(\Sigma_1^*)(\varphi) = \varphi^*(\Sigma_1)$$

are necessarily non-isotopic relative their boundary. Thus, we may again isolate the invariance of the entire map $\mathcal{H}(\Sigma_{0,1}^*)$ to individual classes, with the additional flexibility to *choose* the class $\varphi \in \mathcal{H}(D)$ with which we will study invariance.

As the boundary-preserving isotopy class of Σ and Σ^* are equivalent (isotopies for either are related by a diffeomorphism that reverses the interval factor of $S^3 \times [0, 1]$), Corollary 7.2.3 implies that φ^* -classes are invariants of the boundary-preserving isotopy of Σ and Σ^* . We summarize this as the following result.

Corollary 7.2.3. *For a smooth, closed, oriented surface Σ embedded in the 4-ball with boundary-link $L \subset S^3$, represented by a diagram D , the φ^* -class associated to some class $\varphi \in \mathcal{H}(D)$ is an up-to-sign invariant of the boundary-preserving isotopy class of Σ .*

We again highlight the relevance of the ϕ^* -cycle. Note that the maps $\mathcal{C}(\Sigma^*)$ and $\mathcal{H}(\Sigma^*)$ have codomain supported in the $(0, 0)$ -grading, so the φ^* -class is necessarily the same as the ϕ^* -cycle. As all calculations are based on the ϕ^* -cycle, there is generally no need to bother with the associated φ^* -class. For these reasons, we often use the cycle and class interchangeably. The only cause for caution is that, when defining a φ^* -class, we must ensure that the ϕ^* -cycle with which it is represented is indeed a cycle.

As the induced dual map is independent of the chosen surface diagram (Corollary 7.1.3), we also have diagram invariance of the φ^* -classes, as in the following Corollary.

Corollary 7.2.4. *The φ^* -classes are independent of the chosen diagram.*

7.3. φ^* -distinguished pairs of surfaces

The motivation for defining and studying φ^* -classes is to improve on and extend the distinguishing abilities of φ -classes. Considering the concerns expressed in Section 5.5, there are two areas to address: φ -classes are hard to compute and to distinguish. The latter concern has already vanished: the φ^* -classes are integral invariants, which are easily distinguished. We will see shortly that the former concern is significantly reduced by the flexibility of choosing the φ^* -class with which we distinguish surfaces.

Definition 7.3.1. A family of smooth, oriented, compact surfaces $\Sigma_1, \dots, \Sigma_n \subset B^4$ that are properly embedded and share a common boundary link $L \subset S^3$, represented by a diagram D , are **φ^* -distinguished** by their maps on Khovanov homology if there exists a class $\varphi \in \mathcal{H}(D)$ for which the associated φ^* -classes are pairwise distinct, up to sign, that is $\varphi^*(\Sigma_i) \neq \pm\varphi^*(\Sigma_j)$ for $i \neq j$.

Throughout the remainder of this section, we give pairs of surfaces $\Sigma_{0,1}$ in the 4-ball that are φ^* -distinguished via

$$\varphi^*(\Sigma_0) = 0 \neq \pm 1 = \varphi^*(\Sigma_1)$$

As of yet, we have not constructed natural examples in which the φ^* -class is not 0 or ± 1 , though we have no reason to expect them not to exist (by *natural* we mean excluding cases where we simply alter the coefficient of a φ^* -class).

The flexibility to choose the class φ which φ^* -distinguishes $\Sigma_{0,1}$ is key to our success. How does one choose φ , especially when the Khovanov homology group $\mathcal{H}(D)$ to which it belongs can be exceedingly complex? The current methods for choosing φ are more an art than a science, but we summarize some of our methods here. In our work, we typically began with the orientation-induced smoothing where 0-tracing loops are x -labeled and all other loops are 1-labeled. This labeled state is always a cycle lying in homological grading $h = 0$. However, it may not have the desired quantum grading; a surface Σ induces a $(0, \chi(\Sigma))$ -graded map, so a cycle must lie in the $(0, -\chi(\Sigma))$ -grading in order for it to be mapped to the $(0, 0)$ -supported chain group $\mathcal{C}(\emptyset) = \mathbb{Z}$. While the homological grading (and the underlying diagram) determines the overall balance

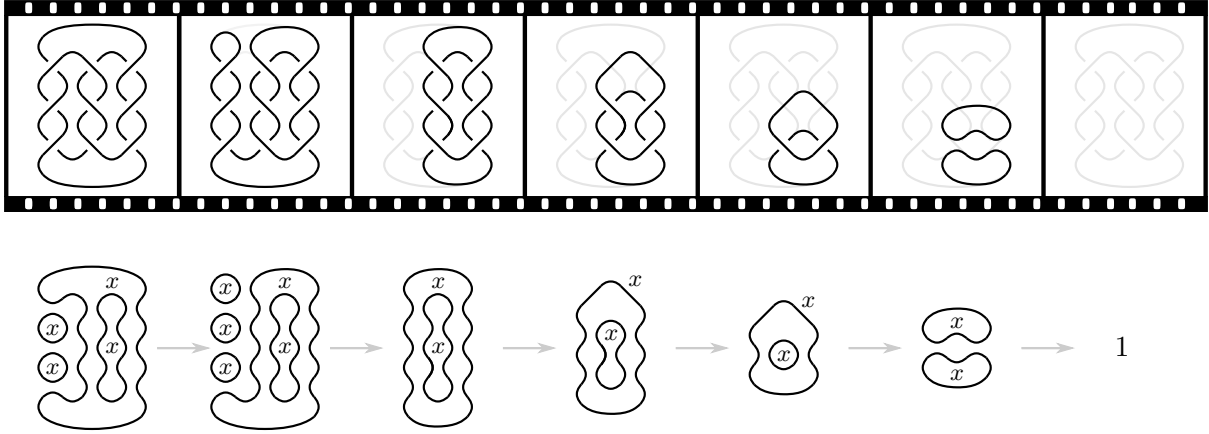


Figure 7.1: The calculation that $\phi^*(D_\ell) = 1$ for the given cycle ϕ . The top line indicates the movie used to describe D_ℓ , while the bottom line tracks the cycle ϕ throughout the chain map induced by each move in the movie.

of 0- and 1-resolutions, the quantum grading can be adjusted by varying the specific choice of crossing resolutions (which may change the number of loops in the smoothing) and the labeling of loops. We made these adjustments, keeping in mind that the result should be a cycle and should be killed by the map induced by one band move but not the other. In our core cases, the slice disks are related by a symmetry of the knot; making asymmetric adjustments to the orientation-induced smoothing helped produce the desired cycle.

Remark 7.3.2. Again, because the induced maps on Khovanov homology do not detect local knotting, any φ^* -distinguished surfaces are not obtained by local knotting.

7.3.1 Two pairs of slice disks

Consider the two slice disks D_ℓ and D_r bounding the knot 9_{46} . We saw in Section 5.3 that these slice disks were φ -distinguished; here we show they are φ^* -distinguished via the class represented by the cycle ϕ given on the bottom-left of Figure 7.1.

We first verify that ϕ is a cycle. Indeed, every 0-smoothing merges two x -labeled components, so by Proposition 2.2.7, ϕ is a cycle representing a homology class. We see immediately that $\phi^*(D_r) = 0$, as the right-hand saddle merges two x -labeled components. On the other hand, we see from Figure 7.1 that $\phi^*(D_\ell) = 1$, proving that D_ℓ and D_r are ϕ^* -distinguished.

Similar calculations can be done for the slice disks in Figure 7.2 bounding the knot $15n_{103488}$. One can quickly recognize that, again, the right-hand saddle merges two x -labeled components, forcing $\phi \mapsto 0$. The left-hand saddle splits a single x -labeled component, and after a bit of work, we see that $\phi \mapsto 1$. We leave it as an exercise to the reader to verify this calculation.

The comparative ease with which we were able to distinguish pairs of slice disks bounding 9_{46} and $15n_{103488}$ gives us hope that, not only can we improve on φ -classes as an invariant, we can use them to produce new results.

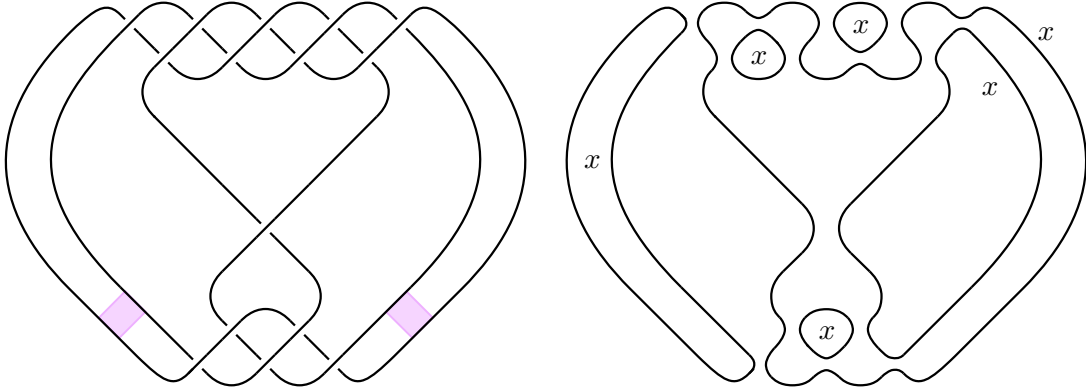


Figure 7.2: A diagram for $15n_{103488}$ and band moves describing a pair of slice disks that are ϕ^* -distinguished by the given cycle ϕ .

Remark 7.3.3. The pairs of slice disks for either knot $m(9_{46})$ and $15n_{103488}$ can be distinguished by their map on fundamental groups induced by the map which includes the knot complement into the slice disk complement. It follows that these pairs of disks are not even *topologically* isotopic rel boundary (or even homotopically isotopic). As the maps on Khovanov homology are invariants of smooth boundary-preserving isotopy, the natural follow-up question is, can the maps on Khovanov homology distinguish topologically equivalent surfaces?

7.3.2 A pair of exotic slice disks

Surfaces that are topologically but are not smoothly isotopic rel boundary are called *exotic* surfaces and have been known to exist in the 4-ball [Akb91, Hay21]. Khovanov previously posed the question: can Khovanov homology detect pairs of exotic surfaces [Kho21]. We answer that question here in the affirmative.

Consider the knot $J = 17nh_{34}$ given by the knot diagram in Figure 7.3. A pair of slice disks D_ℓ and D_r bound J , described by the band moves on the diagram. We first show these slice disks are topologically equivalent, and then use the maps on Khovanov homology to show they are not smoothly equivalent. Topological equivalence relies on the following theorem [CP21, Theorem 1.2] which is proven using surgery theory.

Theorem 7.3.4 ([CP21]). *Any smooth, properly embedded disks in the 4-ball with the same boundary and whose complements have fundamental group $\pi_1 \cong \mathbb{Z}$ are topologically isotopic rel boundary.*

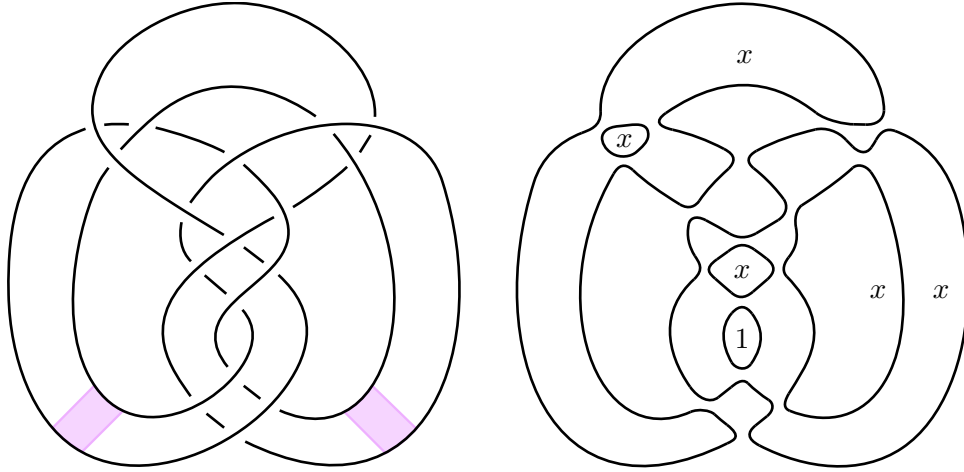


Figure 7.3: A pair of slice disks bounding the knot $J = 17nh_{34}$ that are ϕ^* -distinguished by the given cycle $\phi \in \mathcal{C}(J)$.

Theorem 7.3.5. *The slice disks D_ℓ and D_r are topologically isotopic rel boundary.*

Proof. By construction, the disks have the same boundary. By Theorem 7.3.4, it then suffices to show that the disk-exterior have fundamental group isomorphic to \mathbb{Z} .

A handle diagram for $B^4 \setminus \mathring{N}(D_\ell)$ is shown on the left side of Figure 7.4, obtained using the recipe from [GS99, §6.2]. This can be simplified to the handle diagram on the right. One can use this handle diagram to see that $B^4 \setminus \mathring{N}(D_\ell)$ has homotopy type of $S^1 \times B^3$, which has fundamental group \mathbb{Z} , as desired (c.f., [HS21]). Alternatively, after isotoping the handle diagram further to separate the 0-handles, we can obtain a presentation for the fundamental group of $B^4 \setminus \mathring{N}(D_\ell)$ which simplifies to a presentation for \mathbb{Z} (c.f., [Hay21]).

A handle diagram for the exterior of D_r is obtained from that of D_ℓ by applying a 180° rotation, so a symmetric argument shows $\pi_1(B^4 \setminus D_r) \cong \mathbb{Z}$. □

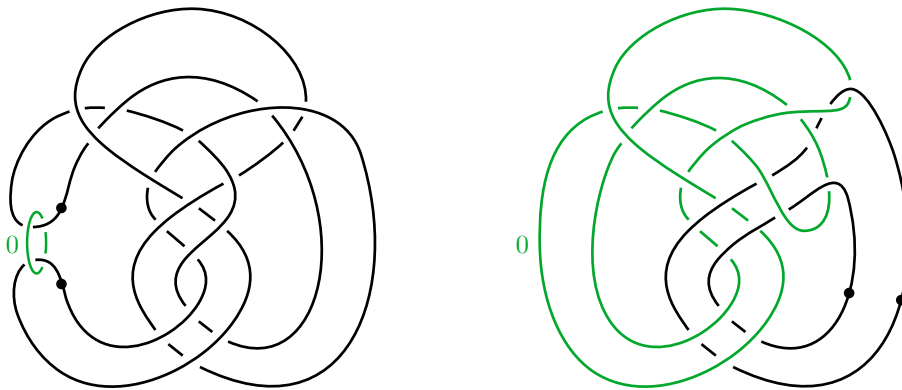


Figure 7.4: A pair of equivalent handle diagrams for the exterior of the slice disk $D_\ell \subset B^4$ bounding the knot J from Figure 7.3.

Theorem 7.3.6. *The slice disks D_ℓ and D_r are not smoothly isotopic rel boundary.*

Proof. It suffices to show that D_ℓ and D_r induce distinct maps on Khovanov homology, or equivalently, that they are φ^* -distinguished by a class $\varphi \in \mathcal{H}(J)$.

Consider the chain $\phi \in \mathcal{C}(J)$ on the right of Figure 7.3. Proposition 2.2.7 guarantees that ϕ is a cycle, as every 0-smoothing on ϕ merges two x -labeled components. Thus, ϕ represents a homology class $\varphi \in \mathcal{H}(J)$. The dual map induced by D_r immediately merges two x -labeled components, so $\varphi^*(D_r) = 0$. On the other hand, we calculate $\phi^*(D_\ell) = 1$ in Figure 7.5. Thus, D_ℓ and D_r induce distinct maps on Khovanov homology and are not smoothly isotopic rel boundary. \square

Corollary 7.3.7. *The slice disks D_ℓ and D_r are exotic.*

7.3.3 Exotic slice disks bounding asymmetric knots

For any $m \in \mathbb{Z}$, there is a ribbon concordance $C_m: J \rightarrow J_m$ from the knot J to the knot J_m depicted on the left side of Figure 7.6, having m half left-handed twists on the left-hand side of the knot. In reverse, we have a cobordism $\overline{C}_m: J_m \rightarrow J$ that performs the additional band move on J_m and caps off the resulting unknot. Attaching the ribbon concordance C_m to the slice disks D_ℓ and D_r bounding J , we obtain a pair of slice disks $D_{\ell,m}$ and $D_{r,m}$ bounding the knot J_m .

Theorem 7.3.8. *For $m \geq 0$, the disks $D_{\ell,m}$ and $D_{r,m}$ are exotic.*

Proof. The slice disks are topologically isotopic because they are constructed by extending a pair of topologically isotopic slice disks by a common link cobordism C_m . More explicitly, we may produce a topological isotopy between $D_{\ell,m}$ and $D_{r,m}$ by extending the topological isotopy between D_ℓ and D_r (from Theorem 7.3.5) across the ribbon concordance C via the identity. By construction, J_m will be fixed throughout.

To distinguish $D_{m,\ell}$ and $D_{r,\ell}$ smoothly, we show they induce distinct maps on Khovanov homology, or equivalently, that they are ϑ_m^* -distinguished by a class $\vartheta_m \in \mathcal{H}(J_m)$. Consider the chain $\theta_m \in \mathcal{C}(J_m)$ on the right-hand side of Figure 7.6. Again, this is a cycle because each 0-smoothing merges a pair of distinct x -labeled components, and so, it represents a class $\vartheta_m \in \mathcal{H}(J_m)$. It is straightforward to check that the map induced by \overline{C}_m sends θ_m to the cycle $\phi \in \mathcal{C}(J)$ defined in Theorem 7.3.6. We then have

$$\theta_m^*(D_{\ell,m}) = \mathcal{C}(D_{\ell,m}^*)(\theta_m) = \mathcal{C}(D_\ell^* \circ \overline{C}_m)(\theta_m) = \mathcal{C}(D_\ell^*)(\phi) = \phi^*(D_\ell) = 1$$

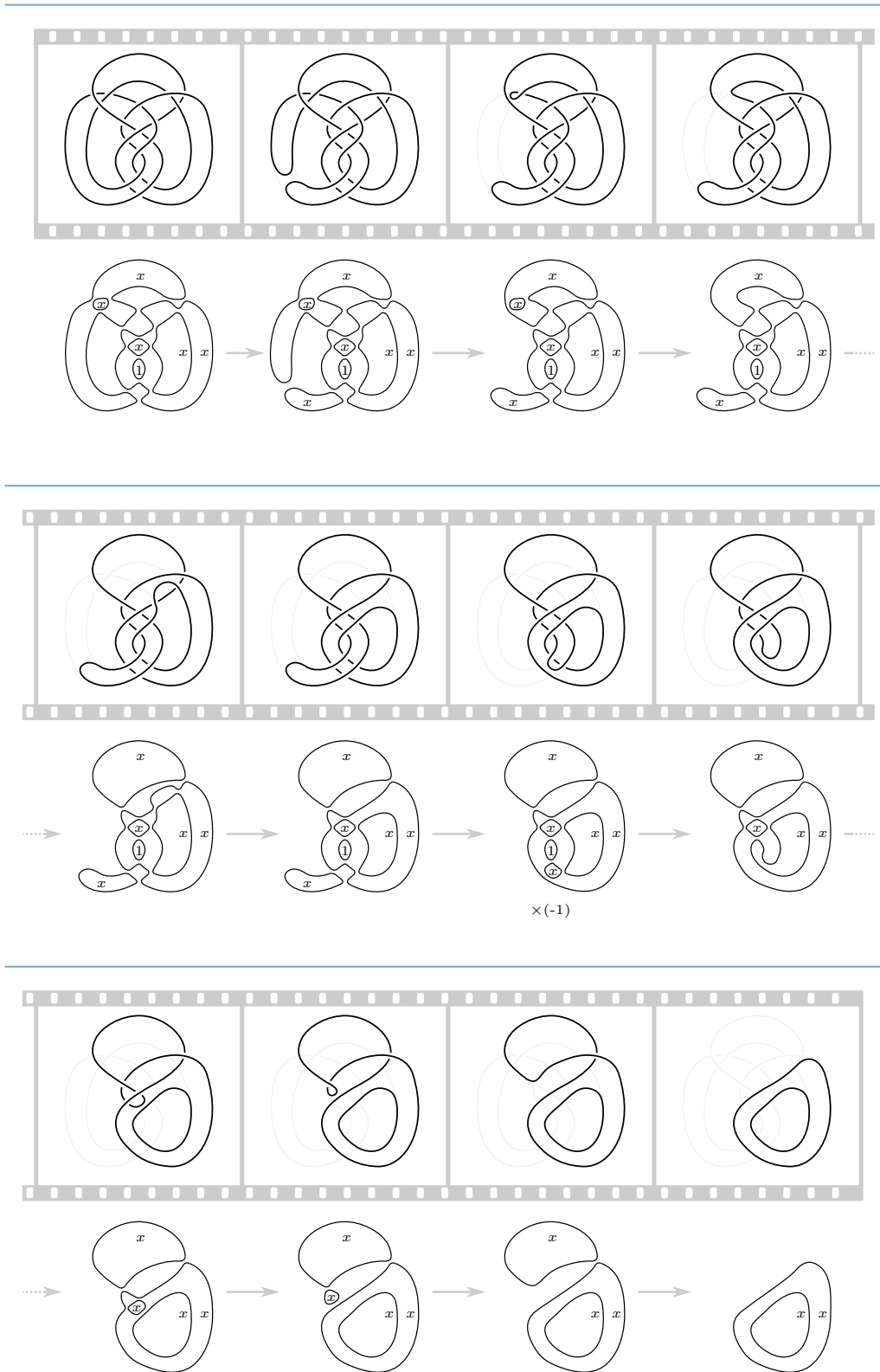


Figure 7.5: A movie description of the slice disk D_ℓ and the behavior of the distinguished cycle $\phi \in \mathcal{C}(J)$ under the cobordism map induced by this slice.

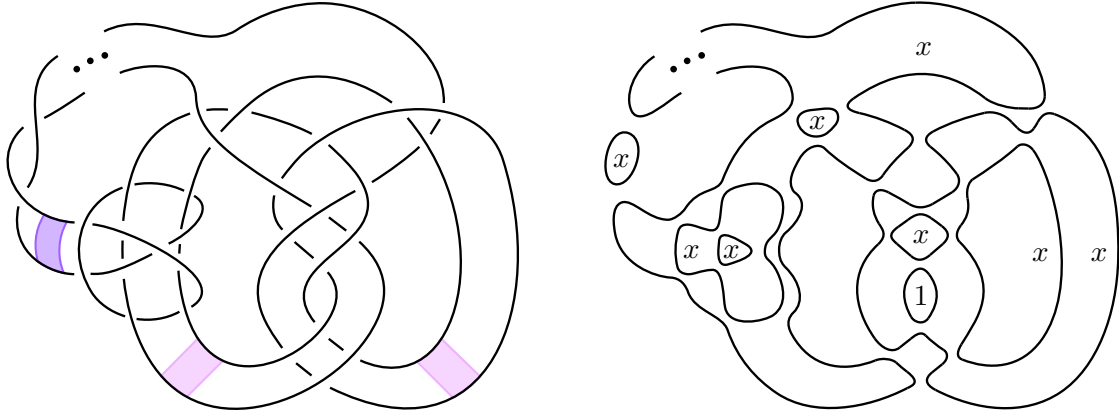


Figure 7.6: A pair of slice disks $D_{m,\ell}$ and $D_{m,r}$ bounding an asymmetric version J_m of the knot J . They are θ_m^* -distinguished by the given cycle $\theta \in \mathcal{C}(J_m)$.

Similarly, we see that $\theta_m^*(D_{r,m}) = \phi^*(D_r) = 0$. Thus, the slice disks $D_{\ell,m}$ and $D_{r,m}$ are ϑ_m^* -distinguished, as desired. \square

Unlike the examples in §7.3.1-7.3.2, which involve slice knots with nontrivial symmetries, the knots J_m are *asymmetric*. That is, every self-diffeomorphism of the pair (S^3, J_m) is isotopic (through diffeomorphisms of the pair) to the identity. This is proven in [HS21, Appendix A2].

7.3.4 Higher genus exotic slices

For $n \geq 0$, there is a genus n link cobordism $\Sigma_n: J \rightarrow J'_n$ from the knot J in Figure 7.3 to the knot J'_n depicted on the left side of Figure 7.7, having n full right-handed twists on the right-hand side of the knot. In reverse, we have a cobordism $\bar{\Sigma}_n: J'_n \rightarrow J$ obtained by performing the additional band moves on J'_n . We obtain a pair of surfaces $\Sigma_{\ell,n}$ and $\Sigma_{r,n}$ bounding J'_n by gluing Σ_n to the slice disks D_ℓ and D_r , respectively.

Theorem 7.3.9. *For $n \geq 0$, the surfaces $\Sigma_{\ell,n}$ and $\Sigma_{r,n}$ are exotic.*

Proof. The proof follows nearly identical to that of Theorem 7.3.8. The surfaces are topologically isotopic because we have extended topologically isotopic disks by the same link cobordism Σ_n . They are not, however, smoothly isotopic, as they are ϱ_n^* -distinguished by the cycle $\rho_n \in \mathcal{C}(J'_n)$ shown on the right-hand side of Figure 7.7. The calculations are similar: $\rho_n^*(\Sigma_{\ell,n})$ is distinguished from $\rho_n^*(\Sigma_{r,n})$ by factoring the induced maps through the cobordism $\bar{\Sigma}_n$ and noting that $\mathcal{C}(\bar{\Sigma}_n)(\rho_n) = \phi$. Therefore, we conclude that $\Sigma_{\ell,n}$ and $\Sigma_{r,n}$ are ϱ_n^* -distinguished. \square

A knot $J_{m,n}$ that is both asymmetric and of higher genus may be produced by, loosely, applying both link cobordisms C_m and Σ_n to the knot J . More explicitly, for $m, n \geq 0$, there is a

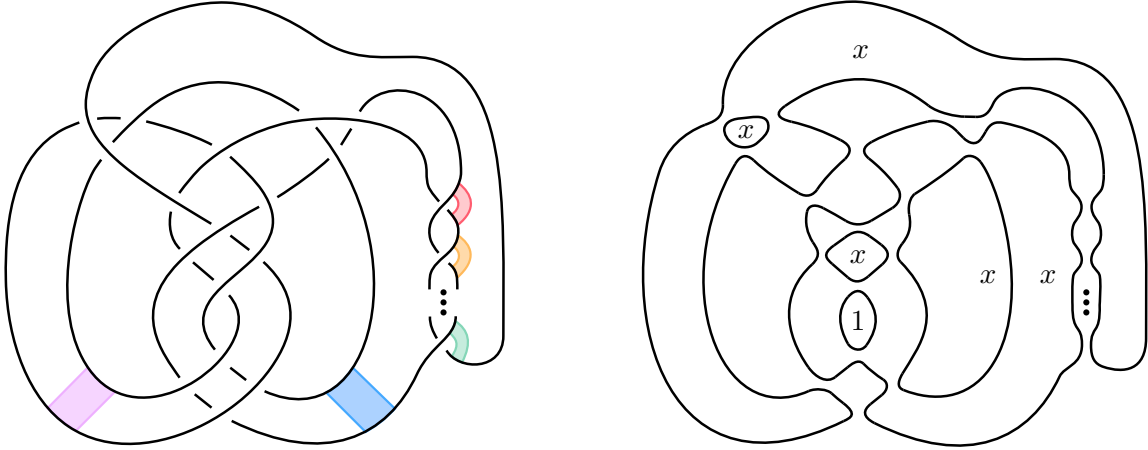


Figure 7.7: A pair of surfaces $\Sigma_{\ell,n}$ and $\Sigma_{r,n}$ bounding a higher-genus version J'_n of the knot J . They are ρ_n^* -distinguished by the given cycle $\rho_n \in \mathcal{C}(J'_n)$.

link cobordism $\Sigma_{m,n}$ from J to the knot $J_{m,n}$ depicted in Figure 7.8, having m half left-handed twists on the left-hand side and n full right-handed twists on the right-hand side of the knot. A pair of genus n surfaces $\Sigma_{\ell,m,n}$ and $\Sigma_{r,m,n}$ bounding $J_{m,n}$ are obtained in the expected manner and are exotically isotopic rel boundary, being $\varphi_{m,n}^*$ -distinguished by a class $\varphi_{m,n} \in \mathcal{H}(J_{m,n})$.

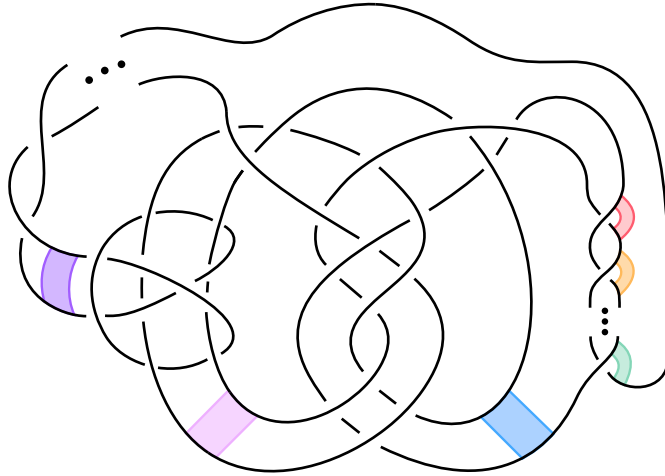


Figure 7.8: A higher-genus, asymmetric version $J_{m,n}$ of J , bounding surfaces $\Sigma_{\ell,m,n}$ and $\Sigma_{r,m,n}$ that are distinguished by their induced maps on Khovanov homology.

7.3.5 Extensions to absolute isotopy

The above results were extended to ambient isotopy of the surfaces in [HS21]. The techniques diverge from our story, which centers Khovanov homology, and so we do not repeat them here. They're amazing though, so definitely check them out. And them's the facts.

Appendix

Appendix A: Categories

Here we describe two main categories: the cobordism category (in dimensions 2 and 3) and the category of R -modules. We also define and describe the symmetric and monoidal properties of these categories. We will use \mathbf{C} to denote a category, $\mathbf{ob}(\mathbf{C})$ to denote the objects in \mathbf{C} , and $\mathbf{mor}(\mathbf{C})$ to denote the morphisms in \mathbf{C} .

Symmetric, monoidal functors

A **monoidal** category (\mathbf{C}, \otimes) is a category \mathbf{C} equipped with a bifunctor $\otimes: \mathbf{C} \times \mathbf{C} \rightarrow \mathbf{C}$ that is associative and has a left and right identity. The notation for the bifunctor varies, as we will see below. A monoidal category (\mathbf{C}, \otimes) is **symmetric** if its bifunctor is symmetric: for all objects $A, B \in \mathbf{ob}(\mathbf{C})$ there is a natural isomorphism between $A \otimes B$ and $B \otimes A$. A symmetric, monoidal functor is a functor between symmetric, monoidal categories that (put loosely) respects the symmetry of the bifunctor.

These definitions (and their notation) are inspired by the following category.

Category of R -modules

The algebraic category we work with is the category Mod_R of R -modules over a finitely-generated, commutative ring R with unity (up to isomorphism). Monoidality in this category is obtained through the tensor product \otimes of R -modules, which is symmetric.

Category of cobordisms

The foundation of this dissertation is the n -dimensional cobordism category Cob^n . This category is critical in the definition of a topological quantum field theory, with which we define Khovanov homology.

Definition. The **cobordism category** Cob^n is a symmetric, monoidal category: the objects

are smooth, closed, oriented $(n - 1)$ -manifolds embedded in \mathbb{R}^n ; the morphisms are smooth, closed, oriented n -manifolds Σ that are properly embedded in $\mathbb{R}^n \times [0, 1]$, considered up to homotopy equivalence and composed by stacking and rescaling the interval factor; the bifunctor is the disjoint union \sqcup with identity the empty manifold \emptyset .

Remark. One might be able to get by without embedding the objects in \mathbb{R}^n , however, we run into more headaches when we wish to decompose the morphisms. In the embedded setting, the interval factor of $\mathbb{R}^n \times [0, 1]$ induces a Morse function on a given morphism.

Remark. In similar resources, the condition that morphisms are considered up to homotopy equivalence is omitted and used to form a quotient category Cob_n^n .

This dissertation focuses on the case $n = 2$ and $n = 3$. Note that the objects in Cob^3 are links and the morphisms are link cobordisms; these are discussed in detail in Section 2.1. The category Cob^2 is discussed in detail below.

(2+1)-dimensions The 3-dimensional cobordism category can be described very explicitly. The objects in Cob^3 are planar 1-manifolds, or simply collections of circles in the plane. The morphisms in Cob^3 are surfaces in $\mathbb{R}^2 \times [0, 1]$, which can be decomposed using the following process. A morphism $S \subset \mathbb{R}^2 \times [0, 1]$ can be isotoped so that, with respect to the interval factor, it has finitely-many, nondegenerate critical values x_1, \dots, x_n . These values correspond to handle attachments, isolated within the surfaces $S_i = S \cap (\mathbb{R}^2 \times [x_i - \varepsilon, x_i + \varepsilon])$. Each S_i is a disjoint union of a finite number of cylinders and exactly one *fundamental cobordism*, illustrated in Figure ???. Away from S_i , the surface is (isotopic to) a product. Fundamental cobordisms are extremely useful, as they allow us to easily describe any morphism in Cob^3 as a composition of many small, simple cobordisms.

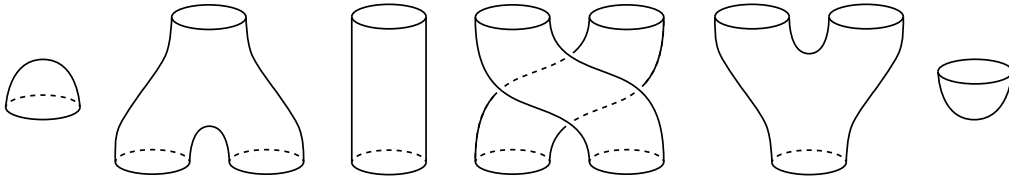


Figure A.1: The fundamental cobordisms (left to right): cap, product, cylinder, permutation coproduct, cup.

As we will often write a cobordism in Cob^3 as a composition of fundamental cobordisms, it will be convenient to develop a shorthand. We denote collection of $n \geq 0$ embedded circles in the plane $\bigsqcup_n S^1 \hookrightarrow \mathbb{R}^2$ by \mathcal{O}^n . When n is small, say $n = 2$, we write $\mathcal{O} \sqcup \mathcal{O}$. Thus, we may write the fundamental cobordisms in Figure ??? as cobordisms on \mathcal{O}^n for some n .

- (\mathcal{X}) the cap, $\mathcal{X}: \bigcirc \rightarrow \emptyset$
- ($\bigcirc\text{-}\bigcirc$) the product, $\bigcirc\text{-}\bigcirc: \bigcirc \sqcup \bigcirc \rightarrow \bigcirc$
- (id) the cylinder, $\text{id}: \bigcirc \rightarrow \bigcirc$
- (perm) the permutation, $\text{perm}: \bigcirc^2 \rightarrow \bigcirc^2$
- (\bigoplus) the coproduct, $\bigoplus: \bigcirc \rightarrow \bigcirc \sqcup \bigcirc$
- (\mathcal{Y}) the cup, $\mathcal{Y}: \emptyset \rightarrow \bigcirc$

This shorthand also allows us to write any morphism in Cob^3 as a composition of fundamental cobordisms, which we will read right to left. For example, a closed sphere can be written $S = \mathcal{X} \circ \mathcal{Y}$ and a closed torus as $T = \mathcal{X} \circ \bigcirc\text{-}\bigcirc \circ \bigoplus \circ \mathcal{Y}$. It will be useful to adopt a shorthand for one additional surface, namely the punctured torus. Let $\mathcal{X}\mathcal{Y}: \bigcirc \rightarrow \emptyset$ denote the composition $\mathcal{X}\mathcal{Y} = \mathcal{X} \circ \bigcirc\text{-}\bigcirc \circ \bigoplus$, and let $\mathcal{Y}\mathcal{X}: \emptyset \rightarrow \bigcirc$ denote the composition $\mathcal{Y}\mathcal{X} = \bigcirc\text{-}\bigcirc \circ \bigoplus \circ \mathcal{Y}$.

The notation \sqcup we used to describe collections of disjoint spheres in the plane can also be used to describe collections of disjoint surfaces in $\mathbb{R}^2 \times [0, 1]$. For example, we might write $\mathcal{X} \sqcup \bigoplus$ to mean the morphism $\bigcirc^2 \rightarrow \bigcirc^3$ where \mathcal{X} acts on one copy of \bigcirc and \bigoplus acts on the other. This is particularly useful when writing out the surfaces S_i used to define the fundamental cobordisms (above), which can be expressed as

$$\text{id} \sqcup \cdots \sqcup \text{id} \sqcup T \sqcup \text{id} \sqcup \cdots \sqcup \text{id} \tag{7.1}$$

where T is one of \mathcal{X} , $\bigcirc\text{-}\bigcirc$, \bigoplus , \mathcal{Y} . The key aspect of the operation \sqcup is that it gives Cob^3 the structure of a symmetric, monoidal category (Cob^3, \sqcup) .

Appendix B: Topological quantum field theories

In this section, we discuss *topological quantum field theories*, or TQFTs. A deep understanding of TQFTs is not necessary to understand this dissertation, however, we wish to draw some attention to one aspect of 2-dimensional TQFTs that is generally omitted from the literature on Khovanov homology: how does one construct a 2-dimensional TQFT and ensure that it is well-defined?

Definition. A $(n + 1)$ -dimensional topological quantum field theory is a symmetric, monoidal functor $\mathcal{G}: (\text{Cob}^{n+1}, \sqcup) \rightarrow (\text{Mod}_R, \otimes)$ satisfying $\mathcal{G}(\emptyset) = R$.

This definition is based on [Ati90]. As we are only concerned with constructing 2-dimensional TQFTs, we restrict to $n = 2$ henceforth.

Building a 2-dimensional TQFT Suppose we are defining a 2-dimensional topological quantum field theory \mathcal{G} . Recall that the objects in the cobordism category Cob^3 are collections of finitely many smooth, disjoint circles in the plane. For such objects, we have $\mathcal{G}(\sqcup S^1) = \otimes \mathcal{G}(S^1)$ by the monoidality of \mathcal{G} . It then suffices to define $\mathcal{G}(S^1)$ and extend via this definition. In short, to define a topological quantum field theory on the objects of Cob^3 , it suffices to choose a finitely-generated R -module V and set $\mathcal{G}(S^1) = V$. By default, we also set $\mathcal{G}(\emptyset) = R$, as in the above definition.

The morphisms in the cobordism category are surfaces embedded in $\mathbb{R}^2 \times [0, 1]$. Recall that after much consideration, these cobordisms can be decomposed into a collection of fundamental cobordisms, as in Figure ???. Thus, it suffices to define \mathcal{G} on each of the fundamental cobordisms, whereby we may decompose any morphism into a collection of local fundamental cobordisms $S = S_n \circ \cdots \circ S_2 \circ S_1$ and functorially define \mathcal{G} across this decomposition by setting

$$\mathcal{G}(S) = \mathcal{G}(S_n) \circ \cdots \circ \mathcal{G}(S_2) \circ \mathcal{G}(S_1)$$

The concern with this definition is that the chosen decomposition of S is not unique, and moreover, morphisms in Cob are considered up to boundary-preserving isotopy. Thus, we immediately run into questions of well-definedness. Does this definition of \mathcal{G} depend on the decomposition of S ? Is \mathcal{G} invariant under isotopy of S ?

Well-definedness To ensure this definition is well-defined, we must verify that it satisfies a set of relations. In particular, any two decompositions of equivalent morphisms (i.e. surfaces in

$\mathbb{R}^2 \times [0, 1]$ related by a boundary-preserving isotopy) into fundamental cobordisms are related by a sequence of births, deaths, or swaps of critical values². These relations on the critical values can be realized as isotopies of surfaces, which we illustrate in Figure B.1. These relations are called the *fundamental relations*. Thus, we conclude that if the morphisms in Mod_R obtained by the definition of \mathcal{G} on the fundamental cobordisms satisfy the equations induced by the fundamental relations, then the definition of \mathcal{G} on any surface (considered up to boundary-preserving isotopy) will be independent of the decomposition into fundamental cobordisms (as well as under boundary-preserving isotopy of the surface).

Note that with the shorthand developed in Appendix A, we can write out the fundamental relations somewhat algebraically:

$$\begin{aligned}
(\bigcirc\bigcirc \sqcup \text{id}) \circ (\text{id} \sqcup \bigoplus) &= \bigcirc\bigcirc \circ \bigoplus = (\text{id} \sqcup \bigoplus) \circ (\bigcirc\bigcirc \sqcup \text{id}) \\
(\boxtimes \sqcup \text{id}) \circ \bigoplus &= \text{id} = \bigcirc\bigcirc \circ (\text{id} \sqcup \boxtimes) \\
\bigcirc\bigcirc \circ (\text{id} \sqcup \bigcirc\bigcirc) &= \bigcirc\bigcirc \circ (\bigcirc\bigcirc \sqcup \text{id}) \\
(\text{id} \sqcup \bigoplus) \circ \bigoplus &= (\bigoplus \sqcup \text{id}) \circ \bigoplus
\end{aligned} \tag{7.2}$$

By assigning notations to the corresponding maps for each fundamental cobordism, we may write these equations out algebraically. When defined carefully, these maps give V the structure of a coassociative, cocommutative coalgebra.

- (ϵ) the map $\mathcal{G}(\boxtimes)$ is a counit $\epsilon: V \rightarrow R$
- (m) the map $\mathcal{G}(\bigcirc\bigcirc)$ is a product $m: V \otimes V \rightarrow V$
- (id) the map $\mathcal{G}(\text{id})$ is the identity map $\text{id}: V \rightarrow V$
- (Δ) the map $\mathcal{G}(\bigoplus)$ is a coproduct $\Delta: V \rightarrow V \otimes V$
- (ρ) the map $\mathcal{G}(\text{perm})$ is a permutation map $\rho: V \otimes V \rightarrow V \otimes V$, $a \otimes b \mapsto b \otimes a$.
- (ι) the map $\mathcal{G}(\boxtimes)$ is a unit $\iota: R \rightarrow V$

With this notation, the corresponding equations from 7.2 become:

$$\begin{aligned}
(m \otimes \text{id}) \circ (\text{id} \otimes \Delta) &= m \circ \Delta = (\text{id} \otimes \Delta) \circ (m \otimes \text{id}) \\
(\epsilon \otimes \text{id}) \circ \Delta &= \text{id} = m \circ (\text{id} \otimes \iota) \\
m \circ (\text{id} \otimes m) &= m \circ (m \otimes \text{id}) \\
(\text{id} \otimes \Delta) \circ \Delta &= (\Delta \otimes \text{id}) \circ \Delta
\end{aligned} \tag{7.3}$$

Therefore, a TQFT \mathcal{G} which assigns the fundamental cobordisms to maps satisfying Equation 7.3 will be well-defined. Any Frobenius system will define a 2-dimensional TQFT [Kho06b].

²This is a nontrivial exercise in Cerf theory.

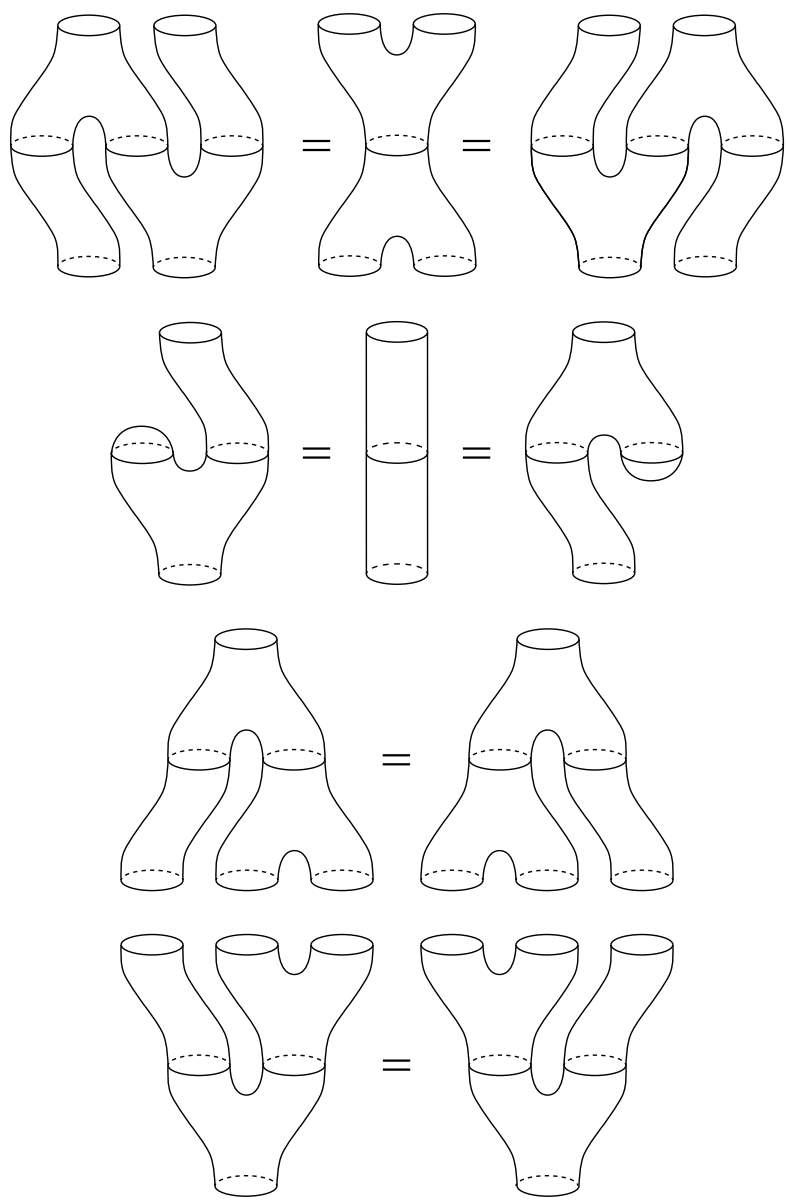


Figure B.1: The fundamental relations for Cob^3 .

Appendix C: Supplementary Code

Distinguishing ϕ -classes from a pair of slice disks with boundary 6_1 The ϕ -cycles associated to a pair of slice disks bounding the knot 6_1 were given in Figure 5.6. We will show these cycles represent distinct homology classes by showing their sum/difference is not a boundary in the chain complex associated to the diagram 6_1 . This is done by running the SageMath program, discussed in Section 6. In particular, we use the enumerations from Figure C.1 and run the given code to determine the cycles in the aforementioned figure are distinct.

```
1 sage: crossings = [[1,5,2,4],[5,1,6,12],[11,7,12,6],
2                 [7,11,8,10],[3,8,4,9],[9,2,10,3]]
3 sage: D = Diagram(crossings)
4 sage: CC = ChainComplex(D)
5 sage: l1 = Generator(D, "011000", "1xx")
6 sage: l2 = Generator(D, "011000", "x1x")
7 sage: l3 = Generator(D, "011000", "xx1")
8 sage: l4 = Generator(D, "010010", "1xx")
9 sage: l5 = Generator(D, "010010", "x1x")
10 sage: l6 = Generator(D, "010010", "xx1")
11 sage: l7 = Generator(D, "001001", "1xx")
12 sage: l8 = Generator(D, "001001", "x1x")
13 sage: l9 = Generator(D, "001001", "xx1")
14 sage: l10 = Generator(D, "000011", "1xx1x")
15 sage: l11 = Generator(D, "000011", "x1x1x")
16 sage: l12 = Generator(D, "000011", "xx11x")
17 sage: l13 = Generator(D, "000011", "xxx11")
18 sage: l14 = Generator(D, "000011", "1x1xx")
19 sage: l15 = Generator(D, "000011", "x11xx")
20 sage: l16 = Generator(D, "000011", "xx11x")
21 sage: l17 = Generator(D, "000011", "xx1x1")
22 sage: r1 = Generator(D, "001100", "1xx")
23 sage: r2 = Generator(D, "001100", "x1x")
24 sage: r3 = Generator(D, "001100", "xx1")
25 sage: r4 = Generator(D, "110000", "1xx")
26 sage: r5 = Generator(D, "110000", "x1x")
27 sage: r6 = Generator(D, "110000", "xx1")
28 sage: r7 = Generator(D, "100100", "xx1")
29 sage: r8 = Generator(D, "000011", "1x1xx")
30 sage: r9 = Generator(D, "000011", "x11xx")
```

```

30 sage: r10 = Generator(D, "000011", "xx11x")
31 sage: r11 = Generator(D, "000011", "xx1x1")
32 sage: c1 = Chain(D, [l1,...,l17,r1,...,r11],
    [1,-1,-1,-1, 1,-1,-1, 1,-1,-1, 1, 1,-1,-1, 1, 1,-1,
    1, 1,-1, 1,-1,-1,-2,-1, 1, 1, 1])
33 sage: c2 = Chain(D, [l1,...,l17,r1,...,r11],
    [1,-1,-1,-1, 1,-1,-1, 1,-1,-1, 1, 1,-1,-1, 1, 1,-1,
    -1,-1, 1,-1, 1, 1, 2, 1,-1,-1,-1])
34 sage: [CC.isCycle(c1), CC.isBoundary(c1)] #Returns [True, False]
35 sage: [CC.isCycle(c2), CC.isBoundary(c2)] #Returns [True, False]

```

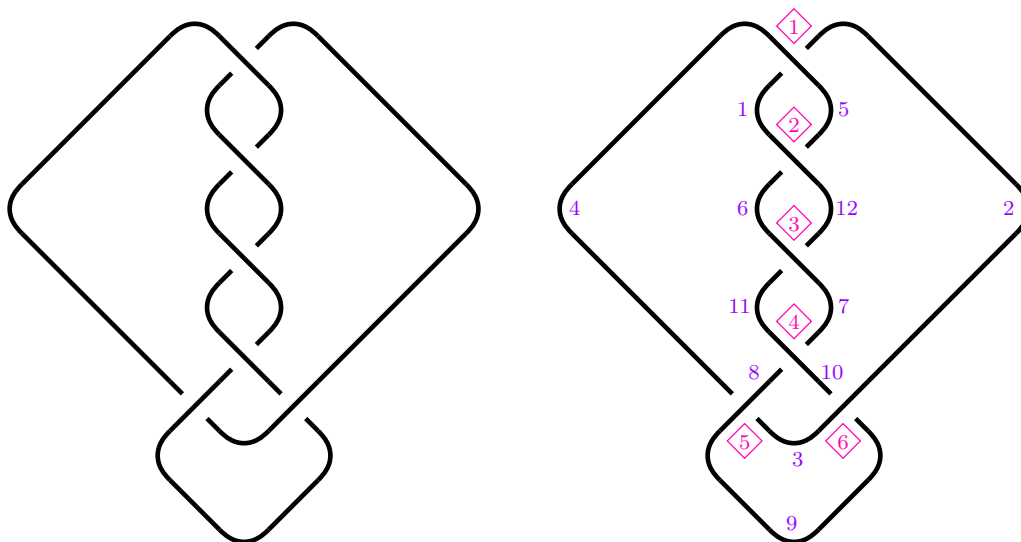


Figure C.1: A diagram for 9_{46} with enumerations of its crossings and strands.

Determining nontriviality of the φ -class associated to a genus-1 surface with bound-

ary 11n34 Below, we give two sets of code which show that the φ -class obtained from the movies in Figures C.3 and C.5 are nontrivial. The code uses the enumerations from Figures C.2 and C.4, respectively.

```

1 sage: crossings = [[1,16,2,17],[2,7,3,8],[17,13,18,12],
    [11,1,12,22],[15,10,16,11],[6,9,7,10],[8,3,9,4],[13,19,14,18],
    [21,15,22,14],[20,6,21,5],[4,20,5,19]]
2 sage: D = Diagram(crossings)
3 sage: CC = ChainComplex(D)
4 sage: g1 = Generator(D, "01000110101", "xx1x")
5 sage: g2 = Generator(D, "01000010111", "xxx1")
6 sage: g3 = Generator(D, "01000110110", "xx1x")
7 sage: g4 = Generator(D, "01000100111", "xx1x")
8 sage: c = Chain(D, [g1,g2,g3,g4], [2,2,2,2])
9 sage: [CC.isCycle(c),CC.isCycle(c)] #Returns [True, False]

```

```

1 sage: crossings = [[1,15,2,14],[13,3,14,2],[15,6,16,7],[12,8,13,7],
    [5,16,6,17],[4,12,5,11],[8,4,9,3],[17,20,18,21],[10,22,11,21],
    [19,24,20,1],[23,18,24,19],[22,10,23,9]]
2 sage: D = Diagram(crossings)
3 sage: CC = ChainComplex(D)
4 sage: g1 = Generator(D, "001101010101", "xxx")
5 sage: g2 = Generator(D, "001110010101", "xxx1x")
6 sage: g3 = Generator(D, "001110001101", "xxxx1")
7 sage: g4 = Generator(D, "001101010010", "xxx1x")
8 sage: g5 = Generator(D, "001101010010", "xxxx1")
9 sage: g6 = Generator(D, "001110010010", "xxx1x1x")
10 sage: g7 = Generator(D, "001110010010", "xxx1xx1")
11 sage: g8 = Generator(D, "001101001010", "xxx")
12 sage: g9 = Generator(D, "001110001010", "xxx1x")
13 sage: c = Chain(D, [g1,g2,g3,g4,g5,g6,g7,g8,g9], [1,1,1,1,1,1,1,1,1])
14 sage: [CC.isCycle(c), CC.isBoundary(c)] #Returns [True, False]

```

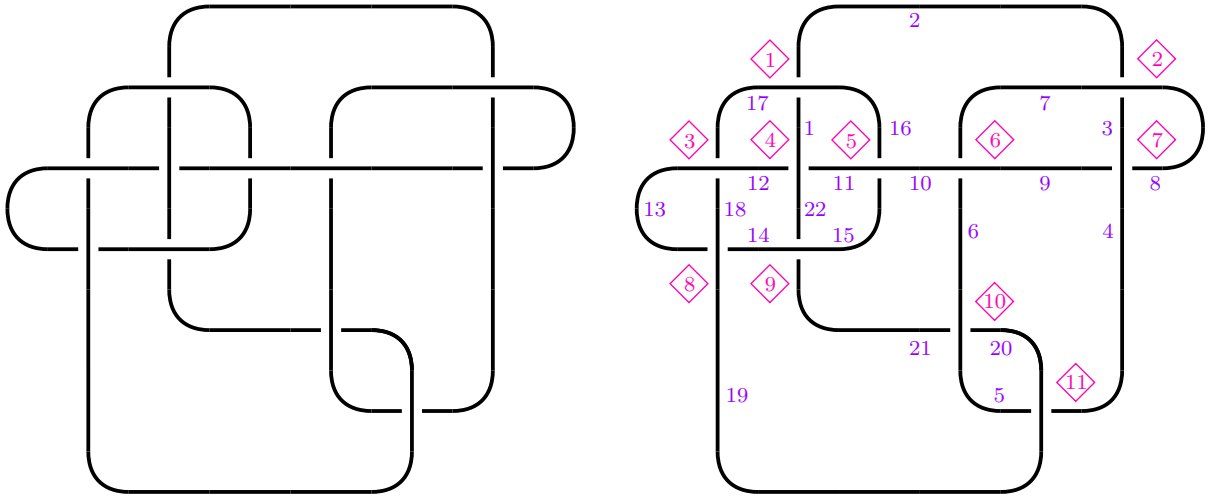



Figure C.2: A diagram for the Conway knot $11n34$ with enumerations of its crossings and strands.

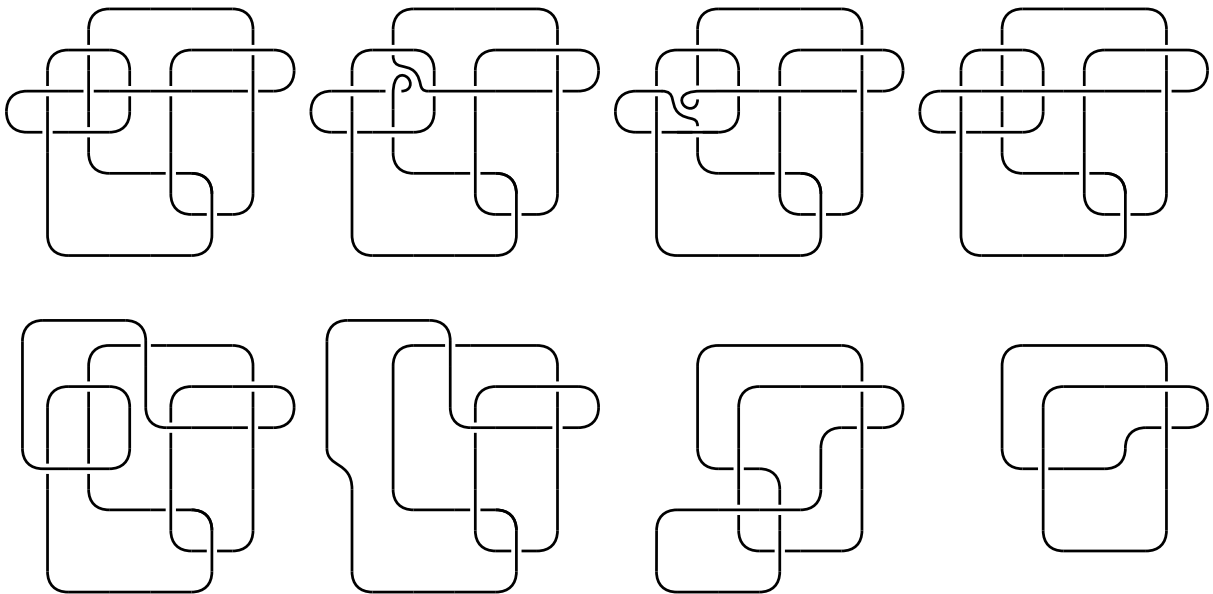


Figure C.3: A shortened movie describing a genus-1 surface bounding the Conway knot; a single crossing change on the left-most diagram produces an unknot diagram, which can be untangled (bottom right, after a final Reidemeister II and I) and capped off.

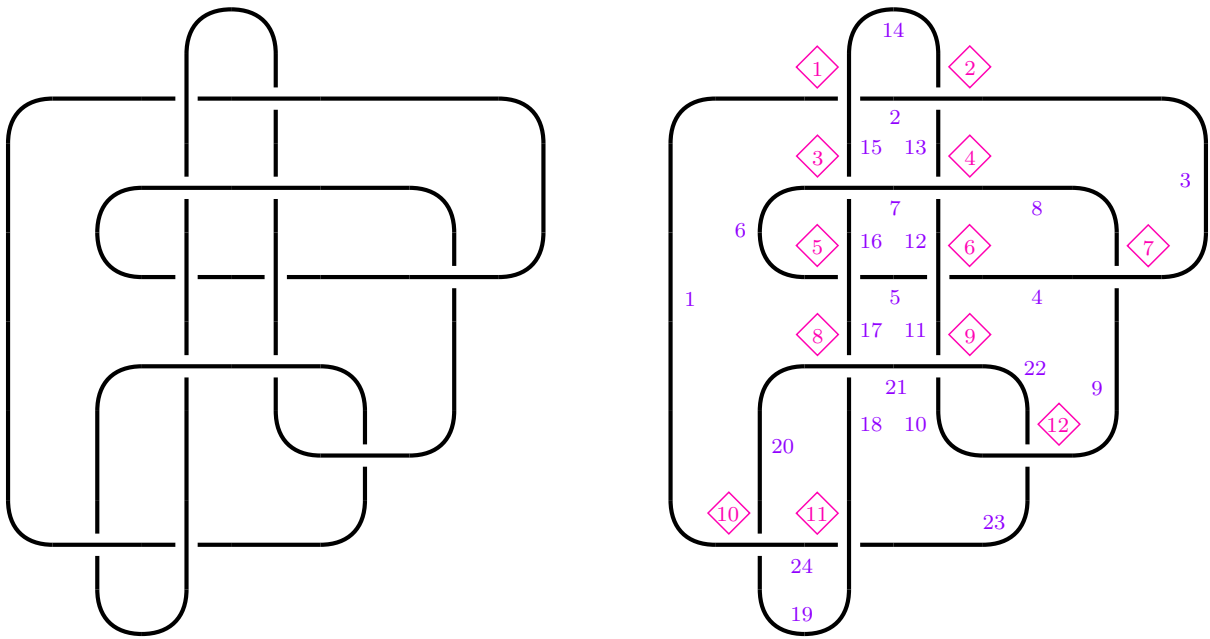


Figure C.4: A diagram for the Conway knot $11n34$ with enumerations of its crossings and strands.

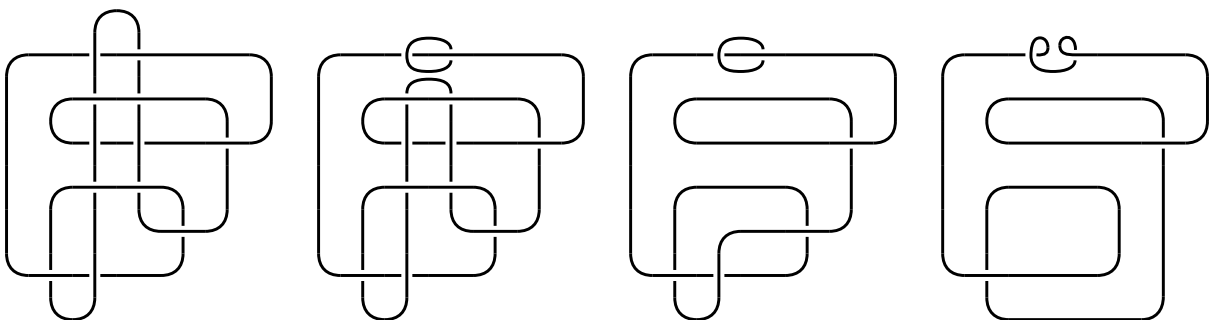


Figure C.5: A shortened movie describing a genus-1 surface bounding the Conway knot, where the last frame can be untangled with Reidemeister I's and capped off.

Bibliography

- [Akb91] **S Akbulut**, *A solution to a conjecture of Zeeman*, *Topology*, 30(3):513–515, 1991.
- [Alf70] **W R Alford**, *Complements of minimal spanning surfaces of knots are not unique*, *Ann. of Math.*, 2(91):419–424, 1970.
- [Ati90] **M Atiyah**, *The geometry and physics of knots*, Cambridge University Press, pages 1–78, 1990.
- [Bat12] **J Batson**, *Personal communication with Paul Melvin*, 2012.
- [BN02] **D Bar-Natan**, *On Khovanov’s categorification of the Jones polynomial*, *Algebr. Geom. Topol.*, 2:337–370, 2002.
- [BN05] **D Bar-Natan**, *Khovanov’s homology for tangles and cobordisms*, *Geom. Topol.*, 9:1443–1499, 2005.
- [CP21] **A Conway**, **M Powell**, *Characterisation of homotopy ribbon discs*, *Advances in Mathematics*, 391:107960, 2021.
- [CRS97] **J S Carter**, **J H Reiger**, **M Saito**, *A combinatorial description of knotted surfaces and their isotopies*, *Adv. Math.*, 127(1):1–51, 1997.
- [CS93] **J S Carter**, **M Saito**, *Reidemeister moves for surface isotopies and their interpretations as moves to movies*, *J. Knot Theory Ramifications*, 2:251–284, 1993.
- [CSS06] **J S Carter**, **M Saito**, **S Satoh**, *Ribbon-moves for 2-knots with 1-handles attached and Khovanov–Jacobsson numbers*, *Proc. Amer. Math. Soc.*, 134(9):2779–2783, 2006.
- [EK71] **R D Edwards**, **R C Kirby**, *Deformations of spaces of imbeddings*, *Ann. Math.*, 93(2):63–88, 1971.
- [Ell09] **A Elliott**, *Graphical methods establishing nontriviality of state cycle Khovanov homology classes*, arXiv:0907.0396, 2009.
- [Ell10] **A Elliott**, *State cycles, quasipositive modification, and constructing H -thick knots in Khovanov homology*, ProQuest LLC, Ann Arbor, MI, 2010, Thesis (Ph.D.)–Rice University.
- [GJ11] **J Greene**, **S Jabuka**, *The slice-ribbon conjecture for 3-stranded pretzel knots*, *Amer.*

- J. Math., 133(3):555–580, 2011.
- [GL20] **O S Gujral, A S Levine**, *Khovanov homology and cobordisms between split links*, arXiv:2009.03406, 2020.
- [GS99] **R E Gompf, A I Stipsicz**, *4-manifolds and Kirby calculus*, number 20 in Graduate Studies in Mathematics, American Mathematical Society, 1999.
- [Hay21] **K Hayden**, *Corks, covers, and complex curves*, arXiv:2107.06856, 2021.
- [HS21] **K Hayden, I Sundberg**, *Khovanov homology and exotic surfaces in the 4-ball*, arXiv:2108.04810, 2021.
- [Jac03] **M Jacobsson**, *Khovanov’s conjecture over $\mathbb{Z}[c]$* , arXiv:math.GT/0308151, 2003.
- [Jac04] **M Jacobsson**, *An invariant of link cobordisms from Khovanov homology*, *Algebr. Geom. Topol.*, 4:1211–1251, 2004.
- [JM16] **A Juhász, M Marengon**, *Concordance maps in knot Floer homology*, *Geom. Topol.*, 20(6):3623–3673, 2016.
- [JZ20] **A Juhász, I Zemke**, *Distinguishing slice disks using knot Floer homology*, *Selecta Math. (N.S.)*, 26(1):Paper No. 5, 18, 2020.
- [Kho00] **M Khovanov**, *A categorification of the Jones polynomial*, *Duke Math. J.*, 101(3):359–426, 2000.
- [Kho06a] **M Khovanov**, *An invariant of tangle cobordisms*, *Trans. Amer. Math. Soc.*, **358**(1):315–327, 2006.
- [Kho06b] **M Khovanov**, *Link homology and Frobenius extensions*, *Fund. Math.*, 190:179–190, 2006.
- [Kho21] **M Khovanov**, *Personal communication with author*, 2021.
- [KL79] **R C Kirby, W B R Lickorish**, *Prime knots and concordance*, *Math. Proc. Cambridge Philos. Soc.*, 86(3):437–441, 1979.
- [Lee02] **E S Lee**, *An endomorphism of the Khovanov invariant*, arXiv:math/0210213, 2002.
- [Liv82] **C Livingston**, *Surfaces bounding the unlink*, *Michigan Math. J.*, **29**(3):289–298, 1982.
- [LS21] **R Lipshitz, S Sarkar**, *A mixed invariant of non-orientable surfaces in equivariant Khovanov homology*, arXiv:2109.09018, 2021.
- [Lyo74] **H C Lyon**, *Simple knots without unique minimal surfaces*, *Proc. Amer. Math. Soc.*, 43:449–454, 1974.
- [LZ19] **A S Levine, I Zemke**, *Khovanov homology and ribbon concordances*, *Bull. Lond.*

- Math. Soc., 51(6):1099–1103, 2019.
- [MN20] **C Manolescu, I Neithalath**, *Skein lasagna modules for 2-handlebodies*, arXiv:math/2009.08520, 2020.
- [MP19] **A N Miller, M Powell**, *Stabilization distance between surfaces*, Enseign. Math., 65(3-4):397–440, 2019.
- [MWW21] **S Morrison, K Walker, P Wedrich**, *Invariants of 4-manifolds from Khovanov-Rozansky link homology*, Geom. Top. (to appear), 2021.
- [Pic20] **L Piccirillo**, *The Conway knot is not slice*, Ann. of Math., 191(2):581–591, 2020.
- [Ras05] **J Rasmussen**, *Khovanov’s invariant for closed surfaces*, arXiv:math/0502527, 2005.
- [Ras10] **J Rasmussen**, *Khovanov homology and the slice genus*, Invent. Math., 182(2):419–447, 2010.
- [Ros98] **D Roseman**, *Reidemeister-type moves for surfaces in four dimensional space*, Banach Center Publications, Knot Theory, 42:347–380, 1998.
- [SS21] **I Sundberg, J Swann**, *Relative Khovanov-Jacobsson classes*, Algebr. Geom. Topol. (to appear), 2021.
- [Swa10] **J Swann**, *Relative Khovanov-Jacobsson classes for spanning surfaces*, ProQuest LLC, Ann Arbor, MI, 2010, Thesis (Ph.D.)–Bryn Mawr College.
- [Tan06] **K Tanaka**, *Khovanov-Jacobsson numbers and invariants of surface-knots derived from Bar-Natan’s theory*, Proc. Amer. Math. Soc., 134(12):3685–3689, 2006.
- [Tro75] **H F Trotter**, *Some knots spanned by more than one knotted surface of minimal genus*, Knots, groups, and 3-manifolds, pages 51–62, *Ann. of Math. Studies, 84*, Princeton Univ. Press, Princeton, N.J., 1975.